SLIDING MODE OBSERVERS FOR OBSERVING THE DYNAMICS OF NUCLEAR REACTOR SYSTEMS

A dissertation submitted in partial fulfilment of the requirements

for the degree of

MASTER OF TECHNOLOGY

in

NUCLEAR SCIENCE AND ENGINEERING

By

Dhaivat Mandavia

(2K13/NSE/02)

Under the guidance of

Dr. A.P. Tiwari
Outstanding Scientist and Head,
Reactor Control System Design Section,
Bhabha Atomic Research Centre,
Mumbai, India

Dr. Nitin Kumar Puri
Assistant Professor,
Department of Applied Physics,
Delhi Technological University,
Delhi, India

Department of Applied Physics,
Delhi Technological University,
(Formerly Delhi College of Engineering),
Bawana Road, Delhi - 110042

June 2015

डॉ. अखिलानन्द पति तिवारी
Dr. Akhilanand Pati Tiwari

सत्यमेव जयते
भारत सरकार
Government of India

उत्कृष्ट वैज्ञानिक एवं अध्यक्ष, रिएक्टर नियन्त्रण प्रणाली अभिकल्पन अनुभाग
Outstanding Scientist & Head, Reactor Control Systems Design Section

Ref: RCSDS/APT/ Date:

CERTIFICATE

This to certify that **Shri. Dhaivat Udayan Mandavia**, IV semester student of M. Tech (Nuclear Science and Engineering) from Delhi Technological University (Formerly Delhi College of Engineering)**,** Delhi - 110042 has successfully completed his project work at Reactor Control System Design Section, Bhabha Atomic Research Centre, Mumbai on "**Sliding Mode Observers for Observing the Dynamics of Nuclear Reactor Systems**" from January 12, 2015 to June 5, 2015. The project report does not contain any proprietary or classified matter.

During the project work, the character and conduct of **Shri. Dhaivat Udayan Mandavia** was found to be exceptionally good.

We wish him all success in his future career.

(A P Tiwari)
Head, RCSDS
E&I Group

रिएक्टर नियन्त्रण प्रणाली अभिकल्पन अनुभाग • Reactor Control Systems Design Section
इलेक्ट्रानिकी एवं यंत्रीकरण वर्ग • Electronics And Instrumentation Group
भाभा परमाणु अनुसंधान केन्द्र, ट्रॉम्बे, मुंबई 400085, भारत • Bhabha Atomic Research Centre, Trombay, Mumbai 400085, India
दूरभाष / Phone: +(91) (22) 25595178 फैक्स / Fax: +(91) (22) 25591803 • ई-मेल / E-mail: aptiwari@barc.gov.in

DELHI TECHNOLOGICAL UNIVERSITY
(Formerly Delhi College of Engineering), Delhi

2014 - 2015
DEPARTMENT OF APPLIED PHYSICS

CERTIFICATE

This is to certify that the major project work entitled "**Sliding Mode Observers For Observing The Dynamics Of Nuclear Reactor Systems**" is a bonafide and authentic work carried out by **Mr. Dhaivat Mandavia (2K13/NSE/02)** in partial fulfilment of Master of Technology (M. Tech) degree in Nuclear Science and Engineering of Delhi Technological University (Formerly Delhi College of Engineering), Delhi during the year 2014-2015. It is certified that all corrections/suggestions indicated for Internal Assessment have been approved as it satisfies the academic requirements in respect of major project prescribed for Master of Technology (M. Tech) degree.

.....
(*Signature of the Internal Assessment Guide*)
Name: Dr. Nitin K. Puri
Date:

.....
(*Signature of the HOD*)
Name: Prof. Suresh Sharma
Date:

.....
(Seal)

Department of Applied Physics,
Delhi Technological University,
(Formerly Delhi College of Engineering), Delhi.

DECLARATION

I, here state that the work which is being presented in the major project, entitled **Sliding Mode Observers For Observing The Dynamics Of Nuclear Reactor Systems** is an authentic record of my own work carried out under the guidance of **Dr. A.P. Tiwari**, Outstanding Scientist and Head, Reactor Control System Design Section, Bhabha Atomic Research Centre, Mumbai and **Dr. Nitin Kumar Puri**, Assistant Professor, Department of Applied Physics, Delhi Technological University (Formerly Delhi College of Engineering), Delhi. The work contained in this major project has not been submitted in part or full, to any other university or institution for carrying out the project in the past.

This dissertation work is submitted to Delhi Technological University (Formerly Delhi College of Engineering) in partial fulfilment for the Master of Technology (M. Tech) in Nuclear Science and Engineering during the academic year 2014-2015.

Dhaivat Mandavia

ACKNOWLEDGMENT

I take this opportunity to express my sincere gratitude to all those people who have been instrumental in the successful completion of this project and because of whom my graduate experience will be cherished forever.

I would like to express my deep sense of gratitude to my external guide, **Dr. A.P. Tiwari**, Outstanding Scientist and Head, Reactor Control System Design Section (RCSDS), Bhabha Atomic Research Centre (BARC), Mumbai. I am fortunate to have worked under his guidance. His immense knowledge, motivation and ingenuity in the subject has been a great value to me. His patience, encouragement and support will be treasured throughout my life.

I am deeply grateful to my technology adviser **Mr. Amit Kumar Mishra,** Scientific Officer, RCSDS, BARC, Mumbai, for the long and fruitful discussions that helped me to overcome the initial difficulties in the project. I am thankful to him for providing moral support and helping me to further explore the new avenues of my life.

I shall always be deeply obliged for the unflinching support and guidance of my internal assessment guide and one my best teachers **Dr. Nitin Kumar Puri** in recommending me to take up this project work. His encouragement and guidance right from the day of meeting inspired me to take up a challenging career.

I wish to thank all my **research fellows** at Bhabha Atomic Research Centre for their insightful comments and suggestions throughout the project work. My **friends** at Delhi Technological University have always helped and supported me. I greatly value their friendship all the time.

I cannot forget to thank **Dr. Suhas Mangoli and family** for providing an enjoyable and memorable stay at their home in Mumbai. Their help to relish the beauty of this fascinating city was indispensable.

Finally, I am forever indebted to my beloved **grandparents** and **mother** whose support and guidance throughout my education was invaluable. Their unconditional love and affection was and will be a source of strength throughout my life.

I conclude my acknowledgements by expressing my wholehearted gratitude to all those people who helped me directly or indirectly to realize this project.

Dhaivat Mandavia

ABSTRACT

The behaviour of the control system under parameter uncertainties is of utmost importance in industrial applications. For designing a robust control system, a necessary effort has to be carried out for achieving desirable control characteristics irrespective of the operating conditions. With the shortcomings in the design of a conventional controller, a theory with proper mathematical background is of imminent need for a control designer. The application of a high speed switching with a suitable switching logic provides attractive feature of possessing a new property which is not present in the substructures. This fundamental idea developed into Variable Structure theory. Having derived from variable structure, sliding mode control is the operational tool of variable structure control. The design of sliding surface is important for control of the system during sliding mode. The distinguishing feature of sliding mode is the independence of the system against model dynamics which testifies the robustness with respect to parametric uncertainties, bounded disturbances and noise.

Numerous applications of sliding mode in controller design is already proposed. The requirement of all states of the system for effective control was an inherent drawback with respect to practical system. Estimation of non-measurable states using the input and information of any measurable state is the fundamental idea of an observer. Luenberger observer for estimation of states is not robust to handle parametric variations and nonlinearities present in the system. Hence, the fundamental idea of sliding mode for observer design is used. This thesis describes the general framework for the design of sliding mode observer with focus on nuclear reactor system. Point Reactor Kinetics (PRK) model which is derived from the neutron diffusion equation is the model to be considered. With only nuclear reactor power as a measurable quantity, the delayed neutron precursor concentration, reactivity, external neutron source, xenon and iodine concentration is estimated. Out of large number of applications of sliding mode, fault detection in a nuclear and non-nuclear component with actuator and sensor faults is carried out. Residual evaluation is carried out using sliding mode observer while validating the residual signal at different instances where fault occurs.

The inherent drawback of chattering due to formulation of first order sliding mode is minimized by using smooth functions. This method would forgo the fundamental idea of robustness of sliding mode. An attempt is made to present the application of higher order sliding mode which minimizes or sometimes eliminates chattering without compromising the robustness. The state estimation of a nuclear reactor system using Super Twisting algorithm is in good agreement with simulated state from PRK model. The independence of states with respect to initial conditions along with faster convergence time is achieved by the application of uniform second order sliding mode algorithm validated using the PRK model.

Contents

List of Figures

List of Tables

Chapter 1

Introduction

The ability to measure the critical parameters of a system under parametric variations, bounded disturbance and noise is one of the most important control problems. Though mathematical model describe the actual physical system, the parameters calculated from the mathematical model are an approximation of the actual system. In most of the cases, the difference which arises between the system model and actual physical system are mainly due to parametric variations and unmodeled high frequency system dynamics. It is well known fact that most of the practical systems are nonlinear in nature which makes the formulation of the accurate mathematical model a complex process. A simpler approach called the linearization is employed but the error by neglecting the nonlinearities present in the system is outside the safety limits of the critical systems. Therefore, there is a significant need to develop a control mechanism to account for nonlinearities and robust against perturbations in parameters.

The conventional controller design is linear with primary analysis using the transfer function of a system. The methods like eigenvalues placement, quadrature minimization provided a simple design of a controller. The control characteristics could easily be altered and control designer applied to various industrial applications. These controllers could not satisfy the perturbations mentioned above while maintaining its designed performance. The application of Variable Structure Control (VSC) provided a new approach in control system design. A control approach involving high speed switching feedback to force the state trajectory on to a designed surface with varying structures defines Variable Structure Control. An efficient switching logic accompanied by a switching gain provides significant advantages.

Sliding Mode Control is one of the operational classes of Variable Structure Control because of its potential advantages and ease in control system design. The inherent advantages offered by sliding mode control against parametric uncertainties and bounded disturbance provided a strong background to carry out further developments. Though there was a long time gap of few decades till the proposed theory on Variable Structure Control was available to all researchers, the development was exemplified by the prominence of sliding mode control. This task is accomplished by sliding mode by quick response to any slight deviation in the parameter which corresponds to addition of discontinuous control. With sliding mode as the operational tool for realization of variable structure control, numerous control applications in aircraft systems, electric motors, robotic systems and many more were developed.

Rapid fluctuations of finite amplitude and finite frequency are the result of finite switching frequency in case of practical systems. This is commonly called as chattering phenomena. This is disastrous effect of application of sliding mode control due to which there is a high loss of energy in systems besides loss in control accuracy. Several works [2, 7, 8] focused on the usage of ‘smooth’ functions like saturation or hyperbolic tangent functions instead of discontinuous

function to minimize chattering. Indeed, this is a significant step towards chattering removal but the loss of robustness by using this approach is a tradeoff which a control designer has to take care of.

The advanced controller design assumes that all the states are observable. This is certainly not valid in case of practical system where a sensor measuring a required state may not be placed due to practical constraints or due to economic considerations. An approach to ignore a state which is immeasurable or in other words an approach to develop a mathematical model by neglecting certain state which is not available is impossible. Therefore, a need to accurately estimate the immeasurable states is of utmost importance. An observer carries out this task by considering the input of the system model along with one of measurable states.

1.1 Motivation

The first observer to estimate the states accurately was developed by Luenberger [14]. The inability to handle parametric uncertainties and applicability to linear systems are some of the drawbacks of Luenberger observer. The application of sliding mode design concept for estimating the state vector is highly advantageous especially the robustness of sliding mode against parametric variations, modeling imperfections, bounded disturbances. Therefore in this thesis we focus on the design of a sliding mode observer.

The application of observer to nuclear reactor system is important because of practical difficulties in measuring all the critical parameters. The critical parameters includes delayed neutron concentration, reactivity, independent neutron source, xenon and iodine concentration with reactor power as the only measurable parameter. In addition, observer can be used in the design of new reactors where hardly any operating data is available. As the safety of a nuclear reactor is dependent on the variation of critical parameters and hence accurate estimation of parameters is indeed required. With a presence of large number of sensors and actuators in a nuclear reactor, there is a finite probability of an occurrence of a fault. The presence of fault in control or sensing a parameter has a severe implication of failure of a nuclear reactor.

In this thesis, application of sliding mode observer for analyzing nuclear reactor system dynamics is carried out. The critical parameters mentioned above are estimated under parametric variations and bounded disturbances. In addition, fault detection is carried out for a nuclear reactor core and steam generator.

The loss of robustness by employing smooth functions in boundary layer approach and hence compromising the fundamental idea of sliding mode is not acceptable. Therefore higher order sliding mode is employed for nuclear reactor system to minimize chattering and preserve the robust nature of sliding mode. Further, usage of uniform algorithms makes the observer design independent of the initial conditions of the system.

1.2 Thesis Contribution

1. A simulation study of first order sliding mode observer for Pressurized Heavy Water Reactor (PHWR) is carried out. The robustness against parametric variations is presented.

2. A second order sliding mode observer for Pressurized Heavy Water Reactor is developed. One of the prominent second order sliding mode algorithms called Super Twisting algorithm is applied for a PHWR. A comparison between first order and second order sliding mode algorithm is highlighted.

3. Uniform Second Order Sliding Mode (USOSM) algorithm is designed to achieve faster convergence time of an observer independent of initial condition of the system. A comparison of this design with the designed Super Twisting Algorithm is presented clearly.

1.3 Organization of Thesis

The thesis is an outcome to design a sliding mode observer for analyzing the nuclear reactor system dynamics.

In Chapter 2, an extensive literature survey is carried out. Though the original idea of this project was published in Russian in 1950s but after few decades, a successful translation with contribution from renowned authors is a noteworthy feature.

In Chapter 3, Point Reactor Kinetics (PRK) model of a nuclear reactor is discussed with a derivation of normalized form. To validate the model, few reactivity transients are considered.

Chapter 4 provides the basic understanding of the original theory of Variable Structure Control (VSC) with its advantages over conventional control theory. The most prominent class of VSC which is the Sliding Mode Control and its distinguishing features is focused at the end of the chapter with few examples.

Chapter 5 gives a basic understanding of an observer. A bird's eye view on one of the popular and simple observer called the Luenberger observer is provided. The inherent disadvantages of Luenberger observer is significantly highlighted and the need for formulating a Sliding Mode Observer is highlighted.

Chapter 6 specifies our discussion on the application of sliding mode observer design to a nuclear reactor application. Simulations are carried out to substantiate the properties of sliding mode by estimating the critical parameters like delayed neutron precursor concentration, reactivity, neutron source, xenon and iodine concentration. In the later part of the chapter, extensive focus on the application of the above design in fault detection of various components in a nuclear power plant is carried out.

Chapter 7 extends the design to an advanced level by introducing a recent theory on Higher Order Sliding Mode (HOSM). A brief overview is followed by an application of Super Twisting Algorithm for estimation of parameters in a nuclear reactor system. A further extension of the previous design is carried out by the design of USOSM algorithm.

Chapter 8 concludes this report with a prospective future work which can be carried out to solve the control problems in a practical nonlinear plant.

Chapter 2

Literature Survey

An extensive survey of emergence of sliding mode control from variable structure control is carried out. To mitigate some of the shortcomings of sliding mode controllers, observers were developed. The linear observers could not estimate practical nonlinear plant with matched disturbances and variation in plant parameters. To overcome these, observers using sliding mode was developed which is the motivation of this work. The applications of sliding mode observers are innumerable but only few applications are considered in this survey.

The history of sliding mode dates back to middle 1950's when the new control method called Variable Structure Control was developed by S.V Emel'yanov and his fellow researchers in the Soviet Union [7]. The proposed theory provided a new outlook in control engineering and potential advantages over the earlier methods was established. One of the distinguishing features of Variable Structure Control was the robustness against model parameter uncertainties, bounded external disturbances and noise effects. The earlier literature of VSC was published in Russian and in the late 1970's the theory was introduced in English literature [1].

The survey paper by Utkin [1] provided a comprehensive understanding of Variable Structure Control. The paper introduced a special class of Variable Structure Control called the Sliding Mode Control. Sliding Mode Control possessed the features of Variable Structure Control with simpler implementation. Therefore Sliding Mode became one of the operational methods of Variable Structure Control [1, 7, 8, 27]. In the coming years, Sliding Mode was successfully applied for motor control, adaptive control algorithms, aircraft control, robotic systems and many more. This was possible by the development of generalized Sliding Mode Control for nonlinear Multi Input Output Systems [8]. Due to addition of discontinuous control and presence of non-idealities in the system, an inherent effect of chattering was present. This effect was a serious disadvantage in case of realization with practical systems. Besides this, some other drawbacks include the application of control for relative degree one system, ability to handle disturbances only under matched conditions [6, 7, 12, 16].

In [37, 38] several variations of sliding mode controllers have been proposed with improvement in the controller design. These controllers possessed better control properties in comparison to the conventional linear design techniques. Most of the developed controllers required the availability of all the states in the system which was not possible practically. This paved the way for development of observer [5, 16].

The theory of observer was initially proposed by Luenberger [14]. This provided a new outlook for obtaining the full state information of the system which was otherwise not possible in

practical systems. An observer was considered as a state estimator where the non-measurable states were estimated by knowing the information about the measurable states. An observer also had the same inputs which were applied to the actual system. A reduced linear observer provided a greater practical flexibility to observe only those states which are non-measurable [5, 13, 14]. In literature [5], this observer is commonly called the 'Luenberger Observer'.

The inability to observe the actual states under plant parametric variations, bounded disturbances in case of practical system was a serious drawback of Luenberger observer [16]. With a strong motive to develop a robust observer, an application of sliding mode for observer design was proposed [6, 16]. The proposed sliding mode observer could make the observer estimation error tend to zero in finite time, while the observer states would asymptotically reach the actual system states [9, 16]. The earliest work on application of sliding mode theory to the development of observers was by Utkin [6] and recently Barbot et al. [28] provided a more robust sliding mode observer. Flippov and Utkin [12, 16] provided a mathematical basis for obtaining a unique solution of nonlinear differential equations with discontinuous terms. The theory of equivalent control [8, 16] was rigorously used in state estimation problems. The bounded disturbance term does not influence the state estimation error but the control signal is the disturbance when equivalent control is achieved without any a priori knowledge [15]. This is a significant property of sliding mode observer in terms of disturbance rejection. Because sliding mode theory was applicable both to linear and nonlinear systems, therefore sliding mode observer was able to model most of the nonlinearities [7, 15].

The problem of high frequency switching does not pose any control problems because there is no requirement of actuator to realize the control signal. Nevertheless, a new approach called the boundary layer approach was developed by [2, 29] where a smooth function was considered for control instead of discontinuous control. The application of several smooth functions like saturation function, hyperbolic tangent function in sliding mode design was considered [29].There is a tradeoff in obtaining the inherent robustness of sliding mode observer over the usage of smooth functions for control [2, 29]. The observer presented by Slotine et al. [2] was better than extended Kalman filter in terms of handling parametric uncertainty. A comprehensive comparative study of Kalman filter and sliding mode observer was carried out by Chen et al. [24].

Another approach for removal of chattering was provided in [18], where the usage of higher order sliding mode was proposed. Robust algorithms are proposed in [18, 20], to preserve the robustness property of sliding mode along with chattering removal. In the literature, the development of higher order sliding mode for a specific application is restricted primarily to second order sliding modes though a generalized sliding mode of any order has already been proposed [18]. Some of the popular second order sliding mode algorithm include Twisting algorithm and Super Twisting algorithm, while Drift algorithm is used for discrete time systems. A remarkable feature in implementing Super Twisting algorithm is the absence of chattering

[26]. In electrical motor, aircraft control and mechanical systems, the usage of super twisting algorithm for control and observation is proposed. To remove the dependence of observer convergence on the initial condition of the system, Fridman et al. [30] proposed a uniform second order sliding mode observer. The convergence time of uniform second order sliding mode observer is significantly less than the corresponding second order sliding mode observer [23, 30]. The requirement of an additional information in terms of derivative of sliding variable (except Super Twisting Algorithm [18]) to realize higher order sliding mode algorithm is difficult to obtain in practice. This is particularly relevant for systems with relative degree greater than two. Even if the differentiation is carried out, the results are degraded especially in noisy environments. Therefore a robust exact differentiator was proposed by Levant [17] with an improvement in terms of independence against initial condition variations, faster convergence of states is proposed in [31].

In [34] a five point nuclear reactor model with state assisted feedback control is discussed. Edwards et al [34] combined the point reactor kinetics model with the thermal hydraulic model to provide a more generalized view of the nuclear reactor core behavior. A nonlinear neutron flux model was proposed by Chernick [3]. Utkin observer was designed for estimation of xenon and iodine concentration in [4]. The properties of sliding mode was not validated in the application of Utkin observer [32].

An intuitive method of fault detection is by direct monitoring of a measured quantity. Due to practical limitations elaborately mentioned in [10], there is a need for development of cost effective and efficient fault detection strategies. In the literature, extensive research is carried out using model based fault detection approach. The actual measured quantity is compared with the model quantity. The significant advantage of model based approach is the minimization in hardware requirement in comparison with prominent techniques of signal analysis and principal component analysis [35]. The model based techniques [35] are linear in nature and therefore cannot handle nonlinearities present in the system. In addition parametric uncertainty is not handled by any of the other methods described. In this thesis, fault detection methods are explored using sliding mode observers.

In this thesis, first order sliding mode observer is designed to estimate precursor concentration, reactivity, neutron source along with xenon and iodine concentration. The estimation of precursor concentration and reactivity is carried out using second order sliding mode observer. An application of sliding mode observer for fault detection in nuclear reactor core and steam generator is carried out using point reactor kinetics and Irving’s model [33].

Chapter 3

Point Reactor Kinetics Model of a Nuclear Reactor

3.1 Introduction

The operating power of a nuclear reactor is dependent on the nuclear material present, the microscopic fission cross section and the neutron flux. Of all these factors, the flux or neutron density is directly related to control of reactor power. Therefore we shall consider the effect of neutron flux under various transients.

In a practical nuclear reactor, the neutrons are produced at different energies and these neutrons are absorbed and escape at different energy. The neutrons produced may be prompt or delayed. When the reactor is critical, the neutron production and loss are nearly equal and the above distinction of prompt and delayed neutrons is not valid. However there is a significant effect of delayed neutrons on the neutron flux and therefore are of importance in case of nuclear reactor control.

With respect to the mathematical model of the reactor, the reactor power will be a continuous function of neutron energy. This makes the analysis quite cumbersome but general conclusions can be reached by using a simple manner as evident in the later stage of this section. However, the identical results of those obtained by detailed modeling, may also be obtained by considering one neutron energy group model. This assumes that production, diffusion, absorption and leakage of neutrons take place at single energy with independence from space variables. This model also assumes that time variation of neutron flux at all points of core is identical. A time dependent behavior of a nuclear reactor due to change in the effective multiplication factor for a homogenous thermal reactor is known as the point reactor kinetics model of nuclear reactor. The word ‘point’ is used because of the approximation of considering the entire reactor core as a point. This model can be easily derived from the diffusion equation of one speed neutrons [36]. The point reactor model can be summarized into

$$\frac{dP(t)}{dt}=\left(\frac{k_{eff}(1-\beta)-1}{\Lambda}\right)P(t)+\sum_{i=1}^{6}\lambda_i C_i(t)+S(t) \qquad 3.1$$

$$\frac{dC_i(t)}{dt}=\left(\frac{\beta_i}{\Lambda}\right)P(t)-\lambda_i C_i(t) \qquad 3.2$$

where

$P(t)\rightarrow$ Reactor Power

$C_i(t)\rightarrow$ Delayed neutron precursor concentration of i^{th} group

$S(t)\rightarrow$ Primary or Independent neutron source

$\beta_i \rightarrow$ Delayed neutron precursor of group i

$\lambda_i \rightarrow$ Decay constant for the delayed neutron precursor of group i

$k_{eff} \rightarrow$ Effective multiplication factor

$\Lambda \rightarrow$ Prompt neutron lifetime

The left side of (3.1) shows the time dependent variation of reactor power. Reactor power can be substituted by neutron flux or neutron generation rate. The first term on right hand side of (3.1) defines the difference between the prompt neutron production rate and the rate of neutron loss. Whereas the second term on right hand side of (3.1) shows the production rate of delayed neutrons. The last term on right hand side of (3.1) is the primary or independent neutron source term which is usually present for low power reactors. This neutron source is present in the point kinetics equations in subcritical state also.

The left side of (3.2) shows the time dependent variation of delayed neutron precursor concentration. The first term on right hand side of (3.2) defines the neutron production rate whereas the second term on right hand side of (3.2) shows the rate of neutron loss.
Reactivity ρ is given by

$$\rho = \frac{k_{eff} - 1}{k_{eff}} \tag{3.3}$$

We can express the result in terms of reactivity ρ by substituting (3.3) in (3.1) and (3.2) as

$$\frac{dP(t)}{dt} = \left(\frac{\rho(t) - \beta}{\Lambda} \right) P(t) + \sum_{i=1}^{6} \lambda_i C_i(t) + S(t) \tag{3.4}$$

$$\frac{dC_i(t)}{dt} = \left(\frac{\beta_i}{\Lambda} \right) P(t) - \lambda_i C_i(t) \tag{3.5}$$

It is easy to infer that (3.4) is a nonlinear equation of $\rho(t)$ and $P(t)$.

3.2 Derivation of normalized form of Point Reactor Kinetics model

Let us consider a steady state of power as P_0. Assume that the independent or primary neutron source is absent. The steady state value of delayed neutron precursor concentration by equating the (3.5) to zero, is given by

$$C_{i0} = \frac{\beta_i}{\Lambda \lambda_i} P_0 \tag{3.6}$$

Normalizing (3.4) with respect to its steady state value P_0,

$$\frac{d}{dt}\left(\frac{P}{P_0} \right) = \left(\frac{\rho(t) - \beta}{\Lambda} \right)\left(\frac{P}{P_0} \right) + \left(\frac{1}{P_0} \right) \sum_{i=1}^{6} \lambda_i C_i$$

Substituting the value of P_0 from (3.6) in the above equation, we get

$$\frac{d}{dt}\left(\frac{P}{P_0}\right)=\left(\frac{\rho(t)-\beta}{\Lambda}\right)\left(\frac{P}{P_0}\right)+\sum_{i=1}^{6}\left(\frac{\beta_i}{\Lambda}\right)\left(\frac{C_i}{C_{i0}}\right)$$

Normalizing (3.5) with respect to its steady state value C_{i0},

$$\frac{d}{dt}\left(\frac{C_i}{C_{i0}}\right)=\left(\frac{\beta_i}{\Lambda}\right)\left(\frac{P}{C_{i0}}\right)-\lambda_i\left(\frac{C_i}{C_{i0}}\right)$$

Substituting the value of C_{i0} from (3.6) in the above equation, we get

$$\frac{d}{dt}\left(\frac{C_i}{C_{i0}}\right)=\lambda_i\left(\frac{P}{P_0}\right)-\lambda_i\left(\frac{C_i}{C_{i0}}\right)$$

The normalized set of equations are written as

$$\frac{dP(t)}{dt}=\left(\frac{\rho(t)-\beta}{\Lambda}\right)P(t)+\sum_{i=1}^{6}\left(\frac{\beta_i}{\Lambda}\right)C_i(t) \qquad 3.7$$

$$\frac{dC_i(t)}{dt}=\lambda_i P(t)-\lambda_i C_i(t) \qquad 3.8$$

Neutronic data used for simulation of response of the point reactor kinetics equations are given in Table 3.1

Table 3.1: Neutronic data for Pressurized Heavy Water Reactor (PHWR)

Group	**Decay Constant (1/s)**	**Delayed neutron fraction**
1	0.0126	$2.1*10^{-4}$
2	0.0301	$1.42*10^{-3}$
3	0.1118	$1.27*10^{-3}$
4	0.3014	$2.58*10^{-3}$
5	1.1363	$7.50*10^{-4}$
6	3.0137	$2.70*10^{-4}$
Total delayed neutron fraction		0.0065
Average decay constant (1/s)		0.0769
Mean neutron generation rate (s)		$3*10^{-5}$

For estimation of xenon and iodine concentration, the data is given in Table 3.2. In addition Table 3.2 provides the data for calculating neutron flux using Chernick model.

Table 3.2: Xenon, Iodine data for PHWR

Mean neutron generation rate (s)	0.083
Microscopic cross section of Xenon (cm^2)	$3.5*10^{-18}$
Constant parameter *c*	1.5
Xenon yield	0.03
Iodine yield	0.056
Decay constant of Xenon (1/s)	$2.1*10^{-5}$
Decay constant of Iodine (1/s)	$2.9*10^{-5}$
Lumped temperature feedback coefficient (cm^2*s)	$1.7*10^{-14}$

The fuel and coolant temperature for a PHWR is given in Table 3.3 and is used in fault detection analysis in Chapter 6.

Table 3.3: Fuel and Coolant temperature data for PHWR

Fraction of reactor power deposited f_f	0.98
Initial Equilibrium power P_0 (MW)	300
Heat capacity of fuel μ_f (MW*s/deg C)	14.8
Heat capacity of coolant μ_c (MW*s/deg C)	220
Mass flow rate multiplied by heat capacity of coolant M (MW/deg C)	$-58.8*n_0+106$
Heat transfer coefficient between coolant and fuel Ω (MW/deg C)	$-25.8*n_0+40$
Coolant temperature reactivity coefficient α_c (/deg C)	-0.00001
Fuel temperature reactivity coefficient α_f (/deg C)	-0.000025

3.3 Transients for validating Point Reactor Kinetics (PRK) model

In this section, we carry out analysis of PRK model with respect to external transients. We assume a high power nuclear reactor where the neutron source term is considered as zero. It is also assumed that the reactor was operating in steady state with zero initial reactivity.

Fig. 3.1 shows the variation of reactor power to a rectangular reactivity input. A positive reactivity of 0.1mk is applied for 40 seconds as shown in Fig. 3.1 (a). There is a prompt jump of reactor power at the point where reactivity is inserted. There is a steady increase in power till 40 seconds. Further there is a drop in power due to decrease in reactivity to zero. The reactor power variation is shown in Fig. 3.1 (b).

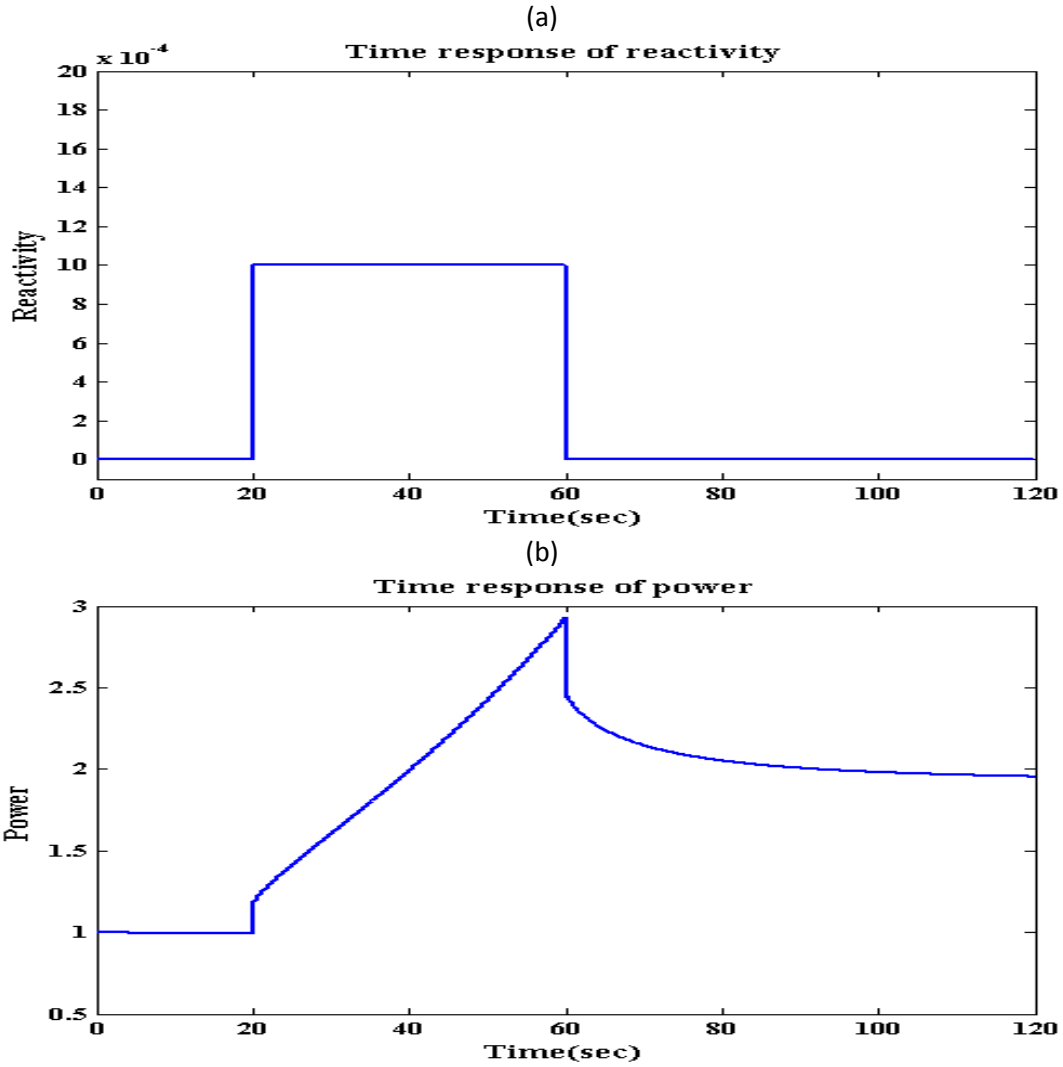

Figure 3.1: Transient response of point reactor kinetics power for rectangular reactivity input. Fig. 3.1(a) represents variation in reactivity. Fig. 3.1(b) shows the corresponding variation in power.

Fig. 3.2 shows the response of reactor power to a large negative step reactivity input. A negative reactivity of 50mk is applied for 10 seconds as shown in Fig. 3.2 (a). We assume that initially the reactor was operating in steady state with zero reactivity. The reactor power variation corresponding to a reactivity transient is shown in Fig. 3.2 (b).

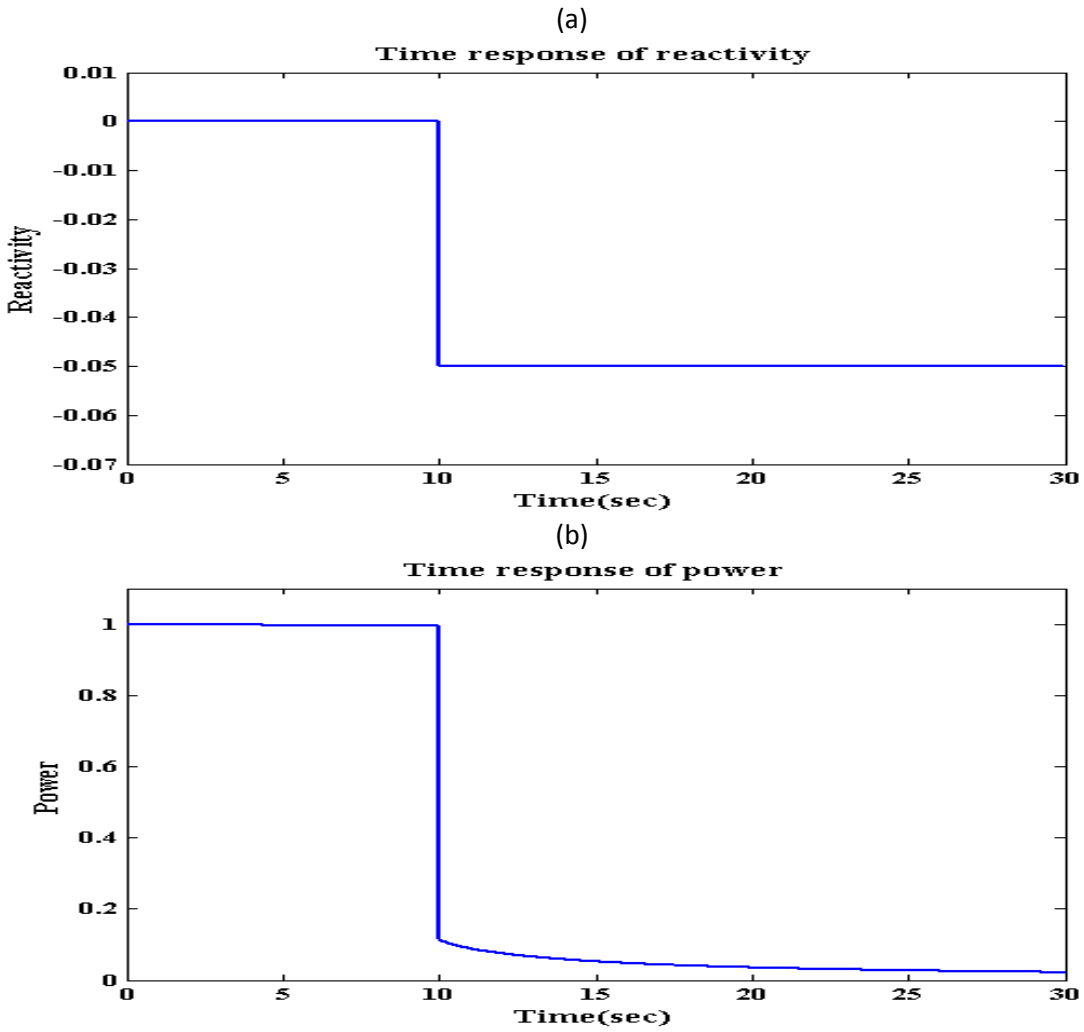

Figure 3.2: Transient response of point reactor kinetics power for large negative step reactivity input. Fig. 3.2(a) represents variation in reactivity. Fig. 3.2(b) shows the corresponding variation in power.

Fig. 3.3 shows the response of reactor power to an up chirp reactivity input. Let us consider a chirp signal defined as $\rho = 0.003\sin 2\pi t\left(0.01 + 0.01t\right)$. We infer that a chirp rate of 0.01 is used. The response of the input reactivity signal is shown in Fig. 3.3 (a). We assume that the reactor was operating in steady state with zero reactivity. The reactor power variation corresponding to a up chirp reactivity transient is shown in Fig. 3.3 (b).

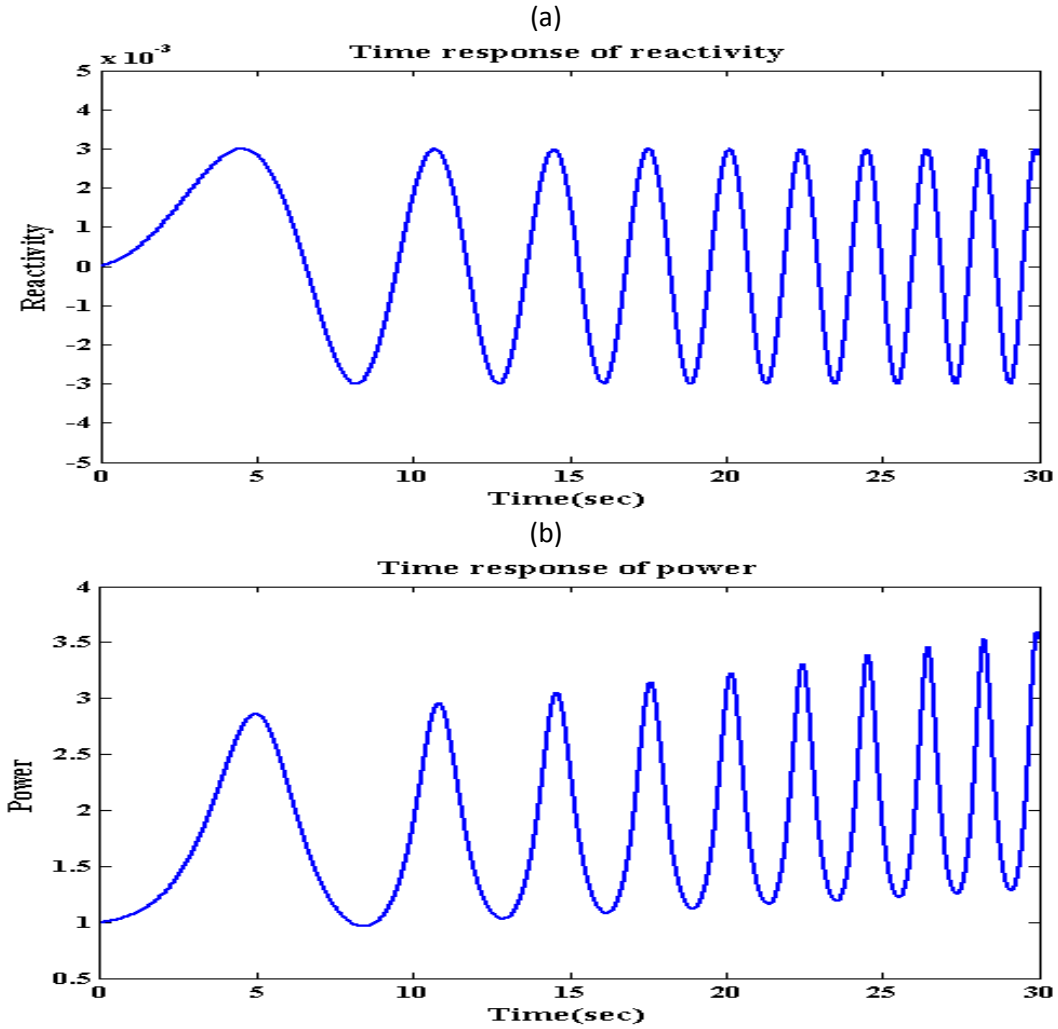

Figure 3.3: Transient response of point reactor kinetics power for up chirp reactivity input. Fig. 3.3(a) represents variation in reactivity. Fig. 3.3(b) shows the corresponding variation in power.

Chapter 4

Introduction to Variable Structure and Sliding Mode Control

In this chapter, a fundamental theory on which sliding mode theory was developed is introduced. The discussion of sliding mode theory with its remarkable properties is highlighted.

4.1 Variable Structure Control (VSC)

Variable Structure Control is a high speed switching feedback control where the control structure of the system varies from one structure to another according to a prescribed switching law. The fundamental goal of VSC is to force the state trajectory to reach onto a user defined surface in finite amount of time and stay thereafter. The user defined surface is commonly called as the switching surface because there is specific gain associated with the region above the switching surface and a different gain below the region of switching surface. The logic which defines the switching action is called the switching logic. The potential advantages of variable structure control outweigh the additional complexity introduced by the switching logic. The 'invariant' property which provided robustness against parameter uncertainty and bounded external disturbances is useful for dynamic process control. In addition, the distinguishing property of VSC is in combination of useful features of its sub structures. Variable Structure System may possess a new property which is non-inherent with respect to any of its sub structures [1]. This property is explained in the following section with necessary examples.

Even though the initial works on Variable Structure Control proposed by Prof. S.V. Emel'yanov was focused on linear second order systems. The VSC has been originated from the classical control techniques related to relay control and bang-bang control. The relative advancement in the coming years focused on nonlinear systems, Multi Input Multi Output (MIMO) systems, stochastic systems and many more. Therefore the application with respect to practical control problems in aircraft control, robot control and many others came into prominence.
The basic feature of variable structure control is explained by considering a general system. In terms of state variable approach,

$$\dot{x} = Ax + Bu \qquad 4.1$$

$$y = Cx$$

where

$$x \in \Re^n \; ; y \in \Re^m \; ; u \in \Re^r$$

$$A \in \Re^{n \times n} \; ; B \in \Re^{n \times r} \; ; C \in \Re^{m \times n}$$

In the linear controller [5] design the input vector x was fixed by knowing the state vector y .

The state feedback control law is represented as

$$u(t) = F\left[x(t), t\right] \tag{4.2}$$

Unlike fixed control law, the control is allowed to switch between permissible states defined by the switching logic. The advantages offered by variable structure control outweigh the additional complexity in designing the switching logic.

Consider a second order system with two structures given by

$\dot{x}_2 = -\alpha_1 x_1$ and $\dot{x}_2 = -\alpha_2 x_1$. Let $\alpha_1 > \alpha_2 > 0$.

The phase portrait of individual structures resembles an ellipse as shown in Fig. 4.1 (a) and (b).

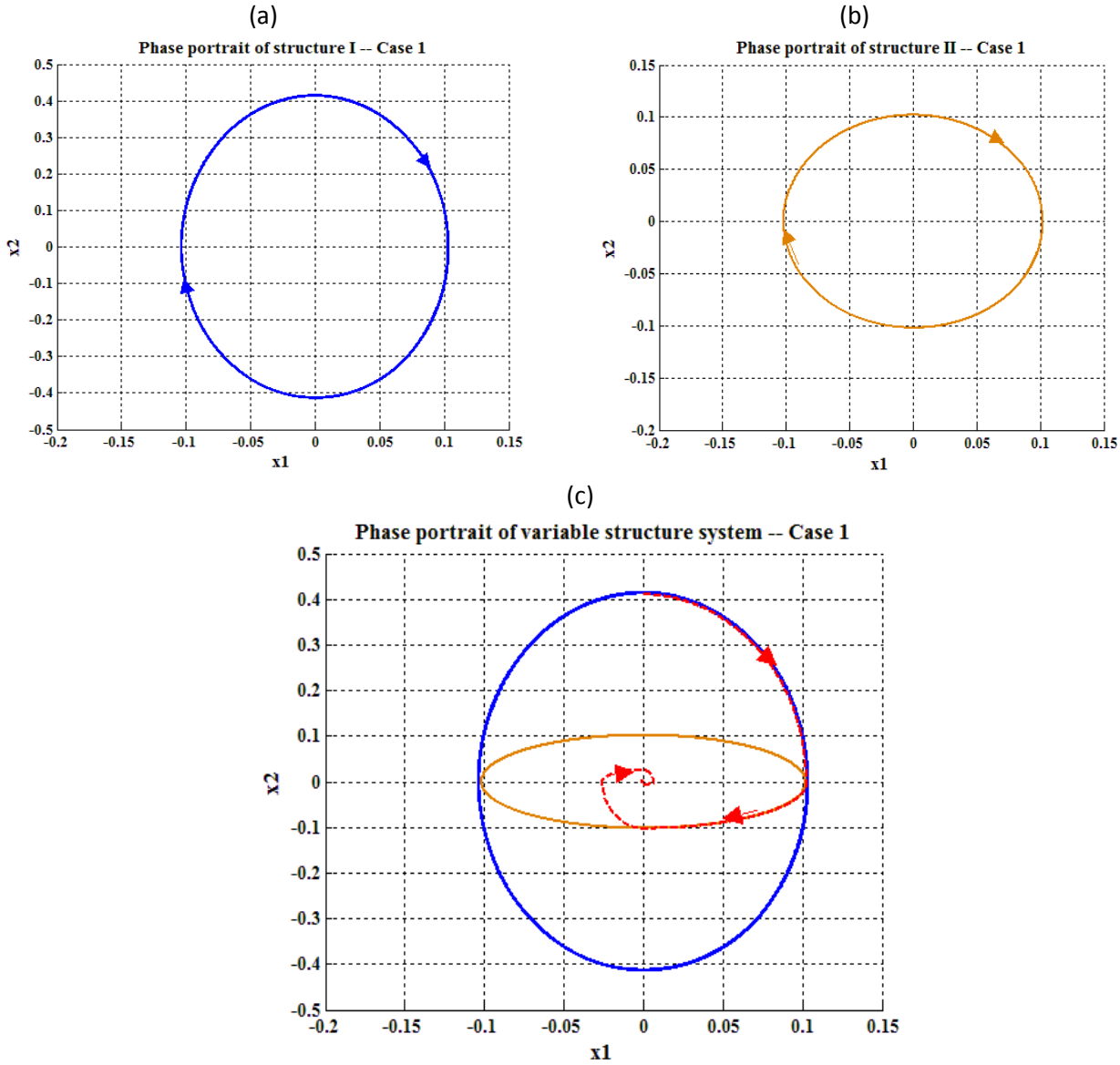

Figure 4.1: Phase portrait of VSS derived from two oscillatory structures. Fig. 4.1(a) and 4.1(b) represents phase portrait of two individual structures. Fig. 4.1(c) shows the phase portrait of resulting VSS.

The structures exhibit oscillatory kind of behavior and therefore it cannot be used in control system design. By applying VSC with a switching logic given by

$$\phi = \begin{cases} \alpha_1 & x_1 x_2 > 0 \\ \alpha_2 & x_1 x_2 \le 0 \end{cases}$$

We achieve asymptotically stable response as shown in Fig. 4.1 (c). The term ϕ is called the feedback gain. Therefore the resulting Variable Structure System will possess a new property which is not present in any of its sub structures. Let us consider another example of a second order system given by

$\dot{x}_2 = \xi x_2 - \alpha x_1$ and $\dot{x}_2 = \xi x_2 + \alpha x_1$. Let $\xi > 0$; $\alpha > 0$

The equilibrium point is represented by origin which is also a saddle point. From the phase portraits shown in the Fig. 4.2 (a) and Fig. 4.2 (b), we conclude that the saddle point is unstable and therefore both the structures are unstable.

Let the chosen switching surface be $s = cx_1 + x_2$ with $c = \lambda$ is the eigenvalue of the system.

We apply VSC with a switching logic given by

$$\phi = \begin{cases} \alpha & x_1 s > 0 \\ -\alpha & x_1 s \le 0 \end{cases}$$

The resulting Variable Structure System is asymptotically stable given by the phase portrait in Fig. 4.2(c).

We note that the convergence of all state trajectories along one stable eigenvector given by $\phi = -\alpha$.

Therefore by employing Variable Structure Control, some useful properties of individual structures are combined resulting in a new property which is not inherent in any of the sub-structures. In general, this new control technique offers significant advantages over the earlier methods and therefore it is suitable for practical nonlinear and MIMO systems.

In addition to the above mentioned advantages, the possibility to obtain a trajectory independent of the trajectories of sub structures is one of the fundamental aspects of variable structure control system. The motion of the special trajectory describes a new motion here after referred to as sliding mode. So a sliding mode consists of a motion of a trajectory which is not a trajectory of any of its sub structures. Therefore Sliding Mode Control is referred to as a special class of variable structure control.

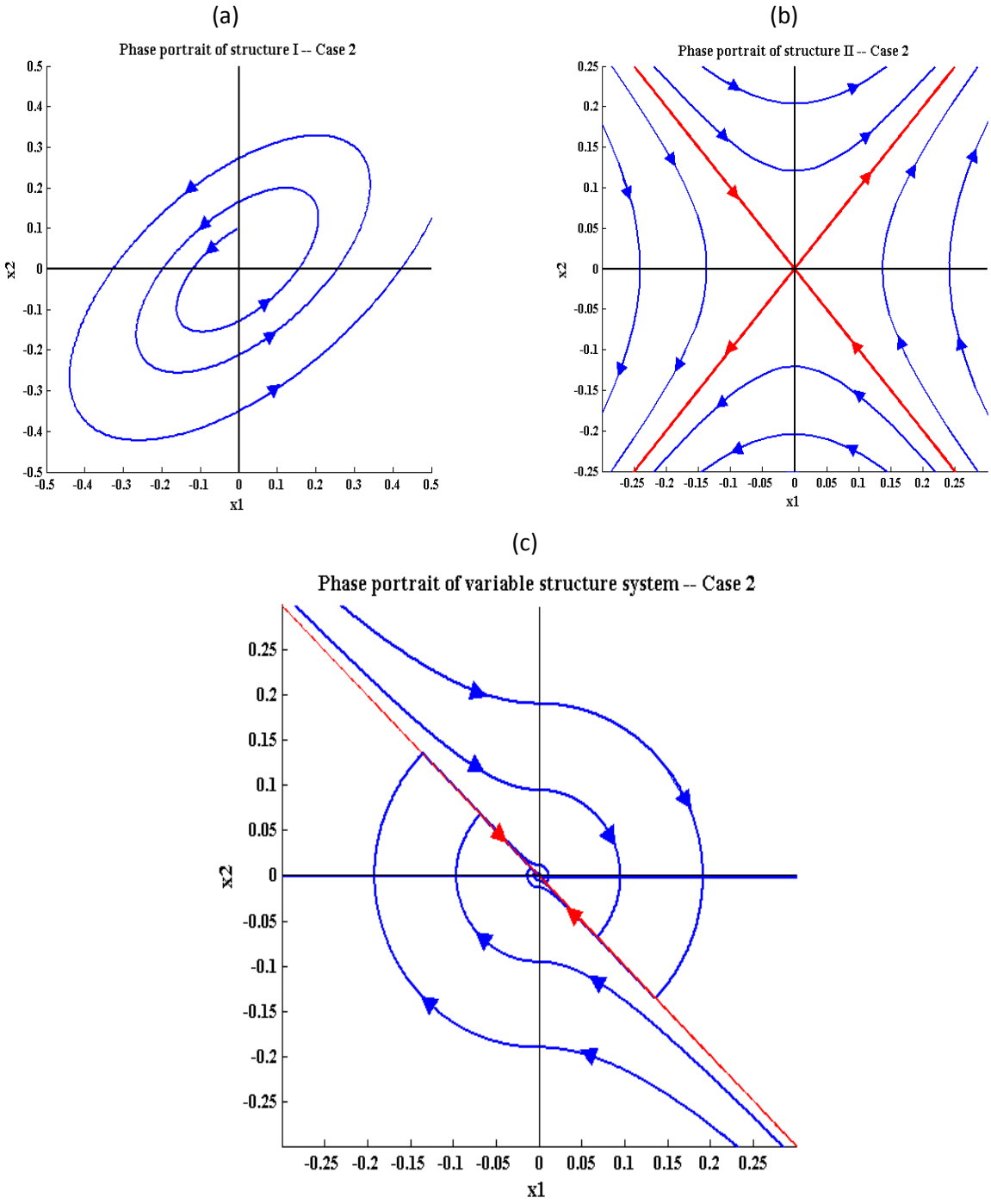

Figure 4.2: Phase portrait of VSS derived from two unstable structures. Fig. 4.2(a) and 4.2(b) represents phase portrait of two individual structures. Fig. 4.2(c) shows the phase portrait of resulting VSS

4.2 Sliding Mode Control (SMC)

Sliding Mode Control consists of an exclusive feature called the 'sliding mode'. To illustrate the sliding mode behavior let us reconsider the VSS with individual structures given by
$\dot{x}_2 = \xi x_2 - \alpha x_1$ and $\dot{x}_2 = \xi x_2 + \alpha x_1$ with $\xi > 0$; $\alpha > 0$.

Let the switching surface be

$$s = c^* x_1 + x_2 \qquad 4.3$$

with $0 < c^* < \lambda$. The phase portrait of the resulting system is shown in Fig. 4.3.

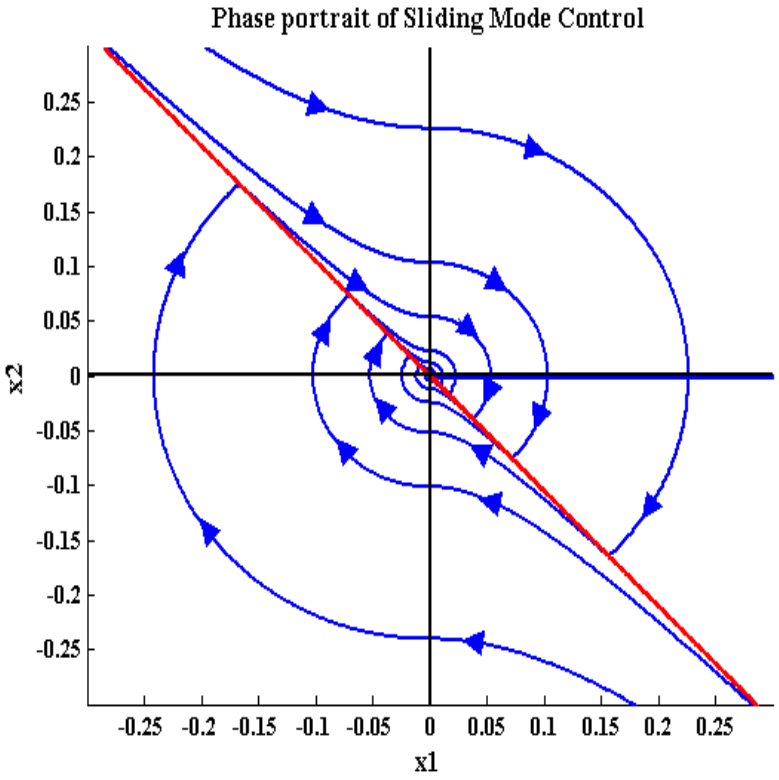

Figure 4.3: Phase portrait of Sliding Mode System

From the Fig. 4.3, it is observed that all the state trajectories are directed towards the switching surface defined by $s = c^* x_1 + x_2 = 0$ and stay on this surface for all time after reaching the surface. These phase trajectories reach the designed switching surface irrespective of the initial condition of the system which can be shown in Fig. 4.4. Therefore, the phase trajectory consists of two representative modes given by *reaching mode* and *sliding mode*. The detailed explanation of these modes will be discussed in the later part of this chapter. An essential condition for sliding mode to occur is that the state trajectories will reach the sliding surface and will continue to remain all the time. This sliding surface is also referred to as sliding manifold in some literature [7, 12]. The magnified portion shown in Fig. 4.4 highlights the chattering behavior and more will be discussed in the later part of this chapter.

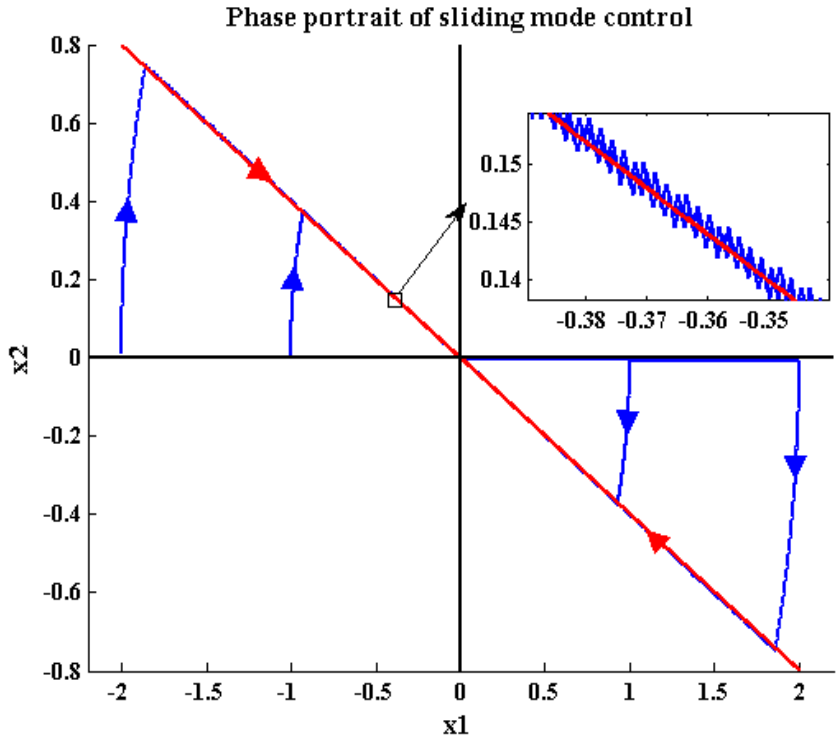

Figure 4.4: Phase portrait of Sliding Mode System with an initial condition of x-axis

In [2], another methodology to obtain the sliding mode was presented. The occurrence of sliding mode is subject to input switching which was a function of one state of the system. This consideration was different to an earlier case given in (4.3) where the sliding mode behavior was dependent on the linear combination of two states.

Let us consider a general second order system as

$$\dot{x}_1 = x_2 \qquad 4.4$$
$$\dot{x}_2 = -\alpha_2 sign(x_1)$$

where

$\alpha_2 \rightarrow$ A positive constant

This system consists of one switching instant. We shall define another second order system consisting of two switching instants given by

$$\dot{x}_1 = x_2 - \alpha_1 sign(x_1) \qquad 4.5$$
$$\dot{x}_2 = -\alpha_2 sign(x_1)$$

where

$\alpha_1 \rightarrow$ A positive constant

Let us carry out a simulation to find the phase portrait of the set of equations defined in (4.4) and (4.5).

From Fig. 4.5, we observe that in the latter case, there is an occurrence of sliding mode where the phase trajectory reaches the equilibrium point in finite amount of time. This behavior is unlike the oscillatory behavior (shown in blue legend) exhibited by set of equations given in (4.4). We can conclude that there is no sliding mode when (4.4) is realized.

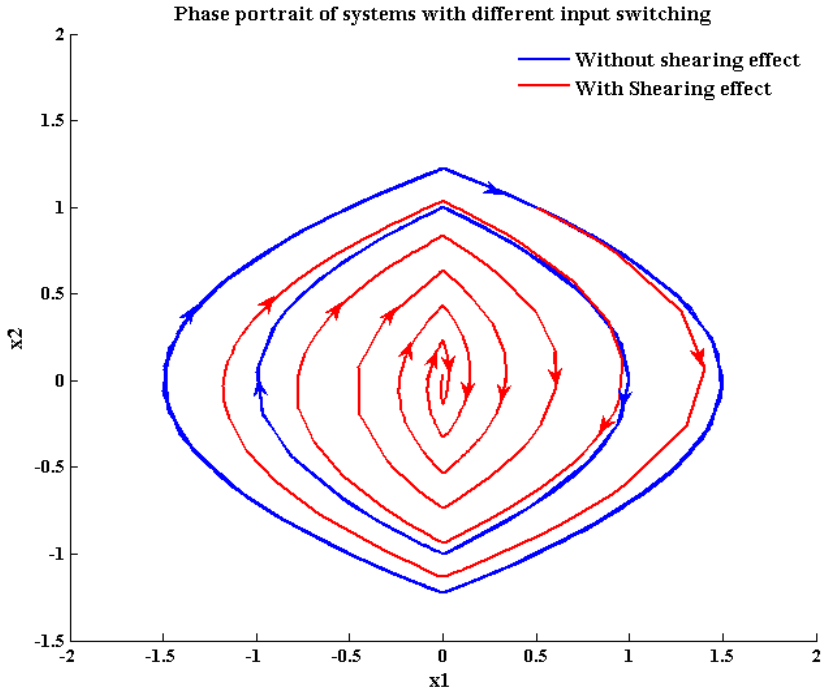

Figure 4.5: Phase portrait of a second order system with and without shearing effect.

A more simpler way to obtain the phase trajectories of a system defined in (4.5) is by shifting the right half plane of the phase trajectories of a system defined in (4.4) by an amount α_1 and left half plane of the phase trajectories by an amount $-\alpha_1$. This behavior is termed as the 'Shearing effect' [2]. Therefore due to shearing effect, a sliding mode exists in the region defined by

$$\left|x_2\right| \le \alpha_1 \tag{4.6}$$

Therefore we define a region surrounding the equilibrium point where the sliding mode behavior exists. The region defined in (4.6) is termed as 'sliding patch' [2]. This patch gives rise to boundary layered approach which results in minimal chattering. The methodologies adopted for chattering minimization is presented in section 4.2.5. Nevertheless the equations governing in the sliding patch are defined from Flippov's concept [16] and elaborate discussion on Flippov's method is presented in section 4.2.4.

4.2.1 Properties of Sliding Mode

The sliding mode behavior assures finite reaching time to a defined sliding surface. As the equilibrium state is the origin, the transient response is given by the behavior after the state trajectory reaches the sliding surface. The distinguishing feature of sliding mode is intuitively known by considering the sliding surface. The sliding surface is completely independent of model and disturbance parameters and only dependent on the parameters defining the switching surface. Therefore, robustness against parametric uncertainties, bounded external disturbances and noise effects is achieved. The sliding surface defined in (4.3) is of lower order than the original system defined by (4.1) and hence a reduced order system can be achieved in sliding mode control. This is certainly useful for a large order practical system.

Consider general system represented by (4.1). The switching is carried out using the logic

$$u = \begin{cases} u^+ & s > 0 \\ u^- & s < 0 \end{cases}$$

such that the state trajectory reaches the switching surface s in finite time.
The controllable canonical form for the given system is represented as

$$\begin{aligned} \dot{x}_1 &= x_2 \ ; \\ &\vdots \\ \dot{x}_{n-1} &= x_n \\ \dot{x}_n &= \sum_{i-1}^{n} -a_i x_i + Bu \end{aligned} \tag{4.7}$$

The switching surface where discontinuities are present is designed as

$$s = c_1 x_1 + c_2 x_2 + ...x_n = 0 \qquad 4.8$$

where

$c_1, c_2, ...$ are the design constants.

If the state trajectories are directed towards the above designed switching surface, then we can say that sliding mode exists. To obtain the sliding mode equation, we solve the (4.8) for x_n and substitute back in (4.7).

$$\dot{x}_i = x_{i+1} \; ; \quad i = 1, 2, ... \, n-2$$

$$\dot{x}_{n-1} = \sum_{i=1}^{n-1} -c_i x_i$$

On analysis of the above set of equations, some important properties can be listed.

(i) The sliding mode equation is of reduced order in comparison with the general system.

(ii) The sliding mode behavior is independent of model parameters and bounded disturbance present in the system. This is a distinguishing feature called the 'invariance' property of sliding mode control. The external disturbances have to satisfy matching conditions so that invariant property is valid. This is explained by considering a general system

$$\dot{x} = A(x) + \Delta A(x) + B(x)u + f(x,t)$$

where ΔA and $f(x,t)$ are the modeling error and external disturbance respectively.

If there is a perturbation in input matrix, then

$$\dot{x} = A(x,t) + \Delta A(x,k,t) + B(x)u + \Delta B(x,k,t)u + f(x,k,t)$$

where k is an uncertain parameter. From the definition of invariance property, it has been shown that [7]

$$\Delta A(x,k,t) = B(x,t)\Delta\tilde{A}(x,k,t)$$

$$\Delta B(x,k,t) = B(x,t)\Delta\tilde{B}(x,k,t)$$

$$f(x,k,t) = B(x,t)\Delta\tilde{f}(x,k,t)$$

for certain $\Delta\tilde{A}$, $\Delta\tilde{B}$ and $\Delta\tilde{f}$ .From Fig. 4.3 and 4.4, we can observe that there is a finite time which the phase trajectory traverses to reach the sliding surface. The phase trajectory can be divided into two modes based on the reaching the sliding surface as *Reaching mode* and *Sliding mode*. Reaching mode can be defined as the mode where the phase trajectory moves from any point defined by the initial condition of the given system to the sliding surface. The time taken by the reaching mode is termed as the reaching time which is finite in sliding mode. In this mode, the state trajectory depends on the model parameters. The second part of the phase trajectory is the mode where the state trajectory moves towards the equilibrium point after reaching the sliding surface. This mode is called the Sliding Mode where the system dynamics

are independent on model parameters and bounded disturbances. Fig. 4.6 explains the two modes where x_0 is the initial condition with the origin as the equilibrium point.

The discontinuous control added results in chattering behavior in case of sliding mode. The effects and remedial measures for chattering in sliding mode are elaborately covered in the sections to follow.

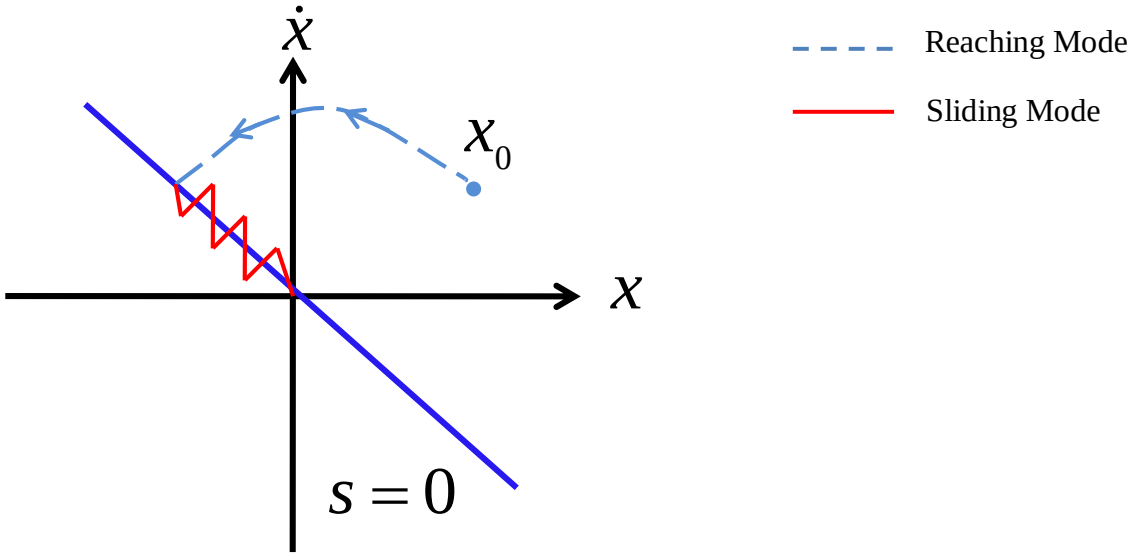

Figure 4.6: Schematic diagram of sliding mode behavior

4.2.2 Realization of Reaching Condition

In Sliding Mode Control design, the system should have a finite reaching time with respect to any initial condition. This can be specified by using any of the methods described below

(a) Direct Switching

A local reaching condition with finite reaching time was proposed in [6] by Utkin. According to this method,

$$\lim_{s\to 0^+}\dot{s}<0 \;\;;\;\; \lim_{s\to 0^-}\dot{s}>0 \qquad 4.9$$

According to [1, 6], the above pair of inequality is the sufficient condition for a sliding mode to exist. But to realize in practice, we require solving $2m$ conditional inequalities even though fixed order switching scheme is adopted.

(b) Lyapunov Function

In this method, a positive definite differentiable function V is chosen such that

$$\dot{V}=\frac{\partial V}{\partial t}+\frac{\partial V}{\partial x}f(t,x)\le 0 \qquad 4.10$$

Then the origin is said to be stable.

For asymptotic stability, $\dot{V} \le 0$ for $x \ne 0$

In our case, we choose the Lyapunov function as $V(x,t) = s^T s$. The conditions to obtain asymptotic stability are

$$(a)\ \dot{V} \le 0 \text{ for } \sigma \ne 0 \qquad 4.11$$

$$(b) \lim_{|\sigma| \to \infty} V = \infty$$

The advantage of using Lyapunov function approach for determining stability is that there is no requirement of explicit solution for a given differential equation. If we choose a positive definite differentiable function V with a decreasing total time derivative along the phase trajectories, then the equilibrium point is said to be stable. This method is rigorously used in the sliding mode examples to calculate the gain parameter.

(c) Reaching Law

The switching dynamics is specified by explicitly defining the switching function. Let the switching function be defined as

$$\dot{s} = -A\,sign(s) - Bf(s) \qquad 4.12$$

where A and B are positive diagonal matrices. (4.12) is called the reaching law where the scalar function f_i satisfies

$$s_i f_i > 0 \quad ; \quad s_i \ne 0,\ i = 1,2,....m$$

where m is the number of inputs.

Several variants of reaching law can be derived from (4.12)

(i) Constant rate reaching law:

$$\dot{s} = -A\,sign(s)$$

(ii) Constant plus proportional rate reaching law:

$$\dot{s} = -A\,sign(s) - Bs$$

(iii) Power rate reaching law:

$$\dot{s}_i = -c_i |s_i|^{\alpha} \operatorname{sgn}(s_i) \text{ where } 0 < \alpha < 1 \ ; \ i = 1 \text{ to } m$$

This method minimizes the chattering [Hung] but the elements of A and B have to be calculated.

4.2.3 Switching Schemes

Let us consider n^{th} order system with m inputs. As described in [7], there can be 2^{m-1} switching surfaces possible. Consequently there will be equal number of sliding modes possible because one differential equation corresponds to one switching surface. There can be a number of ways in which the state trajectory traverses through these sliding modes which shall be referred to as switching schemes.

The various switching schemes available are -

(a) *Fixed order Switching Scheme*: The state traversal corresponds to a pre-assigned path of the sliding mode. In other words, there is progressive movement of sliding modes from lower to higher dimension. For a general system defined earlier, the sliding mode moves from $n-1$ dimension to $n-m$ dimension. We can conclude that this approach is hierarchical with large requirement of control gain and poor sliding mode response.

(b) *Free-Order Switching Scheme:* Unlike the previous scheme, the sliding mode follows a natural path with first reach first switch scheme. As the path followed by the sliding mode depends on the reaching mode, the switching instants are dependent on the initial condition. Eventually, we achieve better switching scheme when compared to the earlier scheme. In practice, we use this scheme if the system has less number of inputs.

(c) *Eventual Sliding Mode Switching Scheme:* The primary goal of this switching scheme is to drive the initial state to the final state defined by the eventual sliding surface with a dimension of (n-m). This scheme does not guarantee a good transient response but the application of control is simple.

(d) *Decentralized Switching Scheme:* In this scheme, the entire system is subdivided into m single input coupled subsystems with scalar gain associated to each sliding mode. This is primarily helpful for large scale systems with large number of inputs.

4.2.4 Solution and Uniqueness of Sliding Mode equations

In general the design procedure for Sliding Mode Control can be summarized as

(1) Design the switching surface with appropriate values of c_i

(2) Addition of discontinuous control such that the state trajectories are directed towards the switching surface for every point on the surface.

(3) Design a control signal to so that the state trajectory reaches the designed switching surface in finite amount of time.

The above procedure of representing the general system in controllable canonical form is valid for linear systems. A set of differential equations necessitates that the right hand side functions satisfy Lipschitz condition $\left\| f\left(x_1\right) - f\left(x_2\right)\right\| < L\left\|x_1 - x_2\right\|$; $L > 0$; $\forall x_1, x_2$. This condition guarantees that the right hand side function does not vary more than some linear function defined by Lipschitz condition.

The sliding mode equations are generally nonlinear differential equations with discontinuous right hand sides which do not satisfy Lipschitz condition. Therefore the existence and uniqueness of sliding mode equations cannot be realized from conventional methods of continuous

differential equations. But the VSC presumes that the model behaves in a unique way during the sliding mode. The mathematical approaches to solve the differential equations with discontinuous right hand sides are grouped under regularization methods. The popular regularization methods are explained here.

Initially, Flippov suggested a mathematical theory for sliding mode equations which accounts for discontinuous terms. By applying the control law given in (4.14) for a general system given in (4.13), we get

$$\dot{x}(t) = f(t, x, u) \tag{4.13}$$

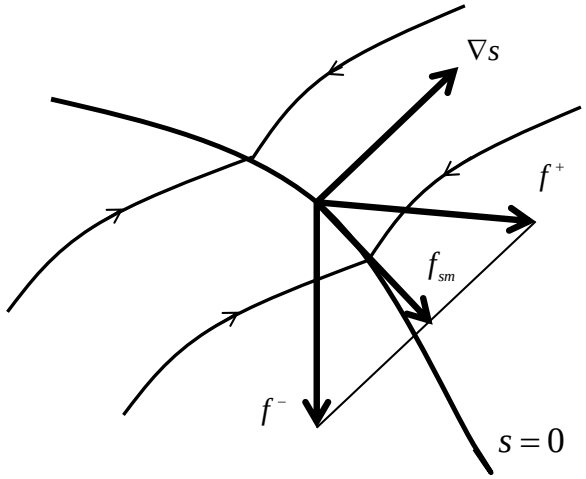

Figure 4.7: Schematic diagram of equivalent control

$$f = \begin{cases} f^{+} & s > 0 \\ f^{-} & s < 0 \end{cases} \tag{4.14}$$

where f^{+} and f^{-} are the velocity vectors subject to control u^{+} and u^{-} respectively.

The system dynamics at $s = 0$ can be defined as the average of the two structures given by

$$\dot{x}(t) = f_0(x) = \mu f_0^{+} + (1-\mu) f_0^{-} \tag{4.15}$$

where

$$0 \le \mu \le 1$$

$$f_0^{+} = \lim_{s \to 0} f^{+}(x,u) \;\; ; \;\; f_0^{-} = \lim_{s \to 0} f^{-}(x,u)$$

The sliding mode is defined along the intersection of the line joining the ends of the velocity vector with the tangential plane as shown in Fig. (4.7).

A generalized approach for multi-input systems is the 'Equivalent Control' approach which considers continuous control unlike Flippov's approach. In other words, Equivalent control approach shall be used to find the sliding mode equations under ideal conditions. In this approach, the initial condition of the system at $t = t_0$ is in sliding manifold $s = 0$ with sliding

mode $\forall t > t_0$. The necessary condition is that the time derivative of the vector $s(x)$ along the system trajectory is equal to zero. The resulting control signal is termed as the equivalent control.

$$s = 0 \; ; \; \dot{s} = 0 \tag{4.16}$$

On solving for a general equation, we get

$$\left[\frac{\partial s}{\partial x}\right]\dot{x} = 0 \tag{4.17}$$

$$\left[\frac{\partial s}{\partial x}\right]\left[f(t,x) + B(t,x)u_{eq} \right] = 0$$

where

$u_{eq} \rightarrow$ Equivalent control signal

For discontinuous systems, we employ *auxiliary* continuous equivalent control approach. The control signal used in the sliding mode shall consist of both low and high frequency terms. The sliding mode behavior primarily depends on the low or average frequency component. Therefore, the equivalent control excluding the high frequency component is nearly equal to the original control excluding the high frequency terms. It is because of this reason that low pass filters are used in the sliding mode design. The application of first order or second order low pass filters in sliding mode design shall be illustrated in Chapter 6.

4.2.5 Chattering

Chattering can be defined as the finite frequency finite amplitude motion in the sliding mode. From Fig 8, we can observe that the motion is discontinuous in sliding mode. The effect of chattering is disastrous when the sliding mode control is realized in actual practice.

The primary causes of chattering are the imperfections or non-idealities present in the actual control system and discrete time nature of the simulation carried out. In the switching logic designed earlier for sliding mode control we had assumed that the switching takes place infinitely or in other words the switching delay was considered to be zero. But in practical systems, it is impossible to switch infinitely fast between two states. This is because of finite time delays present in the actual system. The possible causes may be time delay in control calculation, hysteresis and other delay causing parameters. These factors cause high frequency oscillatory behavior about the equilibrium point which is commonly termed as chattering.

When the switching imperfections described above tend to zero or if the switching frequency is infinite then we describe the sliding mode as *Ideal Sliding Mode*. During ideal sliding mode the distinguishing feature of robustness against model uncertainties and bounded disturbances is achieved with steady state error equal to zero. Conversely if non-idealities are present in the system then *Real Sliding Mode* occurs. In real sliding mode, we consider small vicinity around

the sliding surface where the sliding mode exists. In general real sliding family may be defined as [18]

Definition: *Let* $\left(t, x\left(t,\varepsilon\right)\right)$ *be a family of trajectories, indexed by* $\varepsilon \in \Re^{\mu}$, *with common initial condition* $\left(t_0, x\left(t_0\right)\right)$, *and let* $t \geq t_0$. *Assume that there exists* $t_1 \geq t_0$ *such that on every segment* $\left[t', t''\right]$, *where* $t' \geq t_1$ *the function* $\sigma\left(t, x\left(t,\varepsilon\right)\right)$ *tends uniformly to zero with* ε *tending to zero. In that case we call such a family a real sliding family on the constraint* $s = 0$. *We call the motion on the interval* $\left[t_0, t_1\right]$ *a transient process, and the motion on the interval* $\left[t_1, \infty\right)$ *a steady state process.*

An important property of real sliding mode is that it does not increase the sliding order of the system.

A serious disadvantage of chattering is that the finite amplitude and frequency can induce unmodeled dynamics in the system and therefore the design control algorithm fails. Hence, significant research for removing or minimizing the chattering behavior is discussed in [26]. In this section we consider a few approaches

(a) *Boundary Layer approach*

The control law in case of ideal relay control approach is defined as

$$u\left(s\right) = \operatorname{sgn}\left(s\right) = \begin{cases} +1 & s > 0 \\ -1 & s < 0 \end{cases} \tag{4.18}$$

From (4.18), we can infer that there is a discontinuity at $s = 0$. The control is ideal because the switching is instant at $s = 0$ which is impossible to achieve for a practical system. Therefore the relay control introduces chattering in the sliding mode. To minimize the chattering, we introduce boundary layer around the switching surface which approximates the switching process. In other words, we approximate a discontinuity by a continuous smooth function and thereby minimize the chattering effect. In actual practice we employ an ideal saturation function defined in (4.19)

$$u\left(s\right) = \operatorname{sat}\left(s\right) = \begin{cases} s/|s| & s > \varepsilon \\ s/\varepsilon & s \leq \varepsilon \end{cases} \tag{4.19}$$

Another example of a smooth function is a sigmoid function given in (4.20)

$$\operatorname{sigm}\left(s\right) = \frac{s}{|s| + \varepsilon} \tag{4.20}$$

where

ε is a small positive scalar.

There is an inherent loss of robustness due to implementation of boundary layer approach. The robustness of the system is a function of boundary layer width ε.

Let us illustrate this approach by considering an example. Consider a dynamic system given by

$$\dot{x}_1 = x_2 \qquad 4.21$$

$$\dot{x}_2 = u + f\left(x_1, x_2, t\right)$$

where

$u \rightarrow$ Control signal

$f\left(x_1, x_2, t\right) \rightarrow$ Bounded disturbance

Let the bounded disturbance be $f\left(x_1, x_2, t\right) = \sin\left(2t\right)$. The sliding surface is designed as $s = x_2 + cx_1 \;\; ; \;\; c > 0$. To achieve asymptotic convergence, we employ Lyapunov's stability approach discussed earlier. The control input required for asymptotic convergence is given by

$$u = -cx_2 + \delta_1 sign\left(\sigma\right) \qquad 4.22$$

where

$\delta_1 \rightarrow$ Control gain

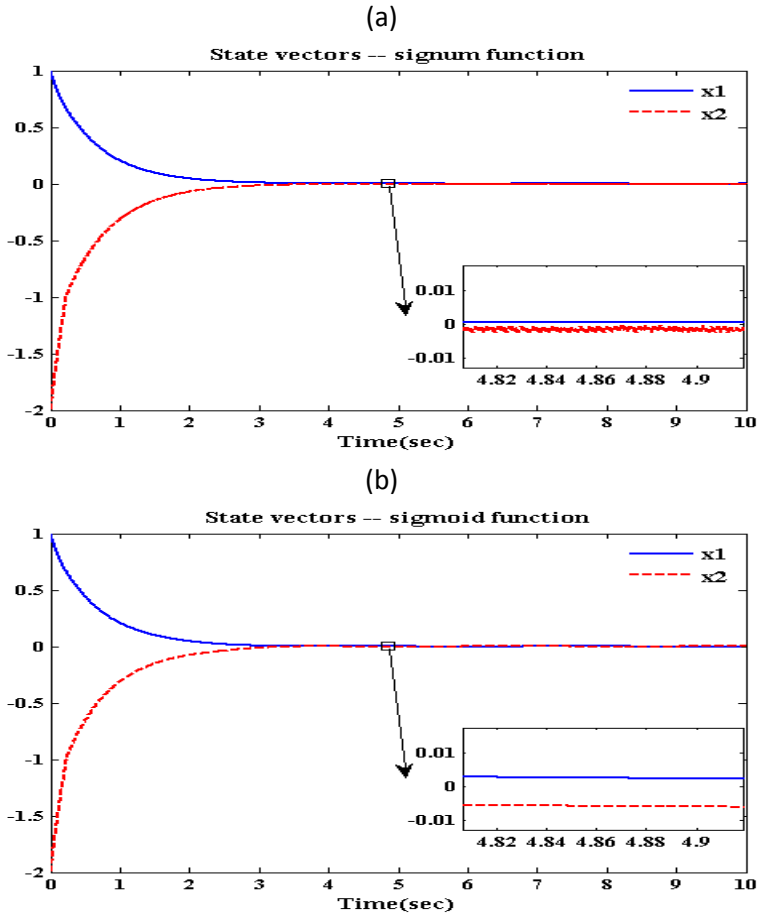

Figure 4.8: An example illustrating SMC. Fig. 4.8(a) represents state variation to an equilibrium value using signum function. Fig. 4.8(b) represents state variation to an equilibrium value using sigmoid function

The state variation of the given system is given in Fig. 4.8. A control signal defined in (4.22) is initially applied. The corresponding state variation is shown in Fig. 4.8(a). By replacing the signum function in (4.22) by a smooth sigmoid function defined in (4.20), the resulting state response for the same dynamic system is shown in Fig. 4.8(b)

We can clearly observe that presence of chattering in Fig. 4.8(a) by using signum function, whereas the chattering is minimized in Fig 4.8(b) by using sigmoid function and thus illustrating boundary layered approach. On comparison of both the results shown in Fig. 4.8, we infer that there is loss of robustness in terms of delay in asymptotic convergence due to application of smooth continuous control.

(b) Higher Order Sliding Mode (HOSM)

The usage of Higher Order Sliding Modes to minimize chattering was first proposed in [18]. This further requires that higher order derivatives of the sliding surface be available which is not possible in practical control system. Therefore it necessitates the usage of robust exact differentiator to estimate the derivatives of the sliding variable. Some of the popular second order sliding algorithms like Twisting algorithm, Super Twisting algorithm are discussed in Chapter 7.

(c) Integration time

One of the possible reasons for chattering behavior in sliding mode is the discrete time nature of the simulation. By decreasing the integration step time, we can approximate correctly to a continuous function. Hence we achieve minimal chattering. This method requires that the control system should have low sampling interval which further affect the economic prospects of the plant.

Chapter 5

Observers

Modern Control theory analysis is based on state variable approach. The advantages of state variable approach over the traditional methods are detailed in [5].
Again let us consider a general system given in (4.1). We shall rewrite the equation for convenience.

$$\dot{x} = Ax + Bu \tag{5.1}$$

where the terms are described in section 4.1.

5.1 Introduction to Observer

The requirement of an entire state vector for a linear state feedback controller was a limitation to obtain the output. The conventional techniques like quadrature minimization, eigenvalues placement could not calculate the output vector if some of the inputs were not available. In most of the practical complex control situations, there are no sensors to actually measure the desired parameters and hence the entire state vector is unavailable. The placement of sensors in the practical system is dependent on space availability, economic consideration, mechanical and electrical characteristics, non-availability of specific sensors and many more. Therefore there is a need to either develop a new approach which considers non availability of state vector or approximate the state vector and find the input vector. The latter method is preferred over the other [14]. In [34], a new class of systems are developed where by designing a static output feedback controller. Output feedback controller is applicable to limited number of systems and its discussion is out of scope of this thesis. Hence we have to estimate the state vector and the device which reconstructs the unknown/unavailable state vector is called an 'Observer'. The output of the plant is sensed by the sensor. Due to the reasons mentioned earlier regarding the placement of sensors, we are able to measure only some of the parameters out of an entire set.

5.2 Luenberger Observer

Let us consider a simple observer with the observer model similar to the system model. Let the observer model be represented as

$$\dot{\hat{x}} = A\hat{x} + Bu \tag{5.2}$$

where $\hat{x}$ is the estimate of x.

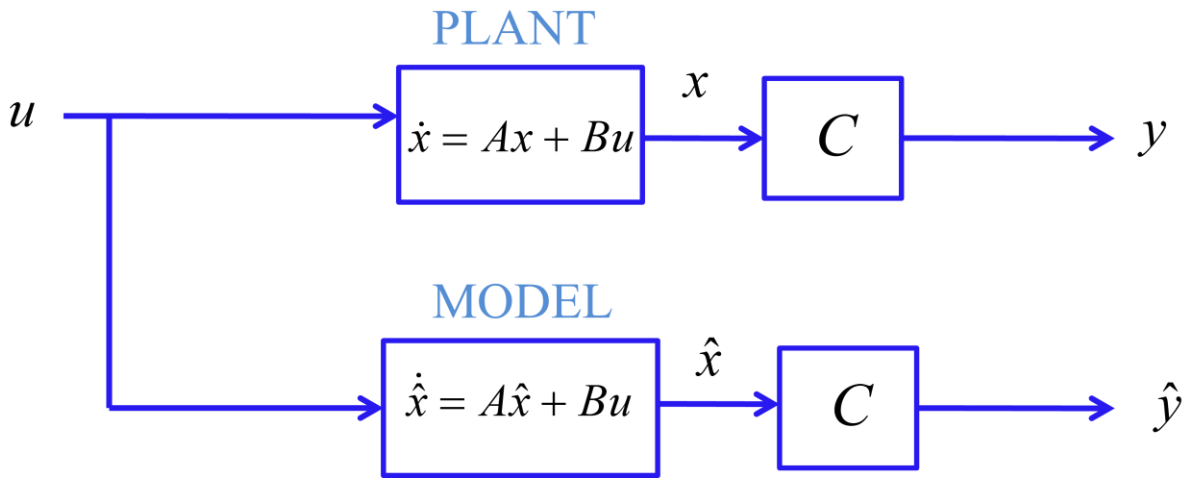

Figure 5.1: Schematic diagram of an open loop estimator

From the Fig. 5.1 it is simple enough to conclude that we obtain a satisfactory response if the initial conditions $x(0)$ and $\hat{x}(0)$ are matched. This estimator is popularly called as 'Open Loop Estimator'.

5.2.1 Design of Full State Luenberger Observer

For an open loop estimator if the initial conditions are not equal, then there is continuous steady state error and the estimator will tend to the actual model after a long period of time. If disturbances present, then the estimator will diverge from the actual model. To solve the above set of problems, we employ a simple feedback path with the difference between measured and model value. This closed loop observer was first proposed by Luenberger [5] and is popularly

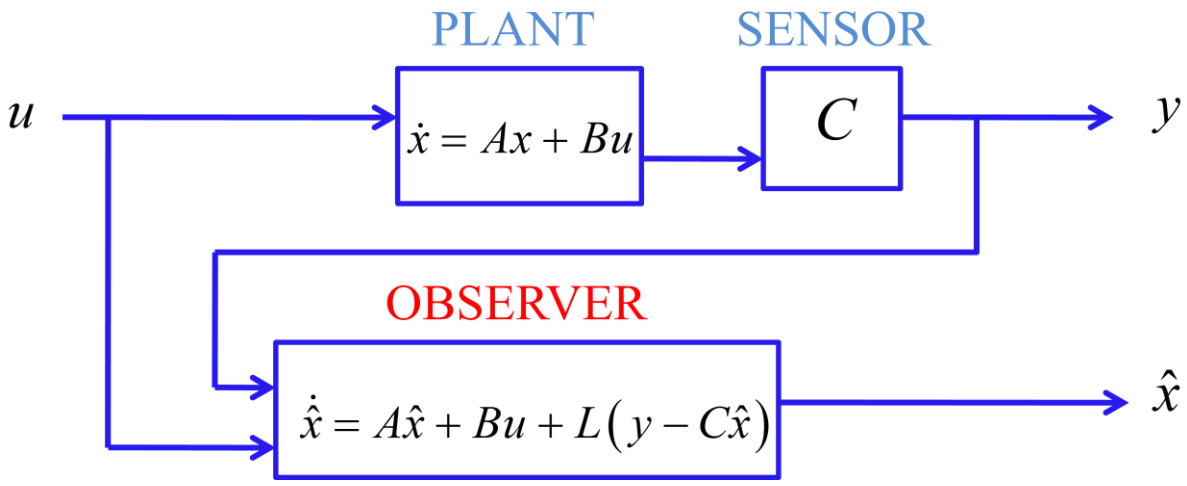

Figure 5.2: Schematic diagram of a Luenberger Observer

From the Fig. 5.2, we can infer that an observer uses both system input and the known output from the system. The designed observer has to estimate all the states of the original system. In other words we need to make the error between the measured value and the estimated value tends to zero in a finite time. It is evident from Fig. 5.3 that the output equation is $y = Cx$. Let the output y be *l* dimensional. For a linear time invariant system, C is a constant. We assume that the pair (A, C) is observable and (A, B) to be controllable. To design a Luenberger observer, we consider the observer model with an additional term similar to a system model. The additional term that is considered is the error between the measured and estimated values multiplied by an input matrix $L \in \Re^{n \times l}$. The estimated state vector is given by

$$\dot{\hat{x}} = A\hat{x} + Bu + L(y - C\hat{x}) \tag{5.3}$$

The error with respect to measurable parameter is given by $\bar{x} = x - \hat{x}$.

Now the entire observer can be represented by a general expression given in (5.3). The corresponding expression is represented in Fig. 5.3.

On subtracting (5.2) from (5.1), we obtain the motion equation given by

$$\dot{\bar{x}} = (A - LC)\bar{x} \tag{5.4}$$

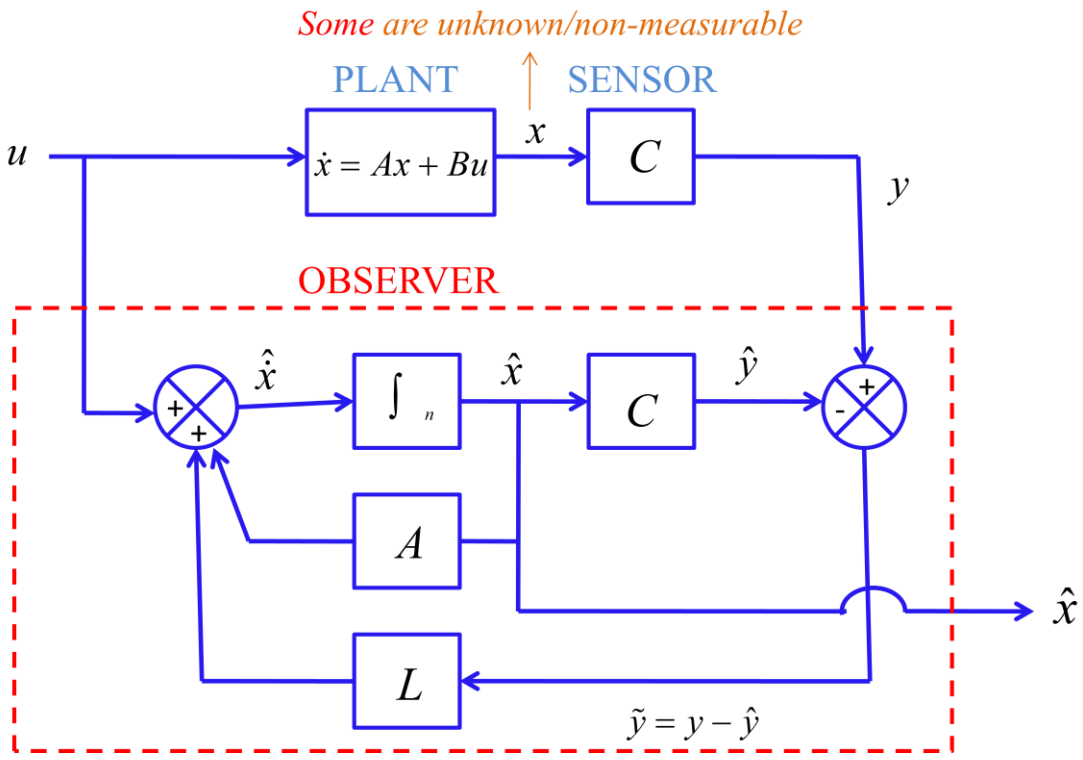

Figure 5.3: Detailed observer structure of a full state Luenberger observer

The characteristic equation for the error is given by $\left|s\mathrm{I}-\left(A-LC\right)\right|=0$

If we choose the parameters of L such that $\left(A-LC\right)$ has stable roots, then $\hat{x}$ will decay to x in a finite time which is independent of initial condition of the system. The dynamics of the error can be varied by the designer unlike the open loop observer. The system matrix and the input matrix of the observer and the plant have to be equal. If there is a parametric variation, then the (5.4) is not valid. However we can choose L such that the system error is below the specified limit. In general, Luenberger observer described earlier cannot handle parametric uncertainties and bounded disturbances present in the system. In addition, Luenberger observer is valid only for linear systems.

The important step in the design of Luenberger observer is the calculation of observer input matrix L . This calculation is similar to the eigenvalues placement technique employed in feedback control design. We do not describe this method because of its lengthy mathematical procedure in case of practical large order systems. Nevertheless we describe a companion form realization which is the most popular method. Let us consider a general system represented by the transfer function

$$\frac{Y\left(s\right)}{U\left(s\right)}=\frac{b_1s^{n-1}+b_2s^{n-2}+.....+b_n}{s^n+a_1s^{n-1}+.....+a_n} \qquad 5.5$$

The above system can be represented in companion form as

$$\dot{x}=Ax+Bu \qquad 5.6$$

$$y=Cx$$

where

$$A=\begin{bmatrix}0 & 0 & ... & 0 & -a_n\\ 1 & 0 & ... & 0 & -a_{n-1}\\ 0 & 1 & ... & 0 & -a_{n-2}\\ \vdots & \vdots & & \vdots & \vdots\\ 0 & 0 & ... & 1 & -a_1\end{bmatrix};\ B=\begin{bmatrix}b_n\\ b_{n-1}\\ b_{n-2}\\ \vdots\\ b_1\end{bmatrix};\ C=\begin{bmatrix}0 & 0 & ... & 0 & 1\end{bmatrix}$$

We can conclude that the pair $\left(A,C\right)$ is completely observable and therefore this companion form is referred to as *observable* canonical form. The evaluation of observer error matrix can be calculated easily by inspection. The observer error matrix is given by

$$(A-LC)=\begin{bmatrix} 0 & 0 & ... & 0 & -a_n - L_1 \\ 1 & 0 & ... & 0 & -a_{n-1} - L_2 \\ 0 & 1 & ... & 0 & -a_{n-2} - L_3 \\ \vdots & \vdots & & \vdots & \vdots \\ 0 & 0 & ... & 1 & -a_1 - L_n \end{bmatrix}$$

with the characteristic equation given by

$$s^n + (a_1 + L_n)s^{n-1} + ... + (a_{n-2} + L_3)s^2 + (a_{n-1} + L_2)s + (a_n + L_1) = 0 \quad 5.7$$

By solving the above equation, we can obtain the observer gains and hence the observer input matrix.

5.2.2 Design of Reduced State Luenberger Observer

In the previous section, we elaborately covered the full state observer. An estimation of all the states of the system was carried out. In practice, there are some states available from direct measurement. In case of noisy measurement channel, robust noise filtering techniques can be employed. Therefore the focus can be shifted to the states which are not available from measuring devices. The cost of designing a full state observer can be minimized by designing a state observer estimating less number of states. This observer is prominently called a reduced state observer.

The design of a reduced state observer is illustrated in this section. Let us assume that only one state is available from measurement. The state vector is partitioned into two where x_1 represents the measured state and x_e represents the states to be estimated.

$$x = \begin{bmatrix} x_1 \\ x_e \end{bmatrix}$$

Now, the system can be represented as

$$\begin{bmatrix} \dot{x}_1 \\ \dot{x}_e \end{bmatrix} = \begin{bmatrix} a_{11} & a_{1e} \\ a_{e1} & A_{ee} \end{bmatrix} \begin{bmatrix} x_1 \\ x_e \end{bmatrix} + \begin{bmatrix} b_1 \\ b_e \end{bmatrix} u$$

$$y = \begin{bmatrix} 1 & 0 \end{bmatrix} \begin{bmatrix} x_1 \\ x_e \end{bmatrix}$$

The system dynamics of unmeasured state variables are given by

$$\dot{x}_e = A_{ee}x_e + (a_{e1}x_1 + b_e u) \quad 5.8$$

where the bracket term represent the known input for estimation of state variables. Similarly for the measured state variable

$$\dot{y} = \dot{x}_1 = a_{11}y + a_{1e}x_e + b_1 u \quad 5.9$$

On rearranging the terms, we get

$$\left(\dot{y} - a_{11}y - b_1u\right) = a_{1e}x_e$$

where the left hand side is known from the measurement. By comparing (5.6), (5.8) and (5.9) we conclude that both the (5.6) and (5.8) have the same state x_e .The following replacement has to be carried out in the original observer equations to obtain reduced order observer

$$x \leftarrow x_e$$
$$A \leftarrow A_{ee}$$
$$Bu \leftarrow a_{e1}y + b_eu$$
$$y \leftarrow \dot{y} - a_{11}y - b_1u$$
$$c \leftarrow a_{1e}$$

On substitution the above replacements in (5.3)

$$\dot{\hat{x}}_e = A_{ee}\hat{x}_e + \left(a_{e1}x_1 + b_eu\right) + L\left(\dot{y} - a_{11}y - b_1u - a_{1e}\hat{x}_e\right)$$

or

$$\dot{\hat{x}}_e = \left(A_{ee} - La_{1e}\right)\hat{x}_e + \left(a_{e1} - La_{11}\right)y + \left(b_e - Lb_1\right)u + L\dot{y} \qquad 5.9$$

Let $\bar{x}_e = x_e - \hat{x}_e$ be the estimation error. Then the estimation error dynamics is given by

$$\dot{\bar{x}}_e = \left(A_{ee} - La_{1e}\right)\bar{x}_e \qquad 5.10$$

The characteristic equation of error is given by $\left|s\mathrm{I} - \left(A_{ee} - La_{1e}\right)\right| = 0$

Usage of Ackermann's formula [16] gives the observer gains of the reduced order observer. Some implementation problems are associated with reduced order observer. From (5.9) we see that this observer requires derivative of the output of the system as one of the input. It is well known fact that differentiation amplifies noise. Therefore if noise is present in the output of the system which is very common in practical systems, then this reduced observer does not give satisfactory results. To solve this difficulty, we define a new state as

$$x'_e = \hat{x}_e - Ly \qquad 5.11$$

Substituting the newly defined state in (5.9), we get

$$\dot{x}'_e = \left(A_{ee} - La_{1e}\right)\hat{x}_e + \left(a_{e1} - La_{11}\right)y + \left(b_e - Lb_1\right)u \qquad 5.12$$

The above equation is represented in block diagram form as shown in the Fig. 5.4.

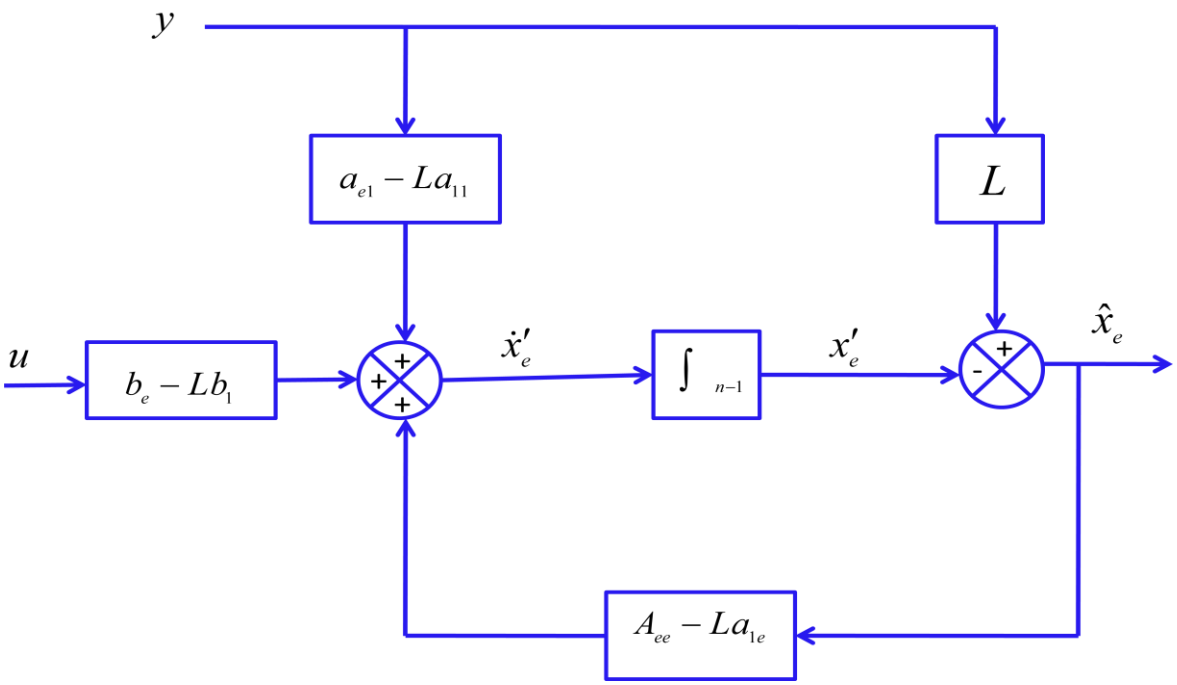

Figure 5.4: Schematic diagram of a reduced order observer with only one measurable state

5.3 Sliding Mode Observer (SMO)

The potential advantages of sliding mode control were successfully utilized in various applications related to aircraft, robot and motor systems [7, 29]. With the development of observer gaining popularity, a need to develop a robust observer was utmost essential. Sliding Mode Observer was designed by considering the distinguishing features of sliding mode. The invariance property of sliding mode was indeed beneficial in designing an observer.

5.3.1 Design of sliding mode observer

Let us consider a system defined by the general equation

$$\dot{x}_1 = x_2 \qquad 5.13$$

$$\dot{x}_2 = f\left(x_1, x_2, t\right)$$

Let us assume that only one state is measurable.

$$y = x_1$$

where

$x_1, x_2 \in \Re \rightarrow$ States of the system

$y \in \Re \rightarrow$ Output state of the system

The function $f\left(x_1, x_2, t\right)$ is bounded by a Lipschitz constant. Mathematically we can express the bound by $\left|f\left(x_1, x_2, t\right)\right| \le L \; ; L > 0$ where $L \rightarrow$ Lipschitz constant.

The formulation of SMO can be carried out as

$$\dot{\hat{x}}_1 = \hat{x}_2 + \delta_1 sign\left(e_1\right) \tag{5.14}$$

$$\dot{\hat{x}}_2 = f\left(\hat{x}_1, \hat{x}_2, t\right) + \delta_2 sign\left(\bar{e}_2\right)$$

The output of an observer is given by

$$\hat{y} = \hat{x}_1$$

where

$\delta_1, \delta_2 \rightarrow$ Observer gain

We note that from the above set of equations, a discontinuous control is added. This discontinuous control is a function of the error between the actual value and the measured value. The only measurable quantity among the two states is represented by y. Mathematically the discontinuous control is a signum function given in (4.18).

We denote the error e_1 as $e_1 = x_1 - \hat{x}_1$ and similarly for another state we define $e_2 = x_2 - \hat{x}_2$.

By subtracting (5.14) from (5.13), we can obtain the error dynamics as

$$\dot{e}_1 = e_2 - \delta_1 sign\left(e_1\right) \tag{5.15}$$

and

$$\dot{e}_2 = f\left(x_1, x_2, t\right) - f\left(\hat{x}_1, \hat{x}_2, t\right) - \delta_2 sign\left(\bar{e}_2\right) \tag{5.16}$$

As $\bar{e}_2$ is used in the discontinuous control, its calculation is explained subsequently. Let us consider a sliding surface given by $s = S\left\{e \,|\, e_1 = 0\right\}$

Let us define a Lyapunov function as

$$V = \frac{e_1^2}{2} \tag{5.17}$$

For asymptotic stability, we need to satisfy the condition where the time derivative of Lyapunov function is always negative. Also the magnitude of Lyapunov function should tend to infinity as the sliding surface tends to infinity. Mathematically,

$(a)\ \dot{V} \le 0$ for s $\neq 0$

$(b)\ \lim_{|s| \to \infty} V = \infty$

To achieve asymptotic stability we consider the first condition. Nevertheless the second condition is always satisfied and hence is not considered for analysis. The time derivative of Lyapunov function is given by

$$\dot{V} = e_1 \dot{e}_1$$

By substituting (5.15) in the above equation, we get

$$\dot{V} = e_1\left(e_2 - \delta_1 sign\left(e_1\right)\right).$$

For the above expression to be negative definite, we can conveniently choose

$$\delta_1 > \max\left|e_2\right| \tag{5.18}$$

In other words, to achieve stability of the designed sliding surface, we can choose the observer gain as per (5.18). Continuing the above analysis, the error vector e_1 and $\dot{e}_1$ tend to zero in finite time. On achieving the sliding surface in finite time, we can define the equivalent value of the first observer. The equivalent value is written as $\left(\delta_1 sign\left(e_1\right)\right)_{eq} = \overline{e}_2 = e_2$ which is the error vector calculated using equivalent control approach. In practical case, to achieve this approach we employ low pass filter to filter out the high frequency terms. These high frequency terms usually arise from the unmodeled system dynamics, actuator and sensor dynamics, unmatched disturbances present in the system. To remove the chattering behavior produced, equivalent control approach is suitable.

Let us consider the Lyapunov function similar to (5.17) and by substituting (5.16) in time derivative of Lyapunov function, we obtain

$$\dot{V} = e_2\left(f\left(x_1, x_2, t\right) - f\left(\hat{x}_1, \hat{x}_2, t\right) - \delta_2 sign\left(e_2\right)\right)$$

By inspection, we can achieve asymptotic stability $\dot{V} \le 0$ by considering

$$\delta_2 > \max\left|f\left(x_1, x_2, t\right) - f\left(\hat{x}_1, \hat{x}_2, t\right)\right| \tag{5.19}$$

The observer gains δ_1, δ_2 are selected by satisfying (5.18) and (5.19) to achieve finite time convergence.

The application of this design is used throughout the entire thesis. We focus on the application of this design to nuclear reactor system. The point reactor kinetic model is introduced in the next chapter which serves as the basic model for analysis.

5.4 Concluding Remarks

From the discussion carried out in section 5.2, we conclude that Luenberger observer is a linear observer and is not robust for parametric variations. We need to design an observer for handling practical noisy data. An attempt has been made in this thesis to present a novel type of observer overcoming the limitations mentioned earlier. This observer is presented elaborately by suitable application of the previously discussed theories. The observer designed using the sliding mode theory is known as the sliding mode observer. In the following section, we introduce sliding mode observer and illustrate the design. The benefits of this observer in nuclear reactor system dynamics is highlighted in the forthcoming chapters.

Chapter 6

Application of Sliding Mode Observer in Nuclear Reactor System Dynamics

Sliding Mode observer is essentially a reduced state observer which possesses remarkable feature to handle in variation in plant parameters. In nuclear reactor system, there are many states which cannot be measured directly with the help of instruments. The limitation of placing a sensor in an actual plant, economic considerations, non-availability of any sensor to record the measurement accurately are some of the reasons where the observer is essential. To design a robust observer accounting for parametric variations and matched disturbances, we conveniently use sliding mode observer. We divide this chapter into two where the first section concentrates on the state estimation. A specific application of sliding mode observer for fault detection in nuclear and non-nuclear parts of a nuclear reactor is considered in the latter part of the section.

6.1 State Estimation of a Nuclear Reactor System using Sliding Mode Observer

In this section, we introduce a step by step design procedure to estimate a set of states with any one or more number of states which are directly measurable. A simple sliding surface is designed to achieve finite time convergence on the surface. Let us again consider point reactor kinetic model defined in (3.4), (3.5).We rewrite the equations for convenience.

$$\frac{dP(t)}{dt} = \left(\frac{\rho(t) - \beta}{\Lambda} \right) P(t) + \sum_{i=1}^{6} \lambda_i C_i(t) + S(t)$$

$$\frac{dC_i(t)}{dt} = \left(\frac{\beta_i}{\Lambda} \right) P(t) - \lambda_i C_i(t)$$

The parameters in the above set of equations are already defined in section 3.1. Practically, we can only measure reactor power. The other parameters are estimated by knowing the reactor power. In other words, we have to design a sliding mode observer to observe the delayed neutron precursor concentration, reactivity and neutron source. We shall present each one of the cases subsequently.

6.1.1 Estimation of Delayed Neutron Precursor Concentration

(i) Single Group Delayed Neutron Precursor

Let us simplify (3.4) by assuming a single group of delayed neutron precursors instead of a six group model. Let us assume that there is no presence of independent neutron source present in the reactor system. By applying the above set of conditions, the point reactor model defined in (3.4) and (3.5) reduces to

$$\dot{P} = \left(\frac{\rho - \beta}{\Lambda} \right) P + \lambda C \tag{6.1}$$

$$\dot{C} = \left(\frac{\beta}{\Lambda} \right) P - \lambda C \tag{6.2}$$

Let us follow the design procedure carried out for a general system in section 5.3. The sliding mode observer for a system model can be designed as

$$\dot{\hat{P}} = \left(\frac{\rho - \beta}{\Lambda} \right) \hat{P} + \lambda \hat{C} + \delta_1 sign\left(e_1 \right) \tag{6.3}$$

$$\dot{\hat{C}} = \left(\frac{\beta}{\Lambda} \right) \hat{P} - \lambda \hat{C} \tag{6.4}$$

where

$\left(\hat{P}, \hat{C} \right) \rightarrow$ Estimates of $\left(P, C \right)$

We again note the addition of discontinuous control function which is dependent on the error vector of the measured variable.

Let the error vector be defined as $\mathrm{e}_1 \rightarrow P - \hat{P}$ and similarly for delayed neutron precursor $\mathrm{e}_2 \rightarrow C - \hat{C}$.

Unlike the design procedure explained earlier, we do not employ equivalent control approach here. This is because the error vector corresponding to delayed neutron precursor tends to zero as time elapses. Therefore we need to define only one Lyapunov function to achieve stability of sliding surface. The error dynamics is given by

$$\dot{e}_1 = \left(\frac{\rho - \beta}{\Lambda} \right) e_1 + \lambda e_2 - \delta_1 sign\left(e_1 \right) \tag{6.5}$$

Lypaunov function can be defined similar to (5.17).By using the condition for asymptotic stability we use the time derivative of Lyapunov function.

$$\dot{V} = e_1 \left(\left(\frac{\rho - \beta}{\Lambda} \right) e_1 + \lambda e_2 - \delta_1 sign\left(e_1 \right) \right) \tag{6.6}$$

For (6.6) to satisfy $\dot{V} < 0$, we need to choose the observer gain as

$$\delta_1 > \max \left| \left(\frac{\rho - \beta}{\Lambda} \right) e_1 + \lambda e_2 \right| \tag{6.7}$$

Simulation Results

Let us carry out a simulation in which we estimate the delayed neutron precursor concentration. Let us consider reactivity transient given by $\rho = 0.1\beta \sin(3.142t)$. For an observer let the reactivity transient $\hat{\rho} = 0.2\beta \sin(2.5t)$ is used. Fig. 6.1 shows the difference in the input reactivity variation with respect to PRK model and an observer. By considering parametric variation with the initial condition $P(0) = 0.5$ and $C(0) = \frac{\beta}{\Lambda\lambda} P(0)$, the analysis is carried out. The data table used for calculation is given in Table 3.1. In this simulation, we have replaced the discontinuous control given by signum function by a smooth function called the saturation function defined in (4.19).

Fig.6.2 (a) shows the time response of a measured state variable. The measured state variable which is the reactor power is having a finite reaching time with asymptotic stability.

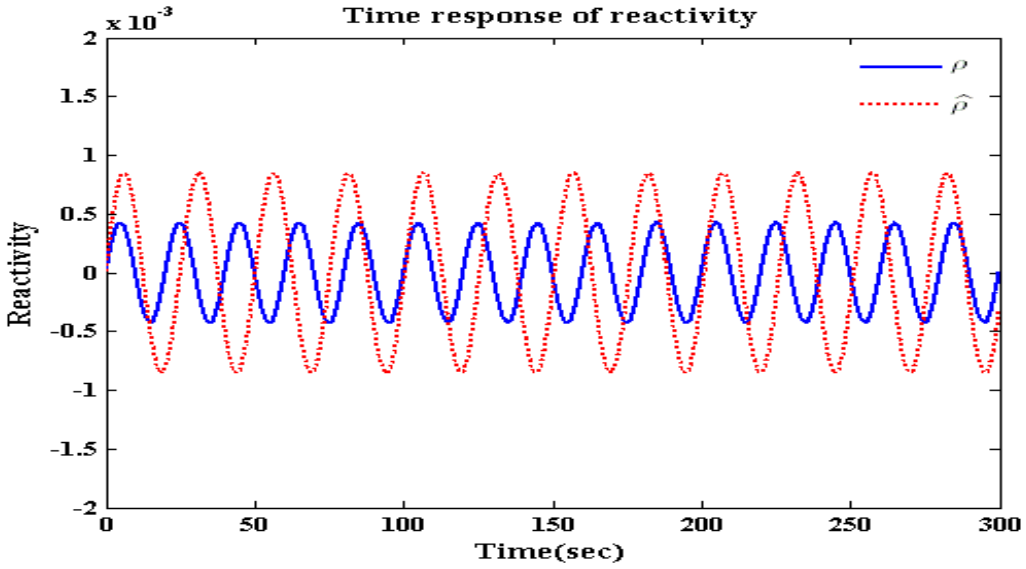

Figure 6.1: Input Reactivity variation for the point reactor kinetics model and an observer for estimation of single group delayed neutron precursor concentration

The estimation of delayed neutron precursor concentration is shown in Fig. 6.2(b). It is easily noted that there is a finite reaching time to a designed sliding surface even in the presence of input parameter mismatch. The convergence to the desired state can be altered by variation in the decay constant of the delayed neutron precursor group or by variation in the observer gain. This variation is clearly shown in the coming sections. The observer gain is calculated by using the expression given in (6.7).

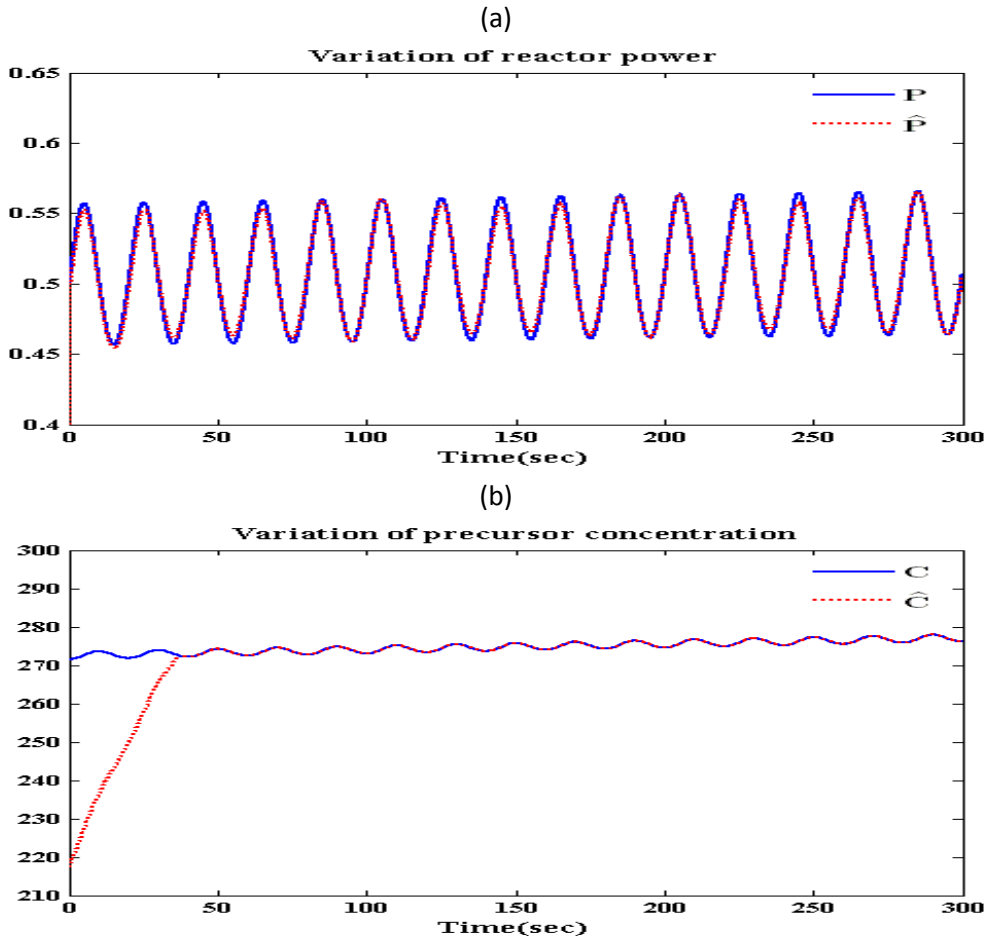

Figure 6.2: Estimation of single group delayed neutron concentration using SMO. Fig. 6.2(a) represents the estimation of reactor power with respect to PRK model. Fig. 6.2(b) shows the estimation of delayed neutron precursor concentration using SMO

(ii) Multi group delayed neutron precursor

By extending the above analysis to a six group delayed neutron precursors, we consider the point reactor kinetic model given in (3.4). Let us assume that there is no presence of independent neutron source present in the reactor system. By applying the above set of conditions, the point reactor model reduces to

$$\dot{P} = \left(\frac{\rho - \beta}{\Lambda} \right) P + \sum_{i=1}^{6} \lambda_i C_i \qquad 6.8$$

$$\dot{C}_i = \left(\frac{\beta_i}{\Lambda} \right) P - \lambda_i C_i \qquad 6.9$$

Let us follow the design procedure carried out for a general system in section 5.3. The sliding mode observer for a system model can be designed as

$$\dot{\hat{P}} = \left(\frac{\rho - \beta}{\Lambda} \right) \hat{P} + \sum_{i=1}^{6} \lambda_i \hat{C}_i + \delta_1 sign\left(e_1 \right) \tag{6.10}$$

$$\dot{\hat{C}}_i = \left(\frac{\beta_i}{\Lambda} \right) \hat{P} - \lambda_i \hat{C}_i \tag{6.11}$$

where

$\left(\hat{P}, \hat{C} \right) \rightarrow$ Estimates of $\left(P, C \right)$.

We again note the addition of discontinuous control function which is dependent on the error vector of the measured variable.

Let the error vector be defined as $\mathrm{e}_1 \rightarrow P - \hat{P}$ and similarly for delayed neutron precursor concentration $\mathrm{e}_{i+1} \rightarrow C_i - \hat{C}_i$; $i = 1, 2, ...6$.

In this case also, we do not employ equivalent control approach. This is because the error vector corresponding to delayed neutron precursor tends to zero as the time elapses. A Lyapunov function is defined to calculate the observer gain. In addition, by applying the Lyapunov condition, we calculate the stability with respect to sliding surface. The error dynamics is given by

$$\dot{e}_1 = \left(\frac{\rho - \beta}{\Lambda} \right) e_1 + \sum_{i=1}^{6} \lambda_i e_{i+1} - \delta_1 sign\left(e_1 \right) \tag{6.12}$$

Lypaunov function can be defined similar to (5.17). By using the condition for asymptotic stability we use the time derivative of Lyapunov function.

$$\dot{V} = e_1 \left(\left(\frac{\rho - \beta}{\Lambda} \right) e_1 + \sum_{i=1}^{6} \lambda_i e_{i+1} - \delta_1 sign\left(e_1 \right) \right) \tag{6.13}$$

For achieving Lyapunov stability condition, we need to choose the observer gain as

$$\delta_1 > \max \left| \left(\frac{\rho - \beta}{\Lambda} \right) e_1 + \sum_{i=1}^{6} \lambda_i e_{i+1} \right| \tag{6.14}$$

Simulation Results

Let us carry out a simulation in which we estimate the delayed neutron precursor concentration. In all the cases, we have replaced the discontinuous control given by sign function by a smooth function called the saturation function defined in (4.19).

Case 1:

Let us consider reactivity transient for a PRK model given by $\rho = 0.003\sin\left(3.142t\right)$. For an observer let the reactivity transient $\hat{\rho} = 0.002\sin\left(2.5t\right)$ be used. Fig. 6.3 shows the reactivity transient for the model and an observer. We can easily infer that the input parameter to a point reactor kinetic model is different. By considering parametric variation with the initial condition $P\left(0\right) = 0.5$ and $C_i\left(0\right) = \dfrac{\beta_i}{\Lambda\lambda_i}P\left(0\right)$; $i = 1,2,...6$, the analysis is carried out. The data table used for calculation is given in Table 3.1

Fig. 6.4 (a) shows the time response of a measured state variable. The measured state variable which is the reactor power is having a finite reaching time with asymptotic stability.

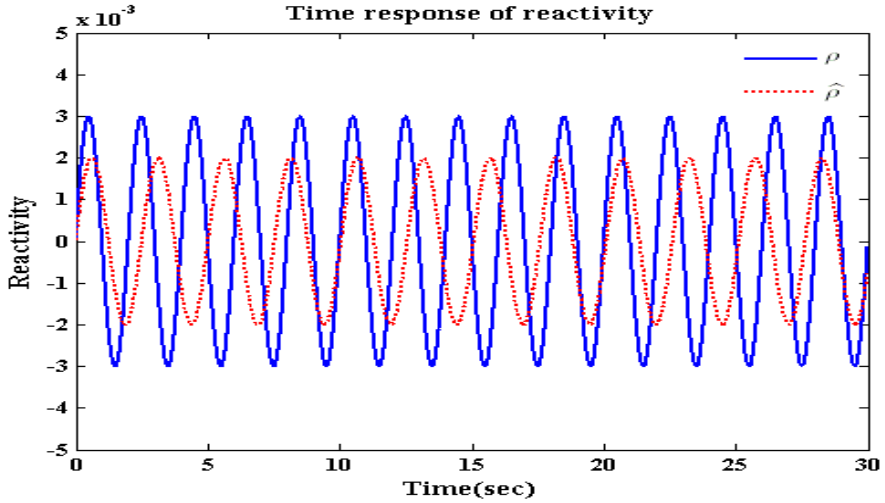

Figure 6.3: Input Reactivity variation for the point reactor kinetics model and an observer for estimation of six group delayed neutron precursor concentration

(a)

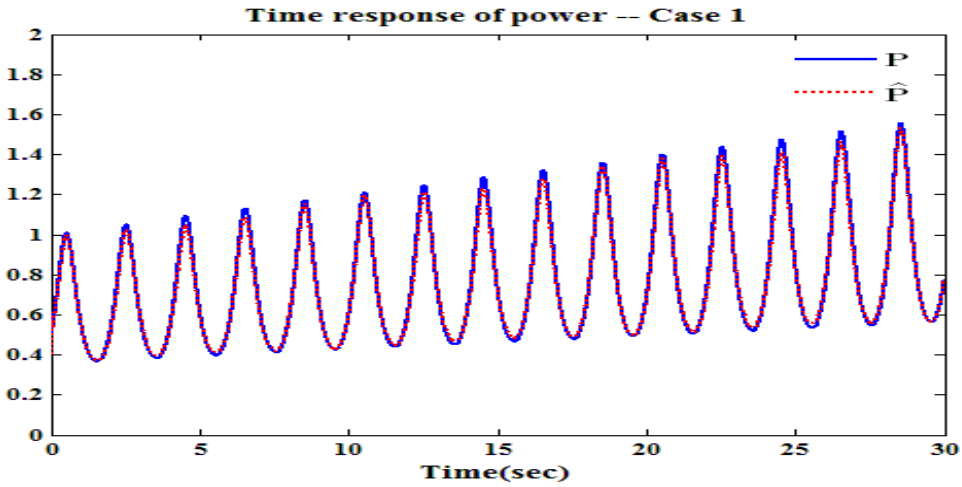

(b)

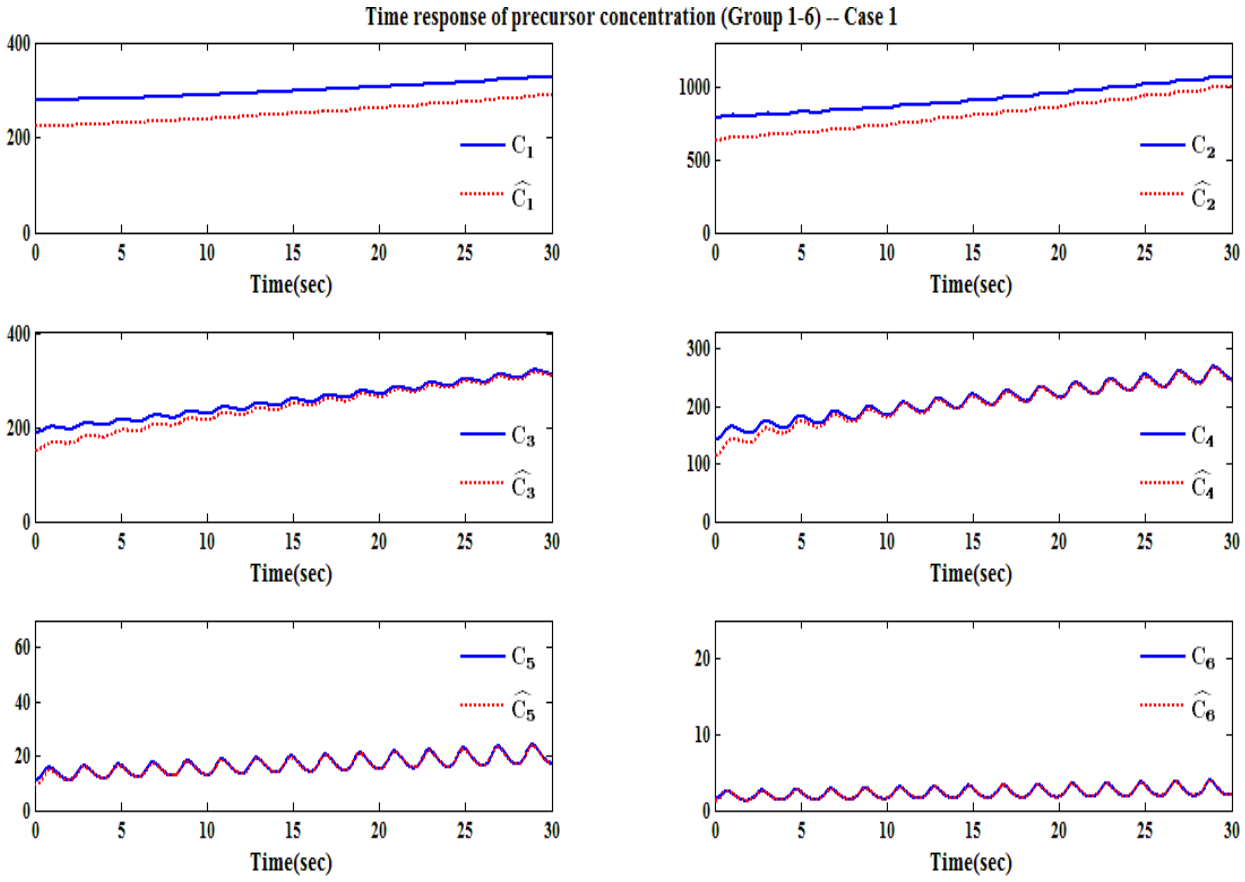

Figure 6.4: Estimation of six group delayed neutron concentration using SMO under input uncertainty. Fig. 6.4(a) represents the estimation of reactor power with respect to PRK model. Fig. 6.4(b) shows the estimation of delayed neutron precursor concentration using SMO

The estimation of delayed neutron precursor concentration of all the groups is shown in Fig. 6.4 (b). It is easily noted that for all the groups there is a finite reaching time to a designed sliding surface even in the presence of input parameter mismatch. The convergence to the desired state can be altered by variation in the decay constant of the delayed neutron precursor group or by variation in the observer gain. This variation is clearly shown in the coming sections.

Case 2:

The input reactivity mismatch with respect to model and an observer is shown in Fig. 6.1. The variation of a delayed neutron fraction with time is also considered as

$$\beta = \begin{cases} 0.007 - \left(1.3 * 10^{-5} t\right) & \beta \geq 0.005 \\ 0.0065 & \text{otherwise} \end{cases}.$$

By considering input and model parametric variation with the initial condition $P(0) = 0.5$ and $C_i(0) = \frac{\beta_i}{\Lambda \lambda_i} P(0)$; $i = 1,2,...6$, the analysis is carried out. The data table used for calculation is given in Table 3.1.

Fig. 6.5(a) shows the time response of a measured state variable. The measured state variable which is the reactor power is having a finite reaching time with asymptotic stability. The estimation of delayed neutron precursor concentration of all the groups is shown in Fig. 6.5(b) It is easily noted that for all the groups there is a finite reaching time to a designed sliding surface even in the presence of input parameter mismatch and plant parameter variation. Therefore sliding mode observer works as a robust observer under parametric uncertainties which was established theoretically in the earlier chapters.

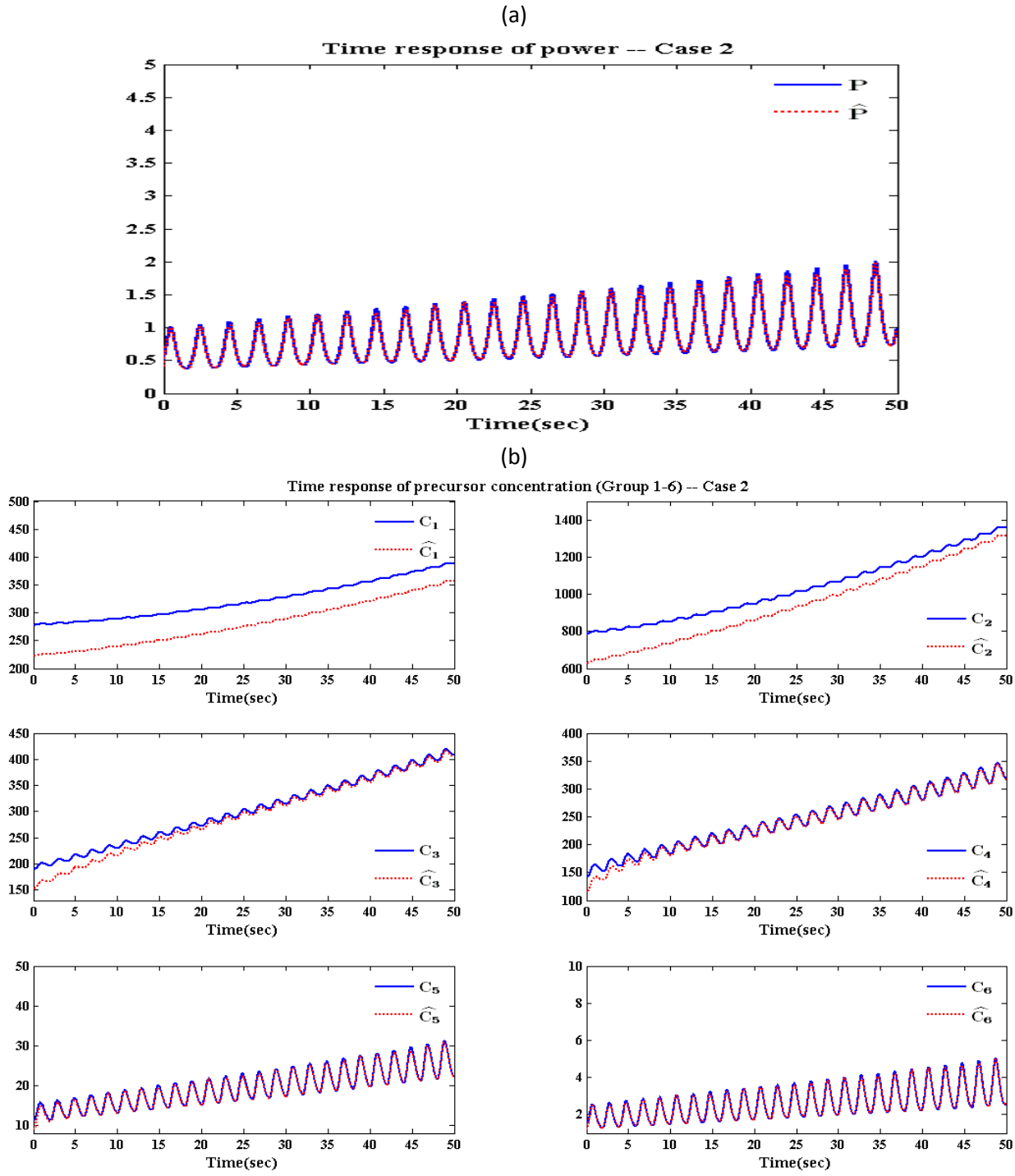

Figure 6.5: Estimation of six group delayed neutron concentration using SMO under parametric and input uncertainty. Fig. 6.5(a) represents the estimation of reactor power with respect to PRK model. Fig. 6.5(b) shows the estimation of delayed neutron precursor concentration using SMO

Case 3:

Let us consider a random reactivity transient given by $\rho = 0.003\text{rand}(t)$ is used as an input to PRK model. For an observer, again consider a random reactivity transient $\rho = 0.003\text{rand}(2t)$ is considered. We can easily infer that the input parameter to a point reactor kinetic model is random and hence different. By considering input parametric variation with the initial condition $P(0) = 0.5$ and $C_i(0) = \frac{\beta_i}{\Lambda\lambda_i} P(0)$; $i = 1,2,...6$, the analysis is carried out. The data table used for calculation is given in Table 3.1

Fig. 6.6 (a) shows the time response of a measured state variable. The measured state variable which is the reactor power is having a finite reaching time with asymptotic stability. The estimation of delayed neutron precursor concentration of all the groups is shown in Fig. 6.6 (b) It is easily noted that for all the groups there is a finite reaching time to a designed sliding surface even in the presence of random reactivity input. This is one of the general cases where the sliding mode observer is designed for random input.

Case 4:

Let us consider an up chirp reactivity transient given by $\rho = 0.008\sin 2\pi t(0.01 + 0.4t)$. For an observer, a constant reactivity transient $\rho = 0.008$ is considered. Fig. 6.7 shows the reactivity variation which is used for an observer. We can easily infer that there is an input parameter mismatch with respect to the model and an observer. By considering input parametric variation with the initial condition $P(0) = 0.5$ and $C_i(0) = \frac{\beta_i}{\Lambda\lambda_i} P(0)$; $i = 1,2,...6$, the analysis is carried out. The data table used for calculation is given in Table 3.1.

Fig. 6.7 (a) shows the time response of a measured state variable. The measured state variable which is the reactor power is having a finite reaching time with asymptotic stability. The estimation of delayed neutron precursor concentration of all the groups is shown in Fig. 6.8. From Fig. 6.8, we can observe that the convergence time varies for every delayed precursor group. Considering 5% tolerance with respect to the actual value, settling time is defined as $(t_s)_i = \frac{4}{\lambda_i}$.

Using the settling time expression for all the groups and using the values given in Table 3.1, we get

$$(t_s)_1 = \frac{4}{\lambda_1} \approx 317 \text{ sec} \; ; \; (t_s)_2 = \frac{4}{\lambda_2} \approx 132 \text{ sec}$$

$$(t_s)_3 = \frac{4}{\lambda_3} \approx 36 \text{ sec} \; ; \; (t_s)_4 = \frac{4}{\lambda_4} \approx 13 \text{ sec}$$

$$(t_s)_5 = \frac{4}{\lambda_5} \approx 3.5 \text{ sec} \; ; \; (t_s)_6 = \frac{4}{\lambda_6} \approx 1.3 \text{ sec}$$

The theoretically calculated settling time for all the groups confirms the simulated result shown in Fig. 6.9. As the decay constant of first group is the lowest, therefore we obtain the highest settling time with respect to all other groups. A converse case is valid for the sixth group. This settling time can be decreased by increasing the observer gain.

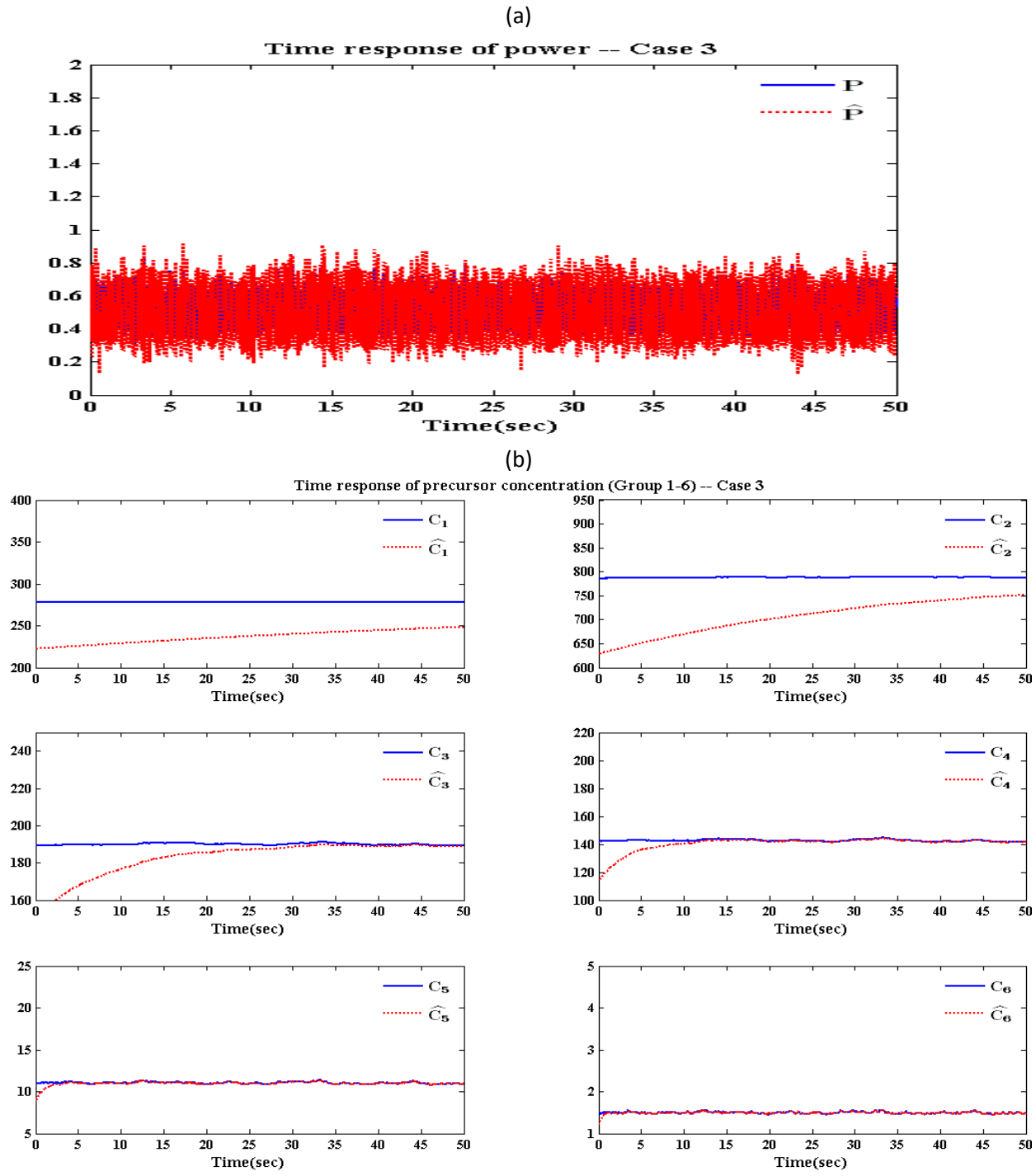

Figure 6.6: Estimation of six group delayed neutron concentration using SMO under random input. Fig. 6.6(a) represents the estimation of reactor power with respect to PRK model. Fig. 6.6(b) shows the estimation of delayed neutron precursor concentration using SMO

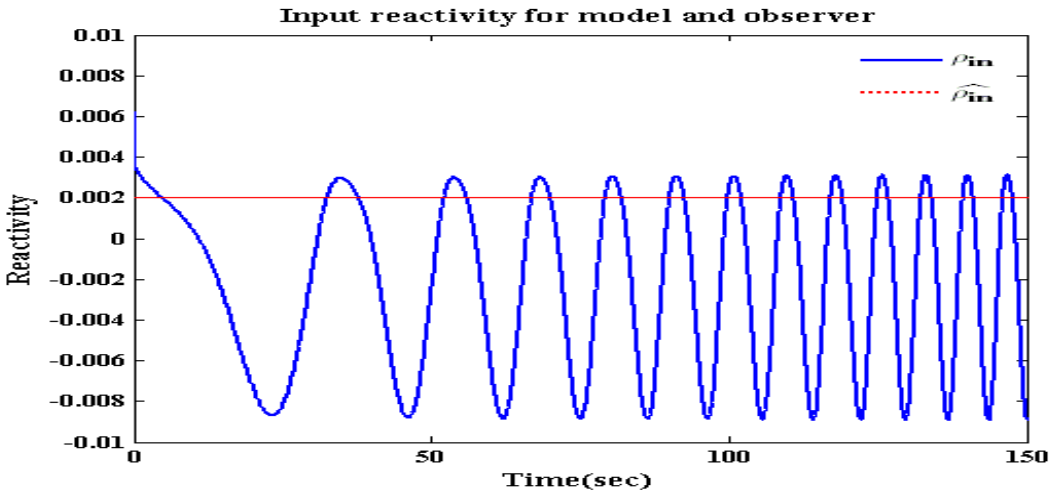

Figure 6.7: Chirp and constant input reactivity for point reactor kinetics model and an observer for estimation of six group delayed neutron precursor concentration

6.1.2 Estimation of reactivity

Let us consider a six group delayed neutron precursor given in (6.8) and (6.9). We follow the design procedure carried out for a general system in 5.3. In this section, we focus on the estimation of reactivity. The sliding mode observer for reactivity estimation can be designed as

$$\dot{\hat{P}} = \left(\frac{\delta_r sign\left(P \cdot e_1\right) - \beta}{\Lambda} \right) \hat{P} + \sum_{i=1}^{6} \lambda_i \hat{C}_i \qquad 6.15$$

$$\dot{\hat{C}}_i = \left(\frac{\beta_i}{\Lambda} \right) \hat{P} - \lambda_i \hat{C}_i \qquad 6.16$$

where

$\left(\hat{P}, \hat{C}\right) \rightarrow$ Estimates of $\left(P, C\right)$

$\delta_r \rightarrow$ Reactivity observer gain

We again note the addition of discontinuous control function which is dependent on the error vector of the measured variable.

Let the error vector be defined as $\mathrm{e}_1 \rightarrow P - \hat{P}$ and similarly for delayed neutron precursor $\mathrm{e}_{i+1} \rightarrow C_i - \hat{C}_i$; $i = 1,2,...6$.

A Lyapunov function is defined to calculate the reactivity observer gain. In addition, by applying the Lyapunov condition, we calculate the stability with respect to sliding surface. The error dynamics is given by

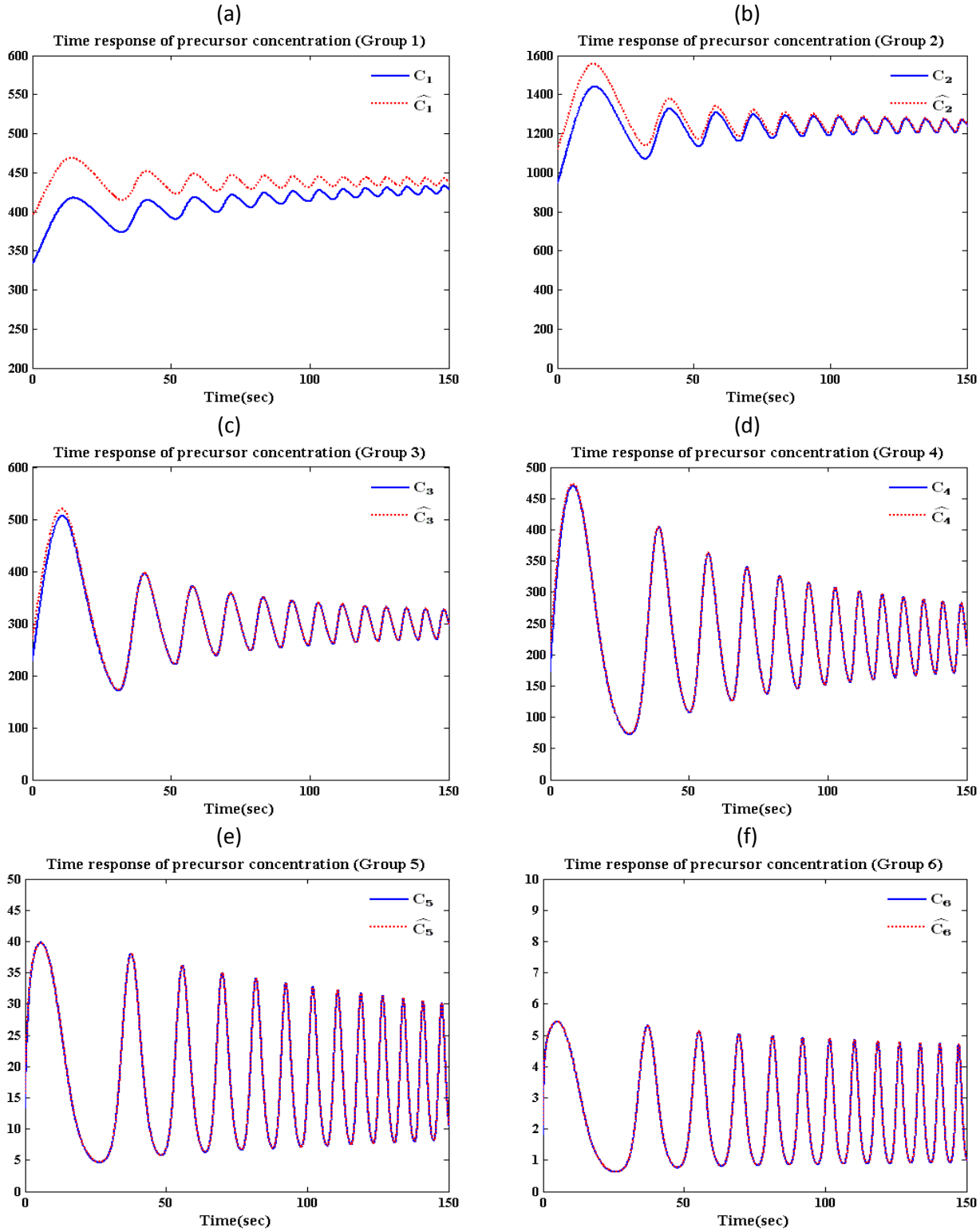

Figure 6.8: Estimation of six group delayed neutron concentration using SMO under input uncertainty.

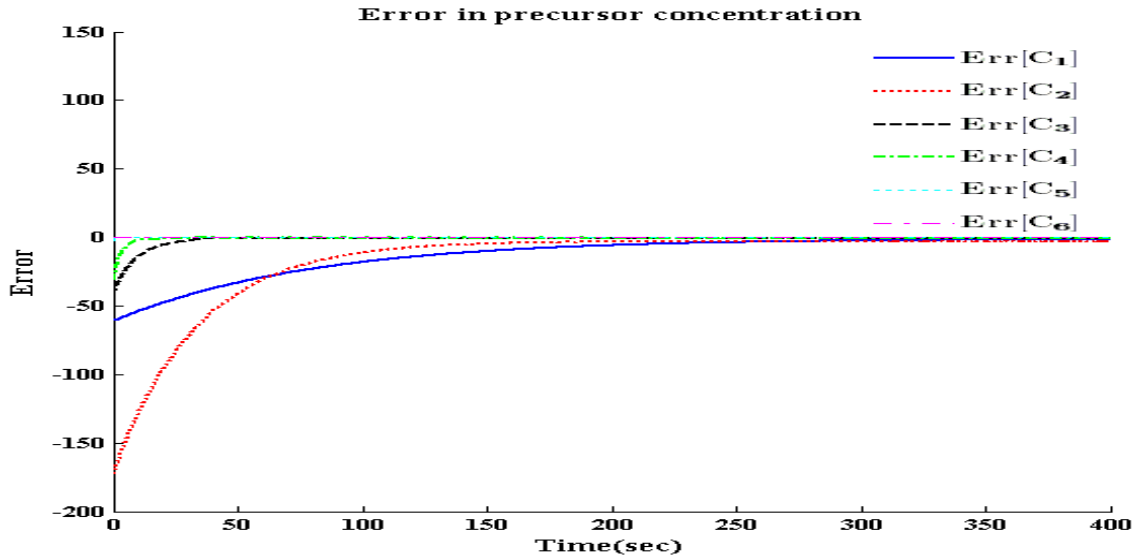

Figure 6.9: Error in estimation of six group delayed neutron concentration using SMO under input uncertainty.

$$\frac{de_1}{dt} = \left(\frac{\rho - \delta_r sign\left(P \cdot e_1\right)}{\Lambda} \right) e_1 \qquad 6.17$$

Lyapaunov function can be defined similar to (5.17). By using the condition for asymptotic stability we use the time derivative of Lyapunov function.

$$\dot{V} = e_1 \left(\left(\frac{\rho - \delta_r sign\left(P \cdot e_1\right)}{\Lambda} \right) e_1 \right) \qquad 6.18$$

For achieving Lyapunov stability condition of negative time derivative, we need to choose the reactivity observer gain as

$$\delta_r > \max\left|\rho(t)\right| \qquad 6.19$$

To obtain the estimated reactivity, we employ equivalent control approach as explained in section 4.2.3. For a practical implementation of equivalent control approach, we employ a low pass filter with a fixed cutoff frequency. When the error defined by e_1 tends to zero, then $\frac{de_1}{dt}$ also tends to zero. By using (6.17), we obtain the estimated reactivity as the low pass filtered value of the discontinuous control. In this case, we have employed a first order low pass filter represented as

$$\tau \frac{dz(t)}{dt} = -z(t) + \delta_r sign\left(P \cdot e_P\right) \qquad 6.20$$
$$\hat{\rho}(t) = z(t)$$

Simulation Results

Let us carry out a simulation in which we estimate the reactivity for different cases. In all the cases, we have replaced the discontinuous control given by sign function by a smooth function called the saturation function defined in (4.19).

Case 1:

Let us consider reactivity transient given by $\rho = 0.008 \sin 2\pi t\left(0.01 + 0.4t\right)$. Fig. 6.7 shows the corresponding reactivity transient. The initial condition $P(0) = 0.5$ and $C_i(0) = \frac{\beta_i}{\Lambda \lambda_i} P(0)$; $i = 1,2,...6$ is used. The data table used for calculation is given in Table 3.1 with a cutoff frequency of first order low pass filter as 100 Hz.

Fig. 6.10 shows that the reactivity is estimated corresponding to the input reactivity variation.

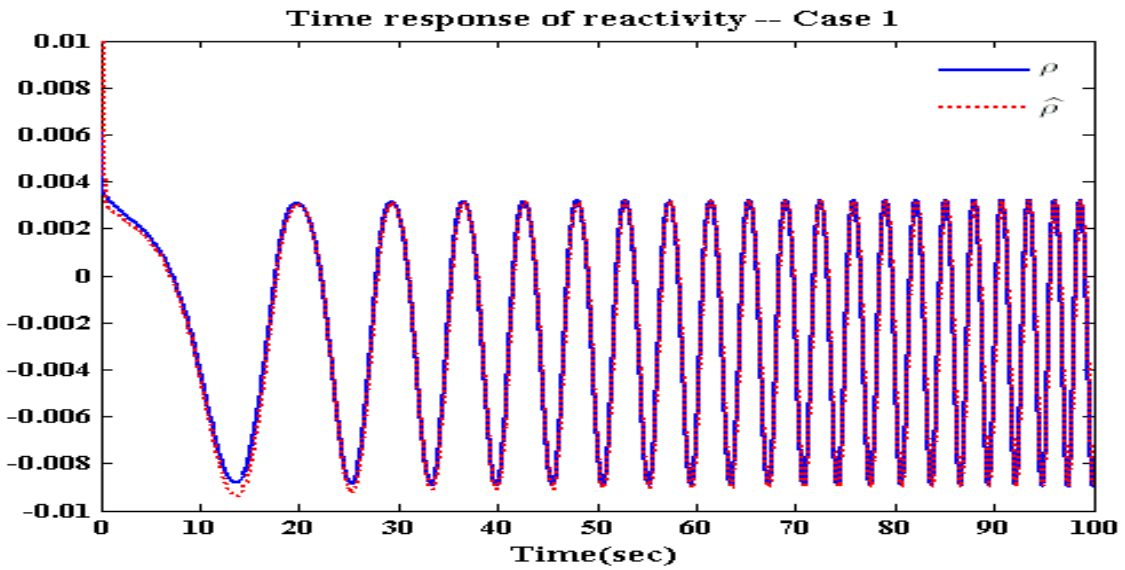

Figure 6.10: Estimation of chirp input reactivity variation using SMO.

Case 2:

Let us consider an arbitrary reactivity input given by

$$\rho = \begin{cases} -0.00065 + \left(2 * 10^{-6} t^{1.2}\right) & t \le 50 \\ 0.00065 - \left(2 * 10^{-6} t^{1.2}\right) & \text{otherwise} \end{cases}$$

The initial condition $P(0) = 0.5$ and $C_i(0) = \frac{\beta_i}{\Lambda \lambda_i} P(0)$; $i = 1,2,...6$ is used. The data table used for calculation is given in Table 3.1 with a cutoff frequency of first order low pass filter as 100 Hz.

Fig. 6.11 shows that the reactivity is estimated with faster convergence time even in case of arbitrary input. Therefore we can conclude that sliding mode observer can be effectively used to observe the reactivity behavior.

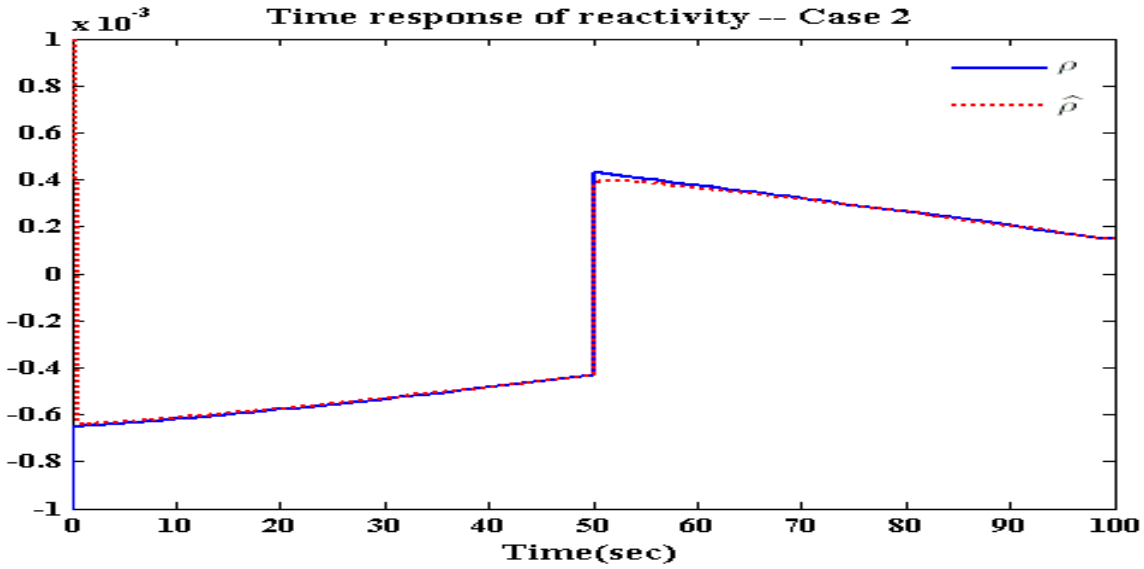

Figure 6.11: Estimation of arbitrary input reactivity variation using SMO.

6.1.3 Estimation of Neutron Source

Let us consider a six group delayed neutron precursor in case of a point reactor kinetic model. In this case, we have to consider the effect of independent neutron source. By using the general point kinetic reactor model given in (3.4), we get

$$\dot{P} = \left(\frac{\rho - \beta}{\Lambda} \right) P + \sum_{i=1}^{6} \lambda_i C_i + S$$

$$\dot{C}_i = \left(\frac{\beta_i}{\Lambda} \right) P - \lambda_i C_i$$

In this section, we need to estimate the neutron source S. This estimation is important for low power reactors where the reactor startup is carried out by using independent or primary neutron source.

Let us follow the design procedure carried out for a general system in section 5.3. The sliding mode observer for independent neutron source estimation can be formulated as

$$\dot{\hat{P}} = \left(\frac{\rho - \beta}{\Lambda} \right) \hat{P} + \sum_{i=1}^{6} \lambda_i \hat{C}_i + \delta_s sign\left(e_P \right) \qquad 6.21$$

$$\dot{\hat{C}}_i = \left(\frac{\beta_i}{\Lambda} \right) \hat{P} - \lambda_i \hat{C}_i \qquad 6.22$$

where

$\left(\hat{P}, \hat{C} \right) \rightarrow$ Estimates of $\left(P, C \right)$

$\delta_r \rightarrow$ Reactivity observer gain

We again note the addition of discontinuous control function which is dependent on the error vector of the measured variable which is the reactor power.

Let the error vector be defined as $\mathrm{e}_1 \rightarrow P - \hat{P}$ and similarly for delayed neutron precursor $\mathrm{e}_{i+1} \rightarrow C_i - \hat{C}_i \; ; i = 1,2,...6$.

A Lyapunov function is defined to calculate the source observer gain. In addition, by applying the Lyapunov condition, we calculate the stability with respect to sliding surface. The error dynamics is given by

$$\frac{de_1}{dt} = \left(\frac{\rho - \beta}{\Lambda} \right) e_1 + S - \delta_s sign\left(e_1 \right) \qquad 6.23$$

Lypaunov function can be defined similar to (5.17). By using the condition for asymptotic stability we use the time derivative of Lyapunov function.

$$\dot{V} = e_1\left(\left(\frac{\rho-\beta}{\Lambda}\right)e_1 + S - \delta_s sign\left(e_P\right)\right) \qquad 6.24$$

For achieving Lyapunov stability condition, we need to choose the reactivity observer gain as

$$\delta_r > \max\left|\left(\frac{\rho-\beta}{\Lambda}\right)e_1 + S\right| \qquad 6.25$$

To obtain the estimated external neutron source, we employ equivalent control approach as explained in section 4.2.3. For a practical implementation of equivalent control approach, we employ a low pass filter with a fixed cutoff frequency. When the error defined by e_1 tends to zero, then $\frac{de_1}{dt}$ also tends to zero. By using (6.23), we obtain the estimated reactivity as the low pass filtered value of the discontinuous control. In this case, we have employed a first order low pass filter represented as

$$\tau\frac{dz(t)}{dt} = -z(t) + \delta_s sign\left(e_1\right) \qquad 6.26$$
$$\hat{S}(t) = z(t)$$

Simulation Results

Let us carry out a simulation in which we estimate the external neutron source. In this simulation, we have replaced the discontinuous control given by sign function by a smooth function called the saturation function defined (4.15).

Let us consider neutron source variation with respect to time as

$$S = \begin{cases} 1 & t \le 3 \\ 2 & \text{otherwise} \end{cases}$$

This neutron source variation is shown in Fig. 6.12. The initial condition $P(0) = 0.5$ and $C_i(0) = \frac{\beta_i}{\Lambda\lambda_i}P(0)$; $i = 1,2,...6$ is used. The data table used for calculation is given in Table 3.1 with a cutoff frequency of first order low pass filter as 100 Hz. By employing equivalent control approach, the independent neutron source estimation is carried out. We observe from Fig. 6.12 that finite reaching time with asymptotic stability is achieved.

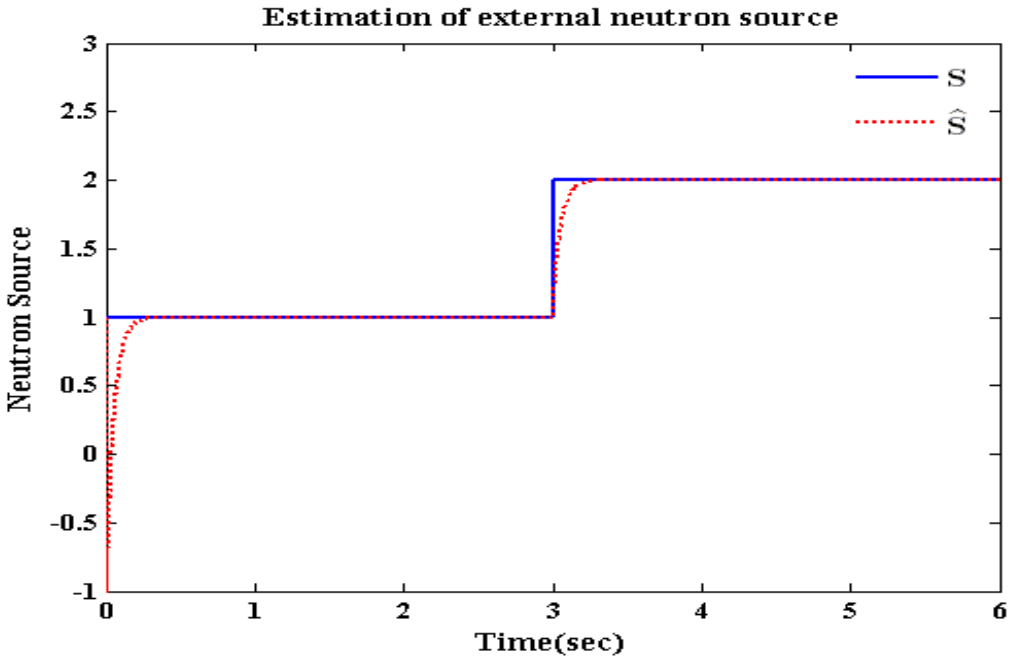

Figure 6.12: Estimation of neutron source using SMO

6.1.4 Estimation of Xenon and Iodine Concentration

Xenon-135(Xe-135) is the one of the most important fission product poison and has a tremendous impact on the operation of a thermal nuclear reactor. Although there are many fission products like Sm-149, I-135, Xe-135 which have influence on the transient behaviour of reactor power. Xe-135 outscores the rest with its large thermal neutron capture cross section nearing to $2.6*10^6$ barn. Chernick [3] provided an elaborate analysis of the dynamics of a nuclear reactor including xenon transients. The expression of flux in such a reactor is given by

$$\dot{\phi} = \frac{\rho}{\Lambda}\phi - \frac{\sigma_X}{\Lambda c \sum_f} X\phi - \frac{\gamma}{\Lambda}\phi^2 \qquad 6.27$$

The dynamics of iodine and xenon are called as the rate equation. The iodine concentration at any time is given by

$$\dot{I} = \gamma_I \sum_f \phi - \lambda_I I \qquad 6.28$$

Where the first term indicates the production of iodine and the second term indicates the decay of iodine over a period of time.

Xenon is one of the decay products in the decay chain of Iodine. Therefore, xenon concentration depends on the iodine concentration at any point of time.

$$\dot{X} = \gamma_X \sum_f \phi + \lambda_I I - \left(\lambda_X X + \sigma_X X\phi\right) \qquad 6.29$$

where the first two terms provide the production rate of xenon. The term represented in the brackets correspond to the loss of xenon in terms of its decay or parasitic absorption.
where

$\phi \rightarrow$ Thermal Flux

$\gamma \rightarrow$ Lumped temperature feedback coefficient

$X \rightarrow$ Xenon – 135 concentration

$I \rightarrow$ Iodine – 131 concentration

$c \rightarrow$ Conversion factor of xenon concentration to reactivity

$\gamma_X \rightarrow$ Xenon – 135 fission yield

$\gamma_I \rightarrow$ Iodine – 131 fission yield

$\lambda_X \rightarrow$ Xenon – 135 decay rate

$\lambda_I \rightarrow$ Iodine – 131 decay rate

$\sum_f \rightarrow$ Macroscopic fission cross section

$\sigma_X \rightarrow$ Microscopic cross section

In (6.27), (6.28) and (6.29, flux ϕ is the only measurable quantity. Therefore

$$y = \phi \tag{6.30}$$

Following the design procedure carried out for a general system in section 5.3, the sliding mode observer for estimation of iodine and xenon concentration can be formulated as

$$\dot{\hat{\phi}} = \frac{\rho}{\Lambda}\hat{\phi} - \frac{\sigma_X}{\Lambda c \sum_f}\hat{X}\hat{\phi} - \frac{\gamma}{\Lambda}\hat{\phi}^2 + \delta_1 sign(e_1) \tag{6.31}$$

$$\dot{\hat{I}} = \gamma_I \sum_f \hat{\phi} - \lambda_I \hat{I} \tag{6.32}$$

$$\dot{\hat{X}} = \gamma_X \sum_f \hat{\phi} + \lambda_I \hat{I} - \lambda_X \hat{X} - \sigma_X \hat{X}\hat{\phi} \tag{6.33}$$

where

$\left(\hat{\phi}, \hat{I}, \hat{X}\right) \rightarrow$ Estimates of $\left(\phi, I, X\right)$

$\delta_1 \rightarrow$ Observer gain

We again note the addition of discontinuous control function which is dependent on the error vector of the measured variable. Let the error vector be defined as $e_1 = \phi - \hat{\phi}$. For iodine and xenon the error vectors are $e_2 = I - \hat{I}$ and $e_3 = X - \hat{X}$ respectively.

A Lyapunov function is defined to calculate the constant observer gain. In addition, by applying the Lyapunov condition, we calculate the stability with respect to sliding surface. The error dynamics of all the three state variables are

$$\frac{de_1}{dt} = \frac{\rho}{\Lambda}e_1 - \frac{\sigma_X}{\Lambda c\sum_f}\left(X\phi - \hat{X}\hat{\phi}\right) - \frac{\gamma}{\Lambda}\left(\phi^2 - \hat{\phi}^2\right) - \delta_1 sign\left(e_1\right) \quad 6.34$$

$$\frac{de_2}{dt} = \gamma_I \sum_f e_1 - \lambda_I e_2 \quad 6.35$$

$$\frac{de_3}{dt} = \gamma_X \sum_f e_1 + \lambda_I e_2 - \lambda_X e_3 - \sigma_X\left(X\phi - \hat{X}\hat{\phi}\right) \quad 6.36$$

In this case, we do not employ equivalent control approach. This is because the error vector corresponding to iodine and xenon concentration tends to zero as the time elapses. To derive this behavior, consider (6.35)

As the error due to neutron flux tends to zero, (6.35) reduces to $\frac{de_2}{dt} = -\lambda_I e_2$

This is a simple differential equation with a solution in the form of $e_2\left(t\right) = e_2\left(0\right)e^{-\lambda_I t}$. It is easy to note that the error decays exponentially to zero because $\lambda_I > 0$.

Similarly we can substitute $e_1 \to 0$ and $e_2 \to 0$ from the above analysis. (6.36) reduces to

$$\frac{de_3}{dt} = -\lambda_X e_3 - \sigma_X\left(X\phi - \hat{X}\hat{\phi}\right)$$

The solution of the above differential equation is given by $e_3\left(t\right) = e_3\left(0\right)e^{-\left(\lambda_X + \sigma_X\hat{\phi}\right)t}$ because $\phi = \hat{\phi}$ when $e_1 \to 0$. The error also decreases exponentially to zero as time increases as $\left(\lambda_X + \sigma_X\phi\right) > 0$.

Now let us calculate the observer gain by defining a Lyapunov function.

$\dot{V} = e_1\dot{e}_1 < 0$

By solving the Lyapunov function, we get

$$\dot{V} = e_1\left(\frac{\rho}{\Lambda}e_1 - \frac{\sigma_X}{\Lambda c\sum_f}\left(X\phi - \hat{X}\hat{\phi}\right) - \frac{\gamma}{\Lambda}\left(\phi^2 - \hat{\phi}^2\right) - \delta_1 sign\left(e_1\right)\right) < 0$$

$$\dot{V} = e_1\left(p - \delta_1 sign\left(e_1\right)\right) < 0$$

where

$$p = \frac{\rho}{\Lambda}e_1 - \frac{\sigma_X}{\Lambda c\sum_f}\left(X\phi - \hat{X}\hat{\phi}\right) - \frac{\gamma}{\Lambda}\left(\phi^2 - \hat{\phi}^2\right)$$

To satisfy the Lyapunov stability condition, we have to select the observer gain such that

$\delta_1 > \max\left|p\right|$ 6.37

Simulation Results

Let us carry out a simulation to illustrate the properties of sliding mode observer and estimate the iodine and xenon concentration. In all the cases, we have replaced the discontinuous control given by signum function by a smooth function called the saturation function defined in (4.15).

Case 1:

Let us consider the reactivity variation as $\rho = |\sin 2t|$ .The initial condition of the system as $\phi(0) = 5\ ;\ I(0) = 2\ ;\ X(0) = 1$ whereas for the observer we use $\hat{\phi}(0) = 1\ ;\ \hat{I}(0) = 5\ ;\ \hat{X}(0) = 2.$

The data table used for calculation is given in Table 3.2. Let us consider a variation in macroscopic fission parameter as an uncertainty. For the system model consider $\sum_f = 1000|\sin(20t)| + 0.1$ and for an observer $\sum_f = 1000|\sin(15t)| + 0.1.$ In other words, we are considering the case of a system with different initial conditions with parametric uncertainty. Fig.6.13 (a) shows the time response of the neutron flux. As neutron flux is the only measured variable, we focus on the results of the estimated iodine and xenon concentration.

Fig. 6.13(b) shows the time response behavior of actual and estimated iodine concentration. From the response, it is clear that the designed sliding mode observer serves as a good estimator. In this thesis, we have not considered the iodine and xenon concentration analysis till the equilibrium value. This may be few hours of simulation time. From Fig. 6.13 (c), we can note the dynamics of xenon concentration in a reactor. In this case also, the sliding mode observer provides a good estimate even in the presence of parametric uncertainty and bounded sinusoidal disturbance.

Case 2:

Let us consider a random reactivity variation as $\rho = rand(t)$ for a system model. For an observer let us consider a random variation in the reactivity as $\rho = rand(2t)$ .The initial condition of the system is $\phi(0) = 5\ ;\ I(0) = 2\ ;\ X(0) = 1$ whereas for the observer we use $\hat{\phi}(0) = 1\ ;\ \hat{I}(0) = 5\ ;\ \hat{X}(0) = 2.$

The data table used for calculation is given in Table 3.2. Let us consider a random variation in macroscopic fission parameter as an uncertainty. For the system model consider $\sum_f = 1000|rand(t)|$ and for an observer $\sum_f = 1000|rand(0.5t)|$. In other words, we are considering the case of a system with different initial conditions with parametric uncertainty defined by the random disturbance. Fig. 6.14 (a) shows the time response of the neutron flux. As neutron flux is the only measured variable, we focus on the results of the estimated iodine and xenon concentration.

Fig 6.14 (b) shows the time response behavior of actual and estimated iodine concentration. From the response, it is clear that the designed sliding mode observer serves as a good estimator even in the presence of random variation. We can conclude that this is one of the most general cases where the designed observer estimates the state variables even in the presence of matched disturbances. From Fig 6.14 (c), we can note the xenon dynamics which increases till the equilibrium value is reached. For homogenous thermal reactors, the time taken by the xenon concentration to reach the equilibrium state is nearly 10 hours. As the intention of presenting this simulation was to estimate xenon and iodine concentration, therefore the simulation time is not considered.

(a)

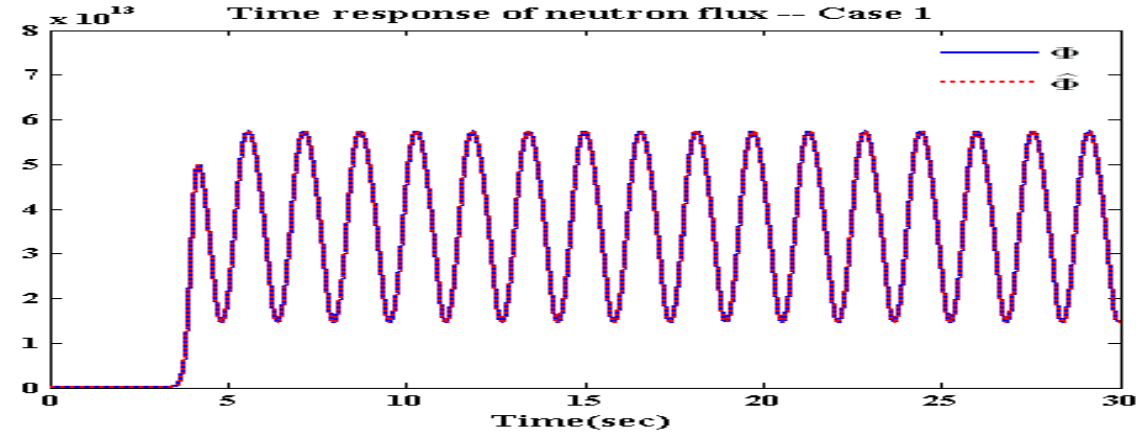

(b)

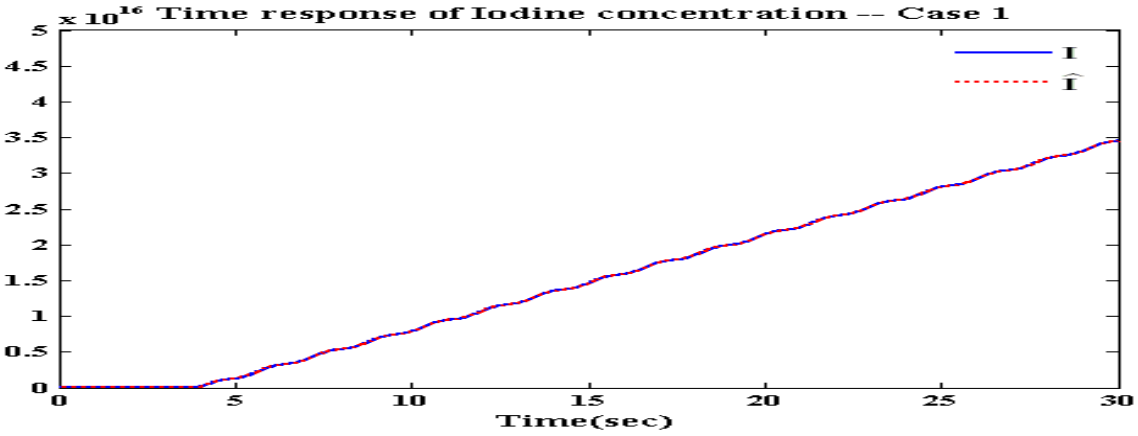

(c)

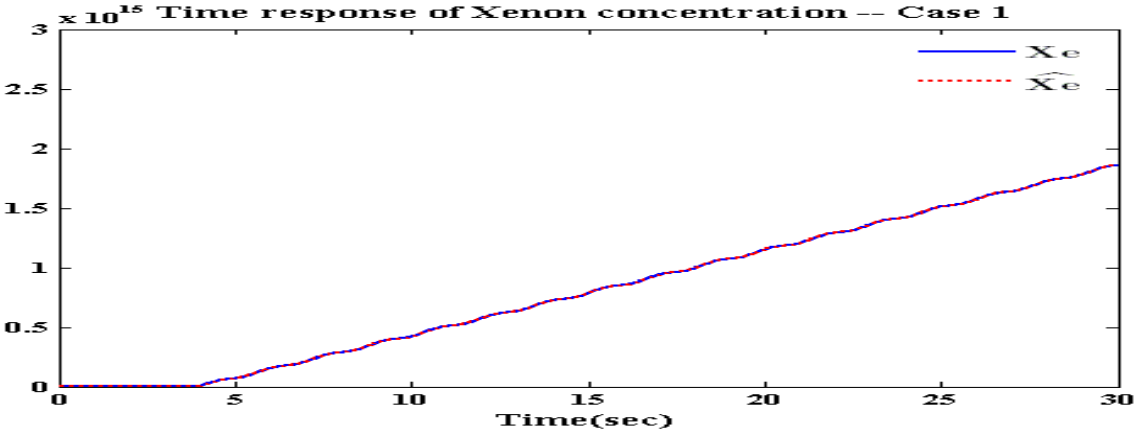

Figure 6.13: Estimation of xenon and iodine concentration using SMO for sinusoidal variation in reactivity. Fig. 6.13(a) gives the neutron flux behavior using Chernick model. Fig. 6.13(b) and (c) shows the estimation of iodine and xenon concentration respectively using SMO

(a)

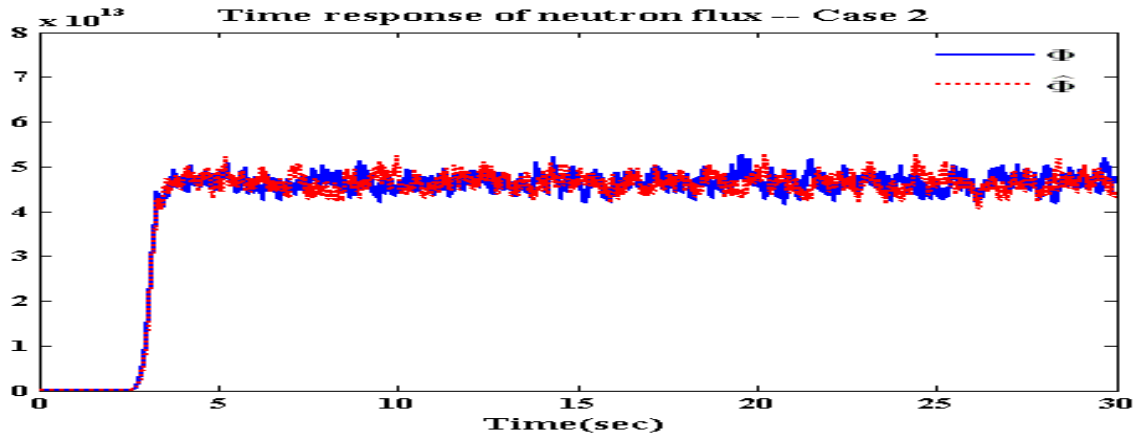

(b)

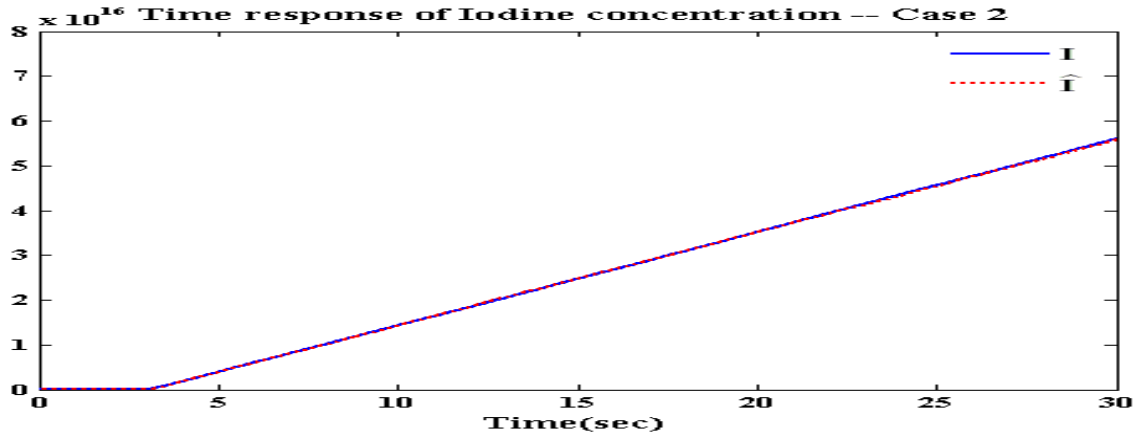

(c)

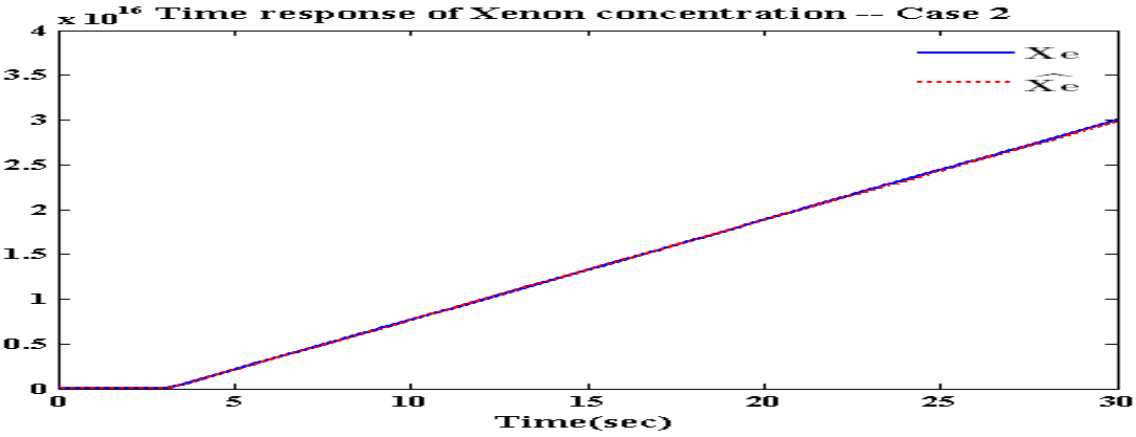

Figure 6.14: Estimation of xenon and iodine concentration using SMO for random variation in reactivity. Fig. 6.14(a) gives the neutron flux behavior using Chernick model. Fig. 6.14(b) and (c) shows the estimation of iodine and xenon concentration respectively using SMO

6.2 Fault Detection using Sliding Mode Observer

A deviation of one of the characteristic variable above a defined threshold value is defined as the fault. There are several types of faults depending on the time during which the fault is present namely, step wise, incipient and intermittent faults [10]. We can model the faults by considering either additive or multiplicative type. In case of additive faults, there is no dependence of model input in the corresponding output whereas in case of multiplicative faults there are changes in the parameters with the variation in the input.

One of the immediate consequences of a fault is the system failure. In a practical system, a fault may correspond to a loss of actuator or a sensor on whose action several inter-related components will not produce desired results and these cumulative behavior leads to the system failure.

The fault detection with specific application to nuclear reactor system dynamics is of utmost concern. This is because, with the occurrence of a fault in any part of the system if not recognized in a timely manner, will compromise on the safety of the system. This is because normal working of the critical systems will lead to safe working of a nuclear reactor. In literature several fault diagnosis techniques are common. These methodologies have been discussed in chapter 2. We use the mathematical model technique of fault detection due to the advantages possessed over the other methods. But model based approaches require that all the state variables that define the model are present. In practice, this is far from reality due to economic and practical considerations. Therefore an observer is highly suitable. In chapter 5 we presented a brief overview of Luenberger and Sliding Mode observer. As discussed in section 5.3, we need to use an observer which can successfully account for the nonlinearities present in the system. In addition an observer should be able to estimate the state variables with finite convergence time irrespective of parametric variations, bounded disturbances and noise. Sliding Mode Observer satisfies all these features and in this thesis, we focus on the use of sliding mode observers to estimate the state variables and finally leading to fault detection.

A basic flow diagram of use of sliding mode observer subject to mathematical model of fault detection is shown in Fig. 6.15.

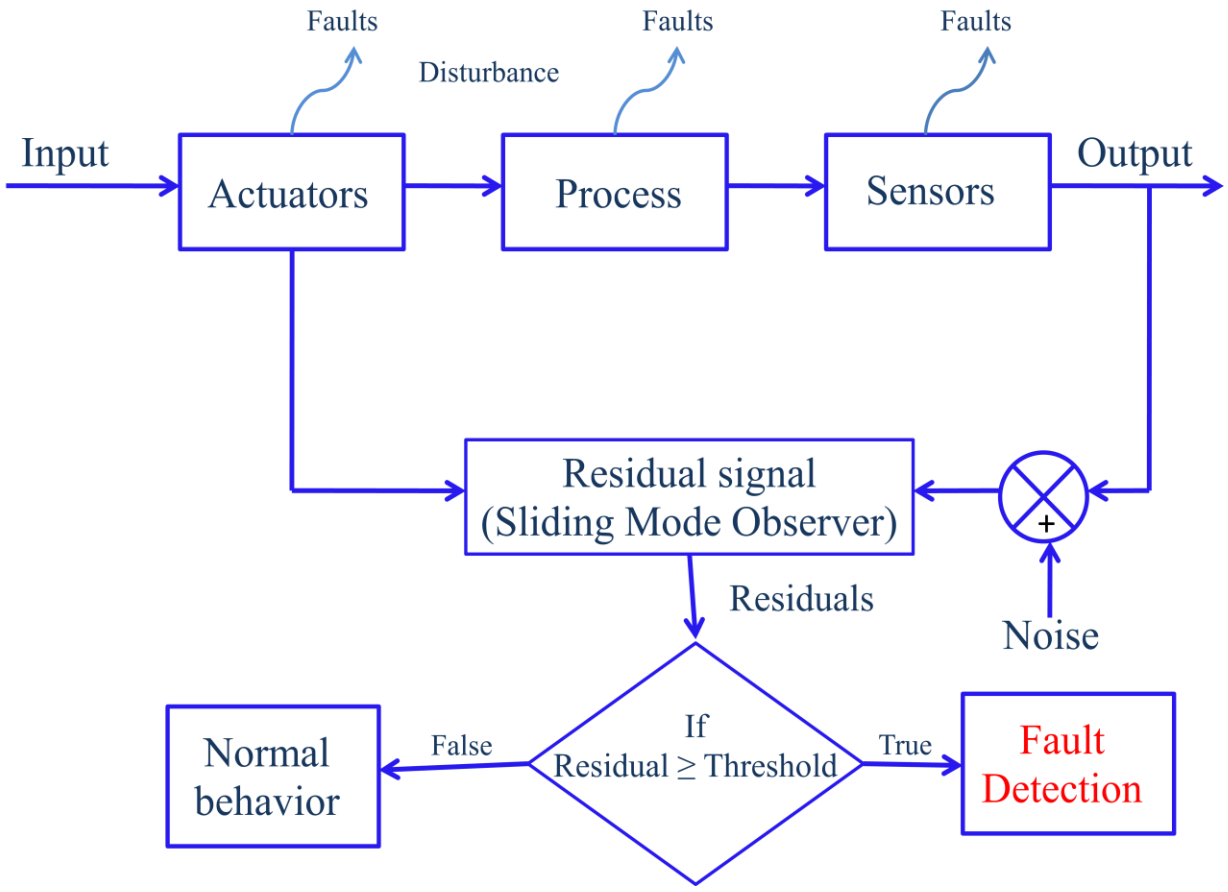

Figure 6.15: General model of Fault Detection System using Sliding Mode Observer

As is evident from Fig.6.15, we need to calculate the residuals which are nothing but the difference between the actual and estimated output. This residual evaluation is carried out with respect to a pre-determined threshold. This threshold is conservative enough to account for a fault. The threshold is selected such that the fault detection system should not give rise to unnecessary interrupts due to the variations of a necessary parameter. A detailed calculation of threshold is out of the scope of this thesis.

6.2.1 Design Methodology of Fault Detection Using Sliding Mode Observers

We present the fault detection system for nuclear and non-nuclear systems in a nuclear reactor. In the first case we discuss the fault detection due to actuator and sensor faults in control rod drive and coolant sensor. In the latter part of this chapter, we consider a failure in the steam generator. To simplify the analysis, let us first consider the evaluation of residue for a general system.

$$\dot{x}_1 = x_2 + u + f_a \qquad 6.38$$

$$\dot{x}_2 = f\left(x_1, x_2, t\right)$$

$$y = x_1 + f_s$$

where

$x_1, x_2 \rightarrow$ States of the system

$y \rightarrow$ Output state of the system

$u \rightarrow$ Control input

$f_a \rightarrow$ Actuator fault

$f_s \rightarrow$ Sensor fault

The function $f\left(x_1, x_2, t\right)$ can be linear or nonlinear but is bounded. On simple inspection of (6.38), we can conclude that an actuator fault directly influences one of the state of the system. In addition, we can conclude that due to a sensor fault, there is an error in measurement of the output.

Using the general case of design of sliding mode observer for a fault free system presented in section 5.3 we get

$$\dot{\hat{x}}_1 = x_2 + u + \delta_1 sign\left(e_1\right) \tag{6.39}$$

$$\dot{\hat{x}}_2 = f\left(\hat{x}_1, \hat{x}_2, t\right) + \delta_2 sign\left(\bar{e}\right)$$

$$\hat{y} = \hat{x}_1$$

where

$e_1 = y - \hat{y}$ is the error vector.

$e_2 = x_2 - \hat{x}_2$ is an another error vector.

$\delta_1, \delta_2 \rightarrow$ Observer gain

After the error due to measurement quantity tends to zero, the time derivative of the error also tends to zero in finite time. Then according to equivalent control approach,

$$\bar{e} = \left(\delta_1 sign\left(e_1\right)\right)_{eq}.$$

The error vector dynamics can be calculated as

$$\frac{de_1}{dt} = e_2 - \delta_1 sign\left(e_1\right) \tag{6.40}$$

$$\frac{de_2}{dt} = f\left(x_1, x_2, t\right) - f\left(\hat{x}_1, \hat{x}_2, t\right) - \delta_2 sign\left(\bar{e}\right) \tag{6.41}$$

To reduce the error e_1 equal to zero in finite time, we employ Lyapunov stability approach. The Lyapunov function is chosen as

$$V = \frac{1}{2} e_1^2$$

The time derivative of the above function is given by

$$\dot{V} = e_1 \dot{e}_1 = e_1\left(e_2 - \delta_1 sign\left(e_1\right)\right)$$

We need to choose $\delta_1 > \max|e_2|$ to satisfy the Lyapunov condition. We can perform a similar working to calculate δ_2.

By considering actuator and sensor faults, the error dynamics is written as

$$\frac{de_1}{dt} = e_2 + f_a + \dot{f}_s - \delta_1 sign(e_1) \tag{6.42}$$

As the error vectors e_1 and e_2 tend to zero after choosing the observer gains by satisfying Lyapunov condition, (6.42) reduces to

$$\left(\delta_1 sign(e_1)\right)_{eq} = f_a + \dot{f}_s$$

The equivalent control signal is obtained by passing the input signal to a low pass filter. Now, the residue can be calculated as

$$r = \left(\delta_1 sign(e_1)\right)_{eq} = f_a + \dot{f}_s \tag{6.43}$$

If faults are present in the system, then sharp spikes are present in the residual signal. To remove false faults which may be due to process changes we need to select a threshold value carefully. If ε is a constant threshold value, then the fault exists for time $t \geq t_f > 0$ where t_f is the duration of fault occurrence if $|r| \geq \varepsilon$. If no faults are present then the residual value is zero.

6.2.2 Fault Detection in the Nuclear Reactor Core

The nuclear reactor core is governed by a system of equations related to reactor power, decayed neutron precursor concentration, fuel and coolant temperature. We have already discussed the point reactor model in great detail in chapter 3. .Let us consider a single group delayed neutron precursor with absence of independent neutron source. Then the point kinetic model for a single delayed group of precursor is given by (6.1) and (6.2),

The effect of fuel rod and coolant dynamics is included in the model. The fuel temperature and coolant temperature is given by

$$\dot{T}_f = \frac{1}{\mu_f}\left[f_f P_{a0} P - \Omega\left(T_f - T_c\right)\right] \tag{6.44}$$

$$\dot{T}_l = \frac{1}{\mu_c}\left[\left(1 - f_f\right) P_{a0} P + \Omega\left(T_f - T_c\right) - M\left(T_l - T_e\right)\right] \tag{6.45}$$

where

$T_f \rightarrow$ Average Fuel Temperature

$T_c \rightarrow$ Average Coolant Temperature

$T_l \rightarrow$ Reactor outlet Temperature

$T_e \rightarrow$ Reactor Inlet Temperature

Now the reactivity considering the coefficients due to fuel and coolant temperature is

$$\rho = \rho_{ext} + \alpha_f \left(T_f - T_{f0}\right) + \alpha_c \left(T_c - T_{c0}\right) P \qquad 6.46$$

where

$\alpha_f, \alpha_c \rightarrow$ Feedback coefficients for fuel and coolant temperature respectively

$T_{f0} \rightarrow$ Equilibrium temperature of fuel

$T_{c0} \rightarrow$ Equilibrium temperature of coolant

Let us consider an actuator fault due to control rod drive mechanism. This is reflected in the reactivity input to the point reactor kinetic equation. Substituting (6.46) in (6.1), with actuator fault, we get

$$\dot{P} = \left(\frac{\left(\rho_{ext} + f_a\right) - \beta}{\Lambda} \right) P + \frac{\alpha_f}{\Lambda} \left(T_f - T_{f0}\right) P + + \frac{\alpha_c}{\Lambda} \left(T_c - T_{c0}\right) P + \lambda C \qquad 6.47$$

Now the sensor faults are considered in power flow channel and coolant temperature channel. Let f_{s1} and f_{s2} be the two sensor faults which correspond to power channel and coolant channel respectively. We need to design a Sliding Mode Observer by addition of discontinuous control. The measurable outputs are power and coolant temperature with corresponding faults which can be written as

$$y_1 = P + f_{s1} \qquad 6.48$$

$$y_2 = T_c + f_{s2}$$

By following the design procedure employed in the earlier chapter, we formulate a general Sliding Mode Observer with two measurable outputs as

$$\dot{\chi}_i = p_i \left(y_i - \chi_i\right) + \delta_i sign\left(y_i - \chi_i\right) \; ; \; i = 1,2 \qquad 6.49$$

where

$\chi_i \rightarrow$ Estimate of y_i

$p_i, \delta_i \rightarrow$ Observer gain

The error vector corresponding to two outputs present in the system can be written as $e_i = y_i - \chi_i \; ; \; i = 1,2$

In this section, we have not calculated the observer gains p_i, δ_i. Nevertheless the procedure illustrated in section 5.3 is to be followed. The important parameter in fault detection analysis is the calculation of residue. We employ equivalent control approach to calculate the residue function.

For a two output case, residue can be denoted as

$$r_i = \left(\delta_i sign\left(e_i\right)\right)_{eq} \; ; \; i = 1,2 \qquad 6.50$$

As discussed in the section 4.3.2, we use a first order low pass filter to filter out the high frequency terms.

Simulation results

We carry out the simulation for analyzing the fault detection mechanism. The faults considered in the system are either from an actuator or a sensor. For ease of understanding we consider one fault at a time.

Case 1:

Let us consider a fault in sensing the reactor power. We also assume that a measurement noise with standard deviation of 0.32 is present in the system. The sensor fault is represented in the Fig. 6.17 (a). The data for other parameters are as given in the Table 3.3. The reactor power variation is shown in Fig. 6.16. There is sudden increase in power at which fault occurs.

The corresponding residual signal is calculated from the procedure outlined above. We employ a low pass filter with cutoff frequency of 100 Hz to realize the equivalent control approach. The corresponding residual signal is shown in Fig. 6.17. From Fig 6.17(b), we can observe that during the sensor fault we obtain spikes when the fault occurs. As this is an impulse fault where the fault gets rectified within a short span of time, we encounter two sharp edged peaks crossing the threshold in the residual signal.

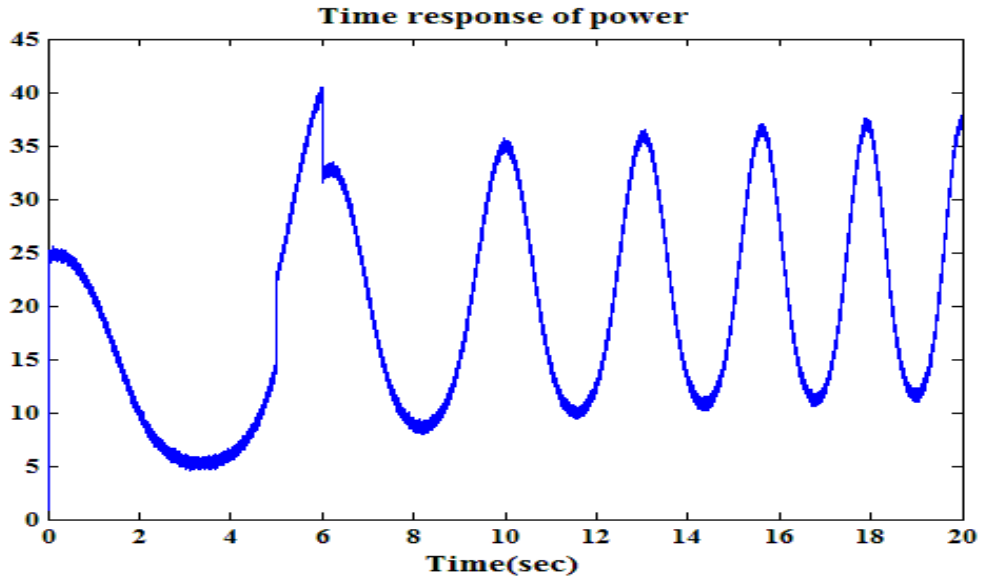

Figure 6.16: Reactor power variation during sensor fault in power measurement channel

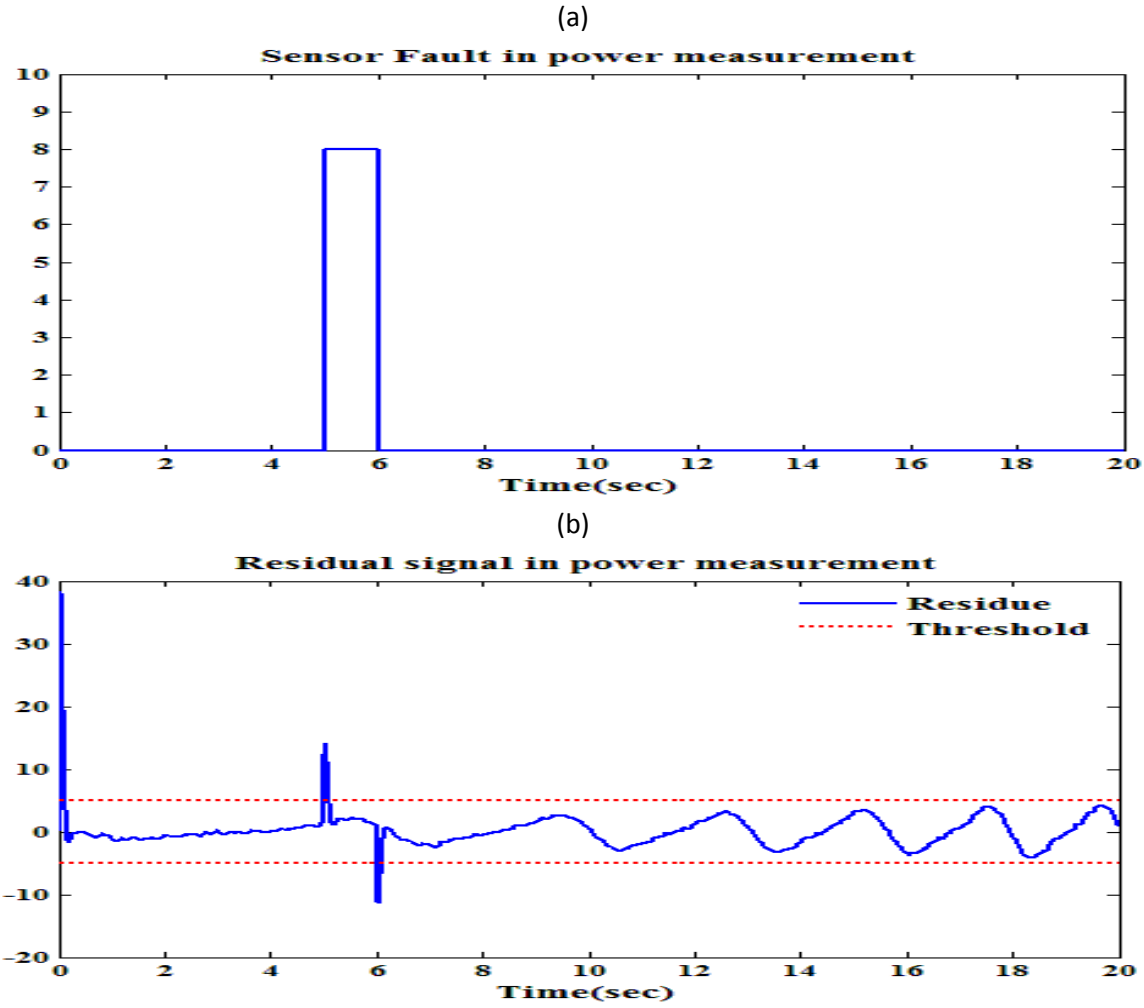

Figure 6.17: Generation of residual signal due to sensor fault in power measurement channel. Fig. 6.17 (a) provides a short pulse signal acting as a sensor fault. Fig. 6.17 (b) shows the corresponding residual signal.

Case 2:

Let us consider a fault in sensing the coolant temperature. The sensor fault is represented in the Fig 6.19 (a). The data for other parameters are as given in the Table 3.3. The coolant temperature variation at which sensor fault occurs shows a sudden increase and gets stabilized after some time as shown in Fig. 6.18.

The corresponding residual signal is calculated from the procedure outlined above. We employ a low pass filter with cutoff frequency of 100 Hz to realize the equivalent control approach. The corresponding residual signal is shown in Fig. 6.19. From Fig 6.19 (b), we can observe that during the sensor fault we get a sharp edge when the fault occurs. As this is a step fault where the fault is present for all the considered time, we encounter only one sharp edged peak crossing the threshold in the residual signal.

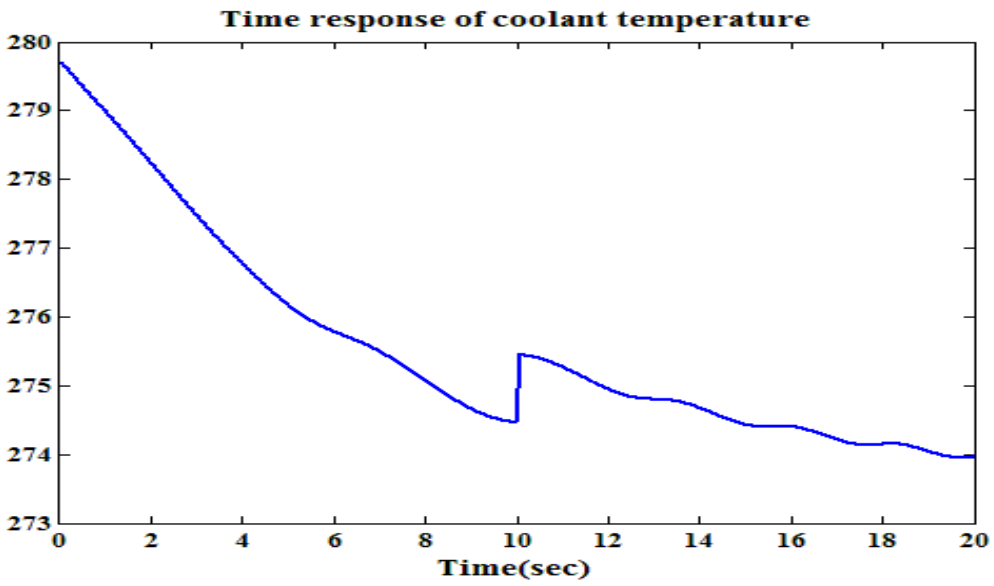

Figure 6.18: Reactor power variation during sensor fault in coolant temperature measurement channel

(a)

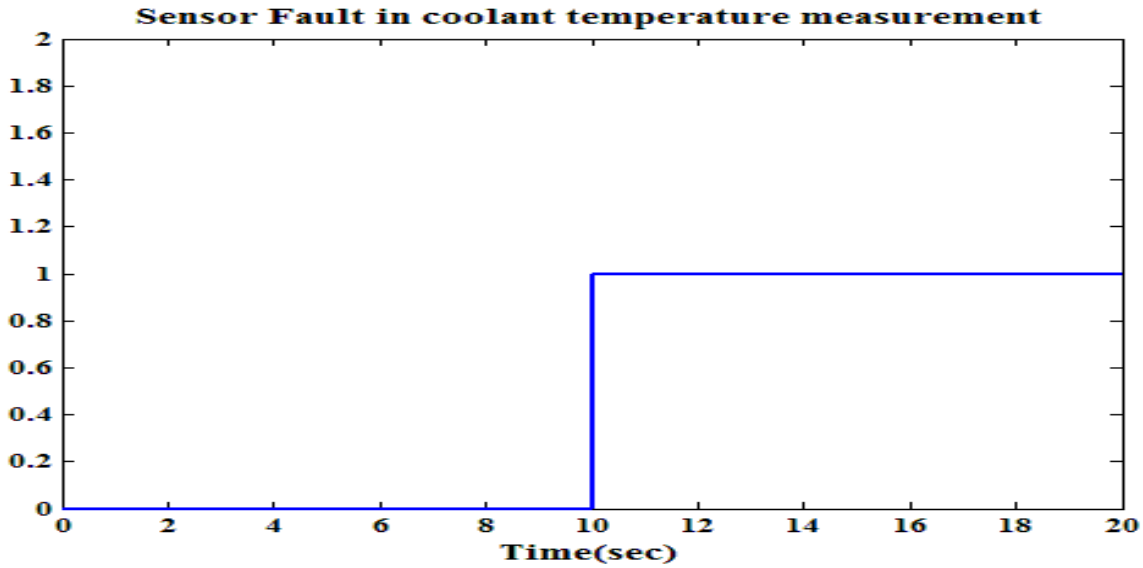

(b)

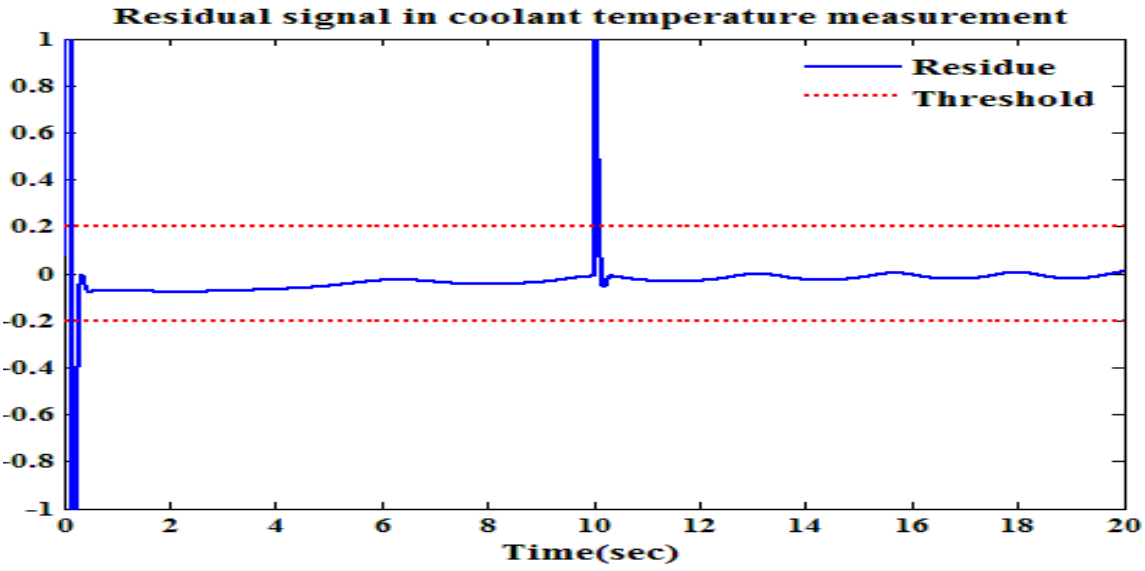

Figure 6.18: Generation of residual signal due to sensor fault in coolant temperature measurement channel. Fig. 6.18 (a) provides a short pulse signal acting as a sensor fault. Fig. 6.18 (b) shows the corresponding residual signal.

Case 3:

Let us consider an actuator fault in the control rod mechanism. This directly affects the reactivity change in the nuclear reactor system. The actuator fault is represented in the Fig. 6.21 (a). The data for other parameters are as given in the Table 3.3. The actuator fault occurs at 15 seconds where there is a sudden increase in reactor power. The response of reactor power is shown in Fig. 6.20.

The corresponding residual signal is calculated from the same procedure. A low pass filter with cutoff frequency of 100 Hz is used for equivalent control after the measurement error tends to zero. The corresponding residual signal is shown in Fig. 6.21. From Fig. 6.21 (b), we can observe that during the actuator fault we obtain sharp spikes exactly at the instant where there is rapid change in the value. As this is an impulse fault where the fault gets rectified within a short span of time, we encounter two sharp edged peaks crossing the threshold in the residual signal.

On comparison of both the faults we can observe that actuator faults produce large oscillations and develop very large signal residues. On the other hand, the sensor faults are sharp signals with very low oscillations. The sensor faults produce independent residue signals and therefore can be isolated easily. But in case of actuator fault, the appearance will be in power measurement channel. Therefore its isolation is difficult. It can be isolated by the presence of oscillations.

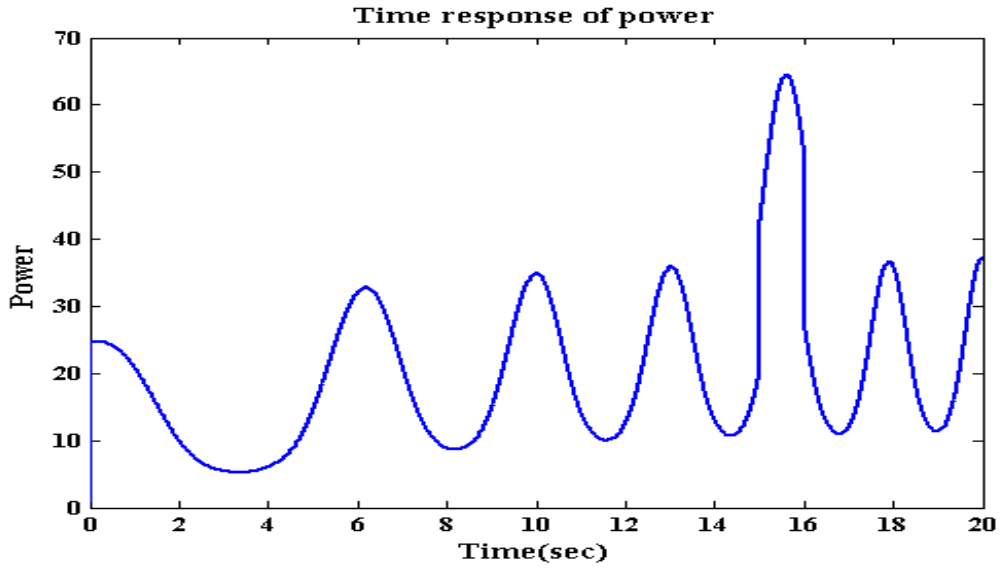

Figure 6.20: Reactor power variation during actuator fault

(a)

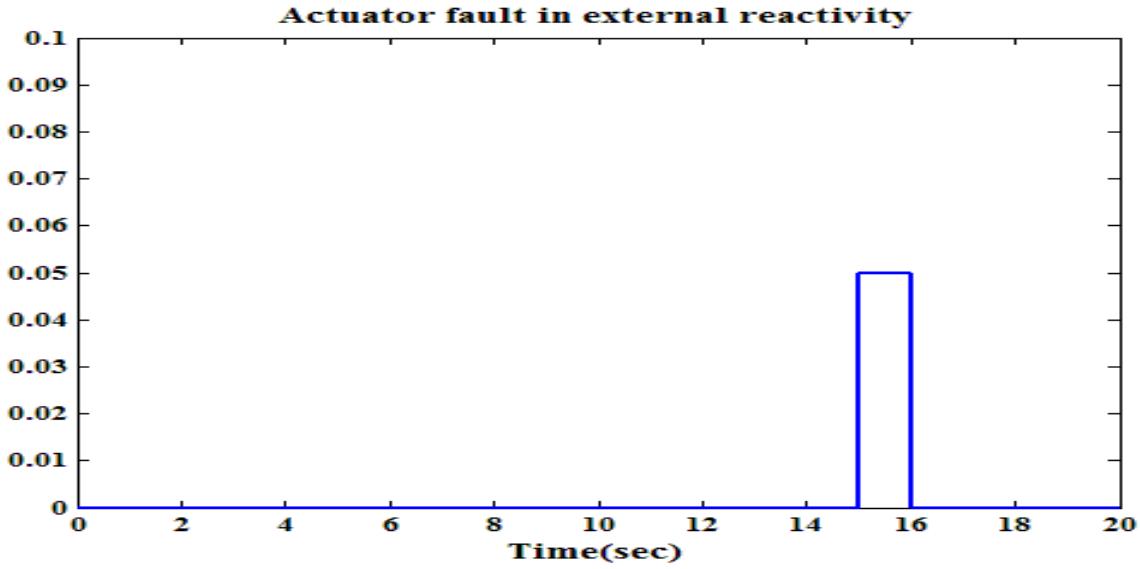

(b)

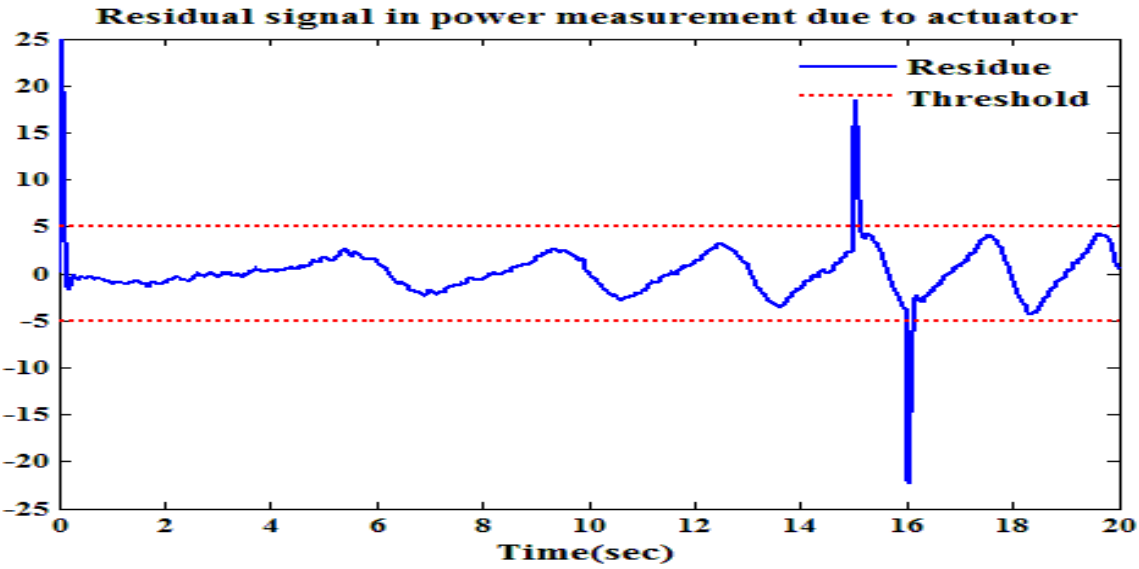

Figure 6.21: Generation of residual signal due to actuator fault in power measurement channel. Fig. 6.21 (a) provides a short pulse signal acting as an actuator fault. Fig. 6.21 (b) shows the corresponding residual signal.

6.2.3 Fault Detection in the Steam Generator

Steam Generator is one of the important non-nuclear components of a nuclear power plant. In steam generator, maintenance of water mass inventory is very important for safe and reliable operation of nuclear power plant. If there is low water level in the steam generator, then there is improper heat transfer between primary and secondary coolant circuits. This will subsequently trip the reactor by damaging the blades of a turbine.

A mathematical model is required to derive the actual insights of the dynamics. It is also necessary to design a controller or an observer with the help of a mathematical model. Irving proposed a comprehensible model to explain the operation of a steam generator [33]. This model is represented as

$$\dot{x}_1 = G_1(u - v) \tag{6.51}$$

$$\dot{x}_2 = -\tau_2^{-1} x_2 - G_2 \tau_2^{-1}(u - v) \tag{6.52}$$

$$\dot{x}_3 = -2\tau_1^{-1} x_3 + x_4 + G_3 u \tag{6.53}$$

$$\dot{x}_4 = \left(-\tau_1^{-1} - 4\pi^2 T^{-2}\right) x_3 \tag{6.54}$$

$$y = x_1 + x_2 + x_3 \tag{6.55}$$

where

$x_1 \rightarrow$ Water level in steam generator

$x_2 \rightarrow$ Reverse dynamic effect

$x_3 \rightarrow$ Mechanical oscillation

$x_4 \rightarrow$ Time derivative of x_3

$f_s \rightarrow$ Sensor fault

$\tau_1, \tau_2 \rightarrow$ Damping constants

$T \rightarrow$ Mechanical oscillation period

$u \rightarrow$ Feed water flow rate

$v \rightarrow$ Steam flow rate

y is the system output which accounts for thermal hydraulic conditions with mechanical effects.

Taking Laplace transform of (6.51-6.55), we get

$$y(s) = x_1(s) + x_2(s) + x_3(s)$$

$$y(s) = \frac{G_1}{s}\left(u(s) - v(s)\right) + \frac{G_2}{\tau_2 s + 1}\left(u(s) - v(s)\right) + \frac{G_3}{\left(s^2 + 2\tau_1^{-1} s + \tau_1^{-2} + 4\pi^2 T^{-2}\right)} u(s) \tag{6.56}$$

G_1/s is the mass capacity effect of the steam generator. The steam flow difference can be given by $(u-v)$. Now $\frac{dx_1}{dt}$ gives the change in the water level due to the steam flow difference. This is an important term because the first term provides the actual water capacity required to remove the primary decay heat. The parameter G_1 is independent of reactor power and hence it remains constant. $G_2(\tau_2 s+1)$ is the thermal negative effect caused by 'swell and shrink' phenomenon. The first order equation representing the swell and shrink phenomenon exhibits decaying exponential response for a step input of flow rate. With respect to a steam generator, the swell and shrink phenomenon is explained as follows. As the steam flow rate increases, the pressure on the upper region of the steam generator decreases. With pressure inversely related to volume at a constant temperature then, the two phase flow mixture expands with an increase in the water level. This phenomenon is called 'Swell'. In the other case, as the feed-water flow rate is increased, the pressure increases. The steam bubbles in the two phase flow mixture collapse with decrease in water level. This phenomenon is called 'Shrink'.

$\frac{G_3}{\left(s^2+2\tau_1^{-1}s+\tau_1^{-2}+4\pi^2T^{-2}\right)}u(s)$ gives the mechanical oscillation effect due to the momentum possessed in the down comer by inflow of the feed water to the steam generator

If the feed-water flow rate is suddenly decreased, then the water level in the down comer falls initially and starts to oscillate. This is because the recalculating flow goes down at the start and then slows down. The oscillation effect gets dampened after some time constants. The value of G_3 is positive and varies with reactor power.

As mentioned in the preceding paragraph, some parameters are linearly varying with respect to reactor power. A proportional integral controller is used for controlling the water level in the steam generator [21]. Mathematically it is represented as,

$$u = K_p\left(e_f + A_l e_l\right) + K_i\int\left(A_f e_f + e_l\right)dt \tag{6.57}$$

where

$e_f = v-u \rightarrow$ Flow error

$e_l = y_{ref} - y \rightarrow$ Level error

$y_{ref} \rightarrow$ Reference water level

$y \rightarrow$ Water level

Following the design procedure carried out for a general system in section 5.3. The sliding mode observer for calculation of residual signal is given by

$$\dot{\hat{x}}_1 = G_1(u-v) + \delta_1 sign(e_1) \tag{6.58}$$

$$\dot{\hat{x}}_2 = -\tau_2'^{-1}\hat{x}_2 - G_2'\tau_2'^{-1}(u-v) + \delta_1 sign(e_1) \quad 6.59$$

$$\dot{\hat{x}}_3 = -2\tau_1'^{-1}\hat{x}_3 + \hat{x}_4 + G_3'u + \delta_1 sign(e_1) \quad 6.60$$

$$\dot{\hat{x}}_4 = \left(-\tau_1'^{-1} - 4\pi^2 T'^{-2}\right)\hat{x}_3 + \delta_2 sign(\bar{e}) \quad 6.61$$

$$\hat{y} = \hat{x}_1 + \hat{x}_2 + \hat{x}_3 \quad 6.62$$

where

$(\hat{x}_1, \hat{x}_2, \hat{x}_3, \hat{x}_4, \hat{y}) \rightarrow$ Estimates of (x_1, x_2, x_3, x_4, y)

The error vector corresponding to only one measurable output (water level in a steam generator) is given by $e_1 = y - \hat{y}$

Applying equivalent control approach, the error vector $\bar{e}$ can be calculated as

$$\bar{e} \rightarrow \left(\delta_1 sign(e_1)\right)_{eq} = x_4 - \hat{x}_4$$

Again in this section, we have not calculated the observer gains δ_1, δ_2. Nevertheless the procedure illustrated in section 5.3 is to be followed. We now focus on calculating the residual signal. Equivalent control approach is used to calculate the residue function. In this case, there is only one measurable quantity, therefore the two output residue considered in (6.50) is reduced to

$$r = \left(\delta_1 sign(e_1)\right)_{eq} \quad 6.63$$

As discussed in the section 4.3.2, we use a first order low pass filter to filter out the high frequency terms.

Simulation Results

To analyze an application of sliding mode observer for fault detection in a steam generator, we carry out the simulation. The fault may be from an actuator or a sensor. The faults considered for this simulation is shown in Fig. 6.22 (a). Following cases are considered to analyze the fault detection in a steam generator at two different power levels.

Table 6.1: Steam Generator model parameters

Parameter	Low Power	High Power
G_1 (mm*s/kg)	0.058	0.058
G_2 (mm*s/kg)	9.63	1.05
G_3 (mm*s/kg)	0.181	0.215
T (s)	119.6	14.2
t_1 (s)	41.9	34.8
t_2 (s)	18.4	3.6
v (kg/s)	57.4	660.2

Case 1:

Let us carry out this mechanism at low power. In other words, let us consider that the steam generator is operating at a power level less than 15% of the total power. The corresponding values for the model and the observer are chosen from Table 6.1.

We also assume that a measurement noise with standard deviation of 0.32 is present in the system. We also assume that there is no flow error. The parameters for Proportional Integral (PI) controller are selected by proper tuning,

The corresponding residual signal is calculated from the procedure outlined above. We employ a low pass filter with cutoff frequency of 100 Hz to realize the equivalent control approach. The corresponding residual signal is shown in Fig. 6.22 (b). From Fig. 6.22 (b), we can observe that during the sensor fault we get sharp edges when an actuator fault or sensor fault occurs. In addition, when a sensor fault occurs, a significantly higher spike is obtained than during an actuator fault. This is justified by considering (6.43) where the residual signal is dependent on the derivative of a discontinuous fault signal.

Case 2:

In this case, we consider the operation of a steam generator at 100% power. The parameters used are selected from the Table 6.1 for power level of 100%. We assume that a measurement noise with standard deviation of 0.32 is present. Contrary to an earlier case where flow error is assumed to be zero, here we consider both level and flow error to be finite. The corresponding parameters of PI controller are chosen.

We carry out a similar procedure for evaluating the residual signal. During high power operation of steam generator, the residual signal is shown in Fig. 6.22 (c). By carrying out a similar analysis discussed in the previous case, larger spikes for sensor faults are resulted than actuator faults. We conclude that the designed fault detection mechanism works for both low power and high power.

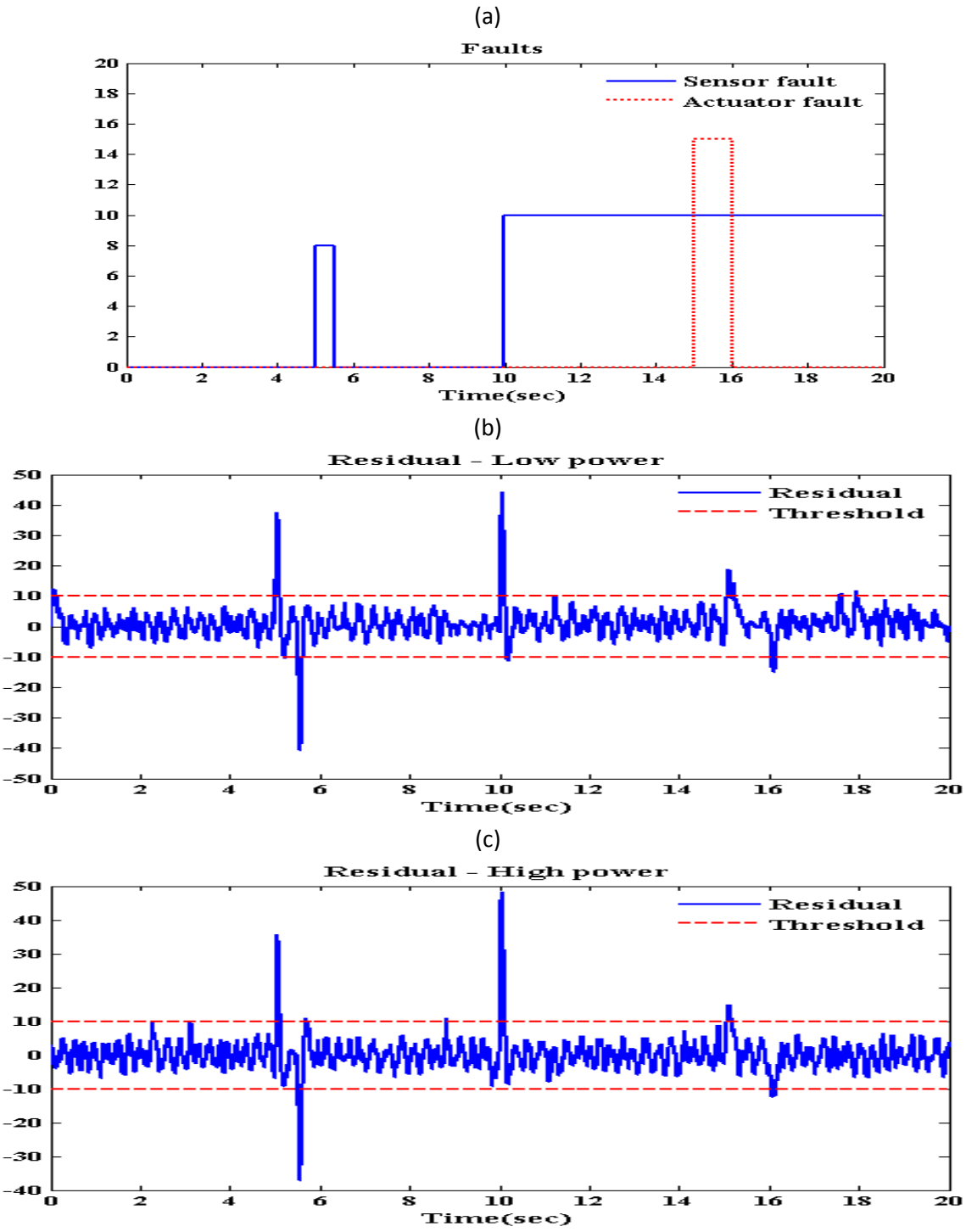

Figure 6.22: Generation of residual signal due to actuator and sensor fault at low and high power operation of a steam generator. Fig. 6.22 (a) provides an account of different types of faults. Fig. 6.22 (b), (c) shows the corresponding residual signal during low and high power respectively.

Chapter 7

Higher Order Sliding Modes

The previous section dealing with the first order sliding modes is based on the same way where a discontinuous control would switch between the states accompanied by a very high feedback gain. From the results presented in section 6.1, we conclude that boundary layer approach was employed to minimize the effect of chattering. This approach also resulted in the loss of robustness [26] due to weak response to any slight deviation in the parameter. Further the fundamental idea of sliding mode is being compensated. A need to develop a method which minimizes the chattering behavior along with the presence of inherent robustness is highly essential.

In this regard, the development of Higher Order Sliding Modes (HOSM) aims to extend the original sliding mode theory by taking higher order time derivatives of the deviation from the constraint. This method preserves the ideas of the original sliding mode theory with an advantage of chattering minimization. Therefore there is an increase in the sliding order and accuracy of the system parameters calculated using this method.

7.1 Mathematical background of HOSM

A brief mathematical theory involving HOSM is dealt in this section. The background of analysis is similar to standard sliding modes and therefore the section 4.2 is used in this chapter. Similar to standard sliding modes of first order, HOSM also considers the solution of a given system in Flippov's sense. In other words, the state trajectory of the system is considered in terms of Flippov's sense. An elaborate discussion of Flippov's method is carried out in the previous section.

The fundamental objective of sliding mode theory is to keep the constraint $s = 0$. This confirms that the state trajectory resides on the designed sliding surface for all the time. We define a term sliding order denoted by r as the number of continuous total derivatives of s in the vicinity of the sliding mode.

From the definition of the sliding mode, it is necessary for a r^{th} order sliding mode to satisfy

$$s = \dot{s} = \ddot{s} = ... = s^{r-1} = 0 \tag{7.1}$$

On analysis of the above equation, we infer that for a r^{th} order sliding, we form a r - dimensional condition for a given system. Also, we note that for a r^{th} order sliding $r-1$ continuous time derivatives are required. In the earlier case of 1-order sliding, $\dot{s}$ is discontinuous. This is an essential drawback of HOSM where extra information is essential to implement HOSM. This extra information in terms of higher order time derivatives may not be available in a real time practical system. An approach to minimize this drawback will be dealt later. An approach of robust exact differentiator estimates the derivatives of the sliding variable in a robust manner.

HOSM may exhibit asymptotic finite time convergence unlike the first order sliding mode. A sliding precision of r^{th} order with respect to the measurement interval is obtained by using HOSM. The definition of higher order sliding mode is described below [26]

Definition 1: *It is said that there exists a first (or second) order sliding mode on manifold* S *in a vicinity of a first (or second) order sliding point* x*, if in this vicinity of point* x *the first (or second) order sliding set is an integral set, i.e. it consists of Filippov's sense trajectories.*

If S is a smooth manifold containing points where the first order sliding mode exists. We can define another manifold S_2 where the condition remains same as in the case of first order sliding modes. This process can be continued to achieve any arbitrary order sliding modes.
With respect to constraint function, we can define HOSM as

Definition 2: *Let the* r *sliding set (7.1) be non-empty and assume that it is locally an integral set in Filippov's sense. Then the corresponding motion satisfying (7.1) is called an* r *-sliding mode with respect to the constraint function.*
The relation (7.1) assures that the all the $r-1$ total time derivatives are continuous.
An important behavior of state trajectory is that the state trajectories do not lie on in the tangential vector space T to the manifold $s=0$. When a switching error is present the trajectory leaves the manifold at a certain angle defined by the discontinuous function. In case of second order sliding all the possible state vectors lie in the tangential space to the sliding manifold even when a switching error is present. In this work, we restrict to a discussion of second order sliding mode only.

7.2 Design of Second Order Sliding Mode Algorithms

Before we begin with the second order sliding mode algorithms, we carry out a generalized approach [18].
Consider the system defined by

$$\dot{x} = f(t,x,u);\ s = s(t,x) \in \Re;\ u = U(t,x) \in \Re \qquad 7.2$$

where

$x \in \Re$, u is the control signal and f, s are smooth functions.

The goal of the sliding mode is to keep $s=0$. Using the relative degree concept explained in Appendix, we divide our approach into two cases.

(a) Relative degree r = 1, that is $\frac{\partial \dot{s}}{\partial u} \neq 0$

(b) Relative degree r $\geq$ 2, that is $\frac{\partial s^{(i)}}{\partial u} = 0\ (i = 1,2,.....r-1)\ ;\ \frac{\partial s^{r}}{\partial u} \neq 0$

Case (a):

This case is similar to the first order sliding mode dealt elaborately in Chapter 4.

Taking the total derivative of s, we get

$$\dot{s} = \frac{\partial}{\partial t} s(t,x) + \frac{\partial}{\partial x} s(t,x)\, f(t,x,u)$$

Differentiating again

$$\ddot{s} = \frac{\partial}{\partial t} \dot{s}(t,x,u) + \frac{\partial}{\partial x} \dot{s}(t,x,u)\, f(t,x,u) + \frac{\partial}{\partial u} \dot{s}(t,x,u)\dot{u}(t)$$

$$\ddot{s} = A(t,x) + B(t,x)\dot{u}(t)$$

Case (b):

Let us consider a system with relative degree two. From the definition of relative degree, we can say that in this case u is one of the state variable with the actual control signal given by $\dot{u}$. Now the system is given by

$$f(t,x,u) = a(t,x) + b(t,x)u(t)$$

where a, b are smooth functions.

Assumptions:

To achieve the goal of keeping $s = 0$, following conditions are assumed

(1) Control values belong to the set $U = \{u : |u| \le U_M\}$, where $U_M > 1$ is a real constant. We define that the solution is well defined if $u(t)$ is continuous $\forall t$.

(2) There exists $u_1 \in (0,1)$ such that for any continuous function $u(t)$ with $|u(t)| > u_1$. For every $t > t_1$, $s(t)u(t) > 0$

(3) There are positive constants s_0, $u_0 < 1$, P, Q such that if $|s(t,x)| > s_0$ then

$$0 < P \le \frac{\partial \dot{s}}{\partial u} \le Q \;\; ; \;\; \forall u \in U$$

(4) There is a positive constant C_0 such that within the region $|s(t,x)| < s_0$ where the following inequality holds for $\forall u \in U;\ \forall t$

$$\left| \frac{\partial}{\partial t} \dot{s}(t,x,u) + \frac{\partial}{\partial x} \dot{s}(t,x,u)\, f(t,x,u) \right| \le C_0$$

From condition (2), we can achieve a control signal $u(t)$ which directs the sliding variable onto a sliding surface independent of initial condition. The sliding mode is bounded by the conditions (3) and (4).

Now, on differentiating the derivative of the sliding variable twice, we get

$$\ddot{s} = A(t,x) + B(t,x)u(t)$$

$$|A(t,x)| \le C_0 \ ; \ 0 < P \le B(t,x) \le Q \ ; \ C_0 > 0$$

The prominent 2-sliding algorithms are discussed with relevant examples are discussed in the next section.

7.2.1 Twisting Algorithm

This algorithm has a distinguishing feature of state trajectories twisting infinite number of times around the origin with finite time convergence.

This algorithm is applicable for relative degree one as well as two. Let us first consider relative degree one system.

The second order sliding mode control problem for relative degree one can be written as

$$\dot{x}_1 = x_2$$
$$\dot{x}_2 = A(t,x) + B(t,x)\dot{u} \qquad 7.3$$

Even though x_2 is immeasurable but its sign can be known by evaluating $\text{sgn}\left(x_1(t) - x_1(t-T)\right)$ where T is the measurement interval. The uncertain smooth functions are defined in a similar way as that of the general case.

$$|A(t,x)| \le C_0 \ ; \ 0 < P \le B(t,x) \le Q \ ; \ C_0 > 0$$

From (7.3), it is clear that we require the time derivative of the sliding variable.

The control algorithm is defined by [18]

$$u(t) = \begin{cases} -u & |u| > 1 \\ -\alpha_1 sign(x_1) & |u| \le 1, x_1 x_2 \le 0 \\ -\alpha_2 sign(x_1) & |u| \le 1, x_1 x_2 > 0 \end{cases} \qquad 7.4$$

where

$$\alpha_2 > \alpha_1 > 0$$
$$\alpha_1 > 4Q/s_0 \quad \text{to achieve finite time convergence.}$$
$$P\alpha_2 - C_0 > Q\alpha_1 + C_0$$

In case of relative degree 2

$$u(t) = \begin{cases} -\alpha_1 sign(x_1) & |u| \le 1, x_1 x_2 \le 0 \\ -\alpha_2 sign(x_1) & |u| \le 1, x_1 x_2 > 0 \end{cases} \qquad 7.5$$

7.2.2 Super Twisting Algorithm

The improvement over the previous method is achieved by using super twisting algorithm. The fundamental limitation of twisting algorithm is it requires real-time measurements of $\dot{x}$ or just of sign of $\dot{x}$. So practically knowing x and $\dot{x}$ is a difficult proposition. Therefore it is advisable for a controller to be designed without the knowledge of $\dot{x}$. We can conclude that this algorithm is applicable for relative degree one.

Consider the same system with the assumptions listed in 7.2.

The control law $u(t)$ consists of two terms [18] as

$$u = u_1 + u_2$$

$$\dot{u}_1 = \begin{cases} -u & |u| > 1 \\ -\alpha sign(s) & |u| \le 1 \end{cases} \qquad 7.6$$

$$u_2 = \begin{cases} -\lambda |s_0|^{\rho} sign(s) & |s| > s_0 \\ -\lambda |s|^{\rho} sign(s) & |s| \le s_0 \end{cases}$$

where

$$\alpha > 4Q/s_0 \quad ; \quad \lambda^2 \ge \frac{4QC_0(\alpha + C_0)}{P(\alpha - C_0)} \quad ; \quad 0<\rho \le 0.5$$ to achieve finite time convergence.

The first term is defined by means of its discontinuous time derivative. The second term is a continuous function of the sliding variable.

We achieve an exponentially stable 2-sliding mode $\rho = 1$ is used in the control law. By using $\rho = 0.5$, we can achieve real sliding algorithm of a second order system. This robust algorithm is widely used in robust exact differentiator which is explained in [17].

7.2.3 Simulation Results

Consider an example illustrating second order sliding mode algorithms. Let the mathematical model be [18]

$$\dot{x}_1 = -5x_1 + 10x_2 + 4x_3 + x_1 \sin t + (u^2 - 1)(x_1 - x_2)$$

$$\dot{x}_2 = 6x_1 - 3x_2 - 2x_3 + 3(x_1 + x_2 + x_3)\cos t$$

$$\dot{x}_3 = x_1 + 3x_3 + 4x_2 \cos 5t + 4\sin 5t + 10(1 + 0.5\cos 10t)\mu(u)\phi(x)$$

where

$$\mu(u) = 3u - \cos 30t \sin u - \frac{u^2}{4}$$

$$\phi(x) = \left[x_1^2 + x_2^2 + x_3^2 + 1\right]^{1/2}$$

The sliding variable is

$$\sigma = \frac{x_3}{\phi}$$

(a) Twisting Algorithm

Using the control law given in (7.4), the phase portrait of the given model using twisting algorithm is shown in Fig. 7.1 (a). We can observe that the state trajectories 'twist' around the origin and finally reach the origin in finite amount of time. From Fig. 7.1 (b), the convergence time is nearly 0.3 seconds. Therefore by employing twisting algorithm subject to control shown in Fig. 7.1 (c) we obtain a finite time convergence.

(b) Super Twisting Algorithm

Using the control law given in (7.6), the response of the system is as shown below. Fig. 7.2 (a) provides the phase portrait of the given model using super twisting algorithm. We can observe that the state trajectories twist around the origin similar to the previous case. From Fig. 7.2 (b) the convergence time is nearly 0.15 seconds which is less than that of the twisting algorithm. We can conclude that super twisting algorithm is more robust than twisting algorithm and its applicability to relative degree one system is another potential advantage. The control signal applied in this case is shown in Fig. 7.2(c).

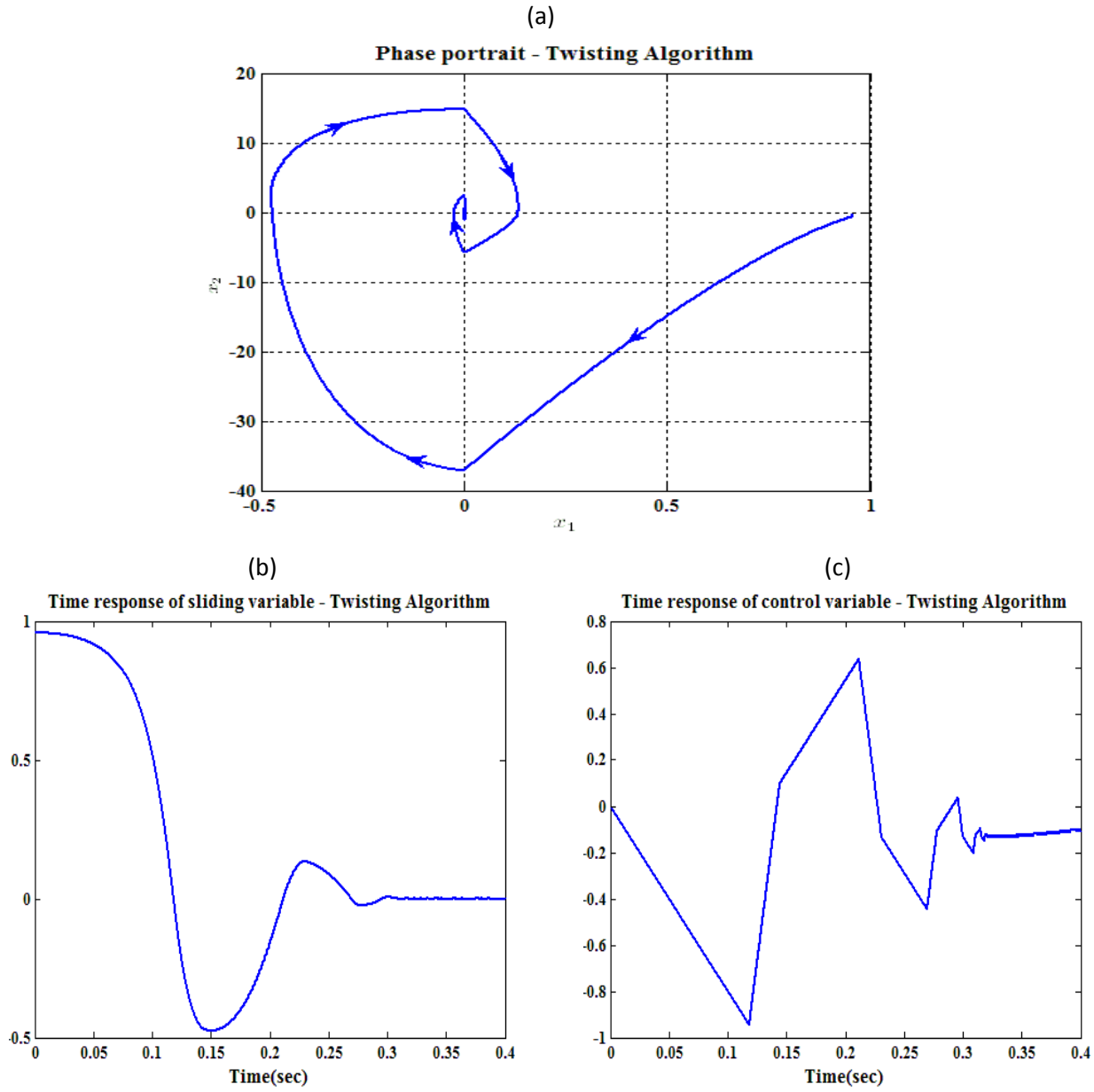

Figure 7.1: Application of Twisting Algorithm to illustrate HOSM. Fig. 7.1 (a) gives the phase portrait. Fig. 7.1 (b) provides the variation of the sliding variable. Fig. 7.1 (c) gives the applied control signal to achieve finite time convergence.

(a)

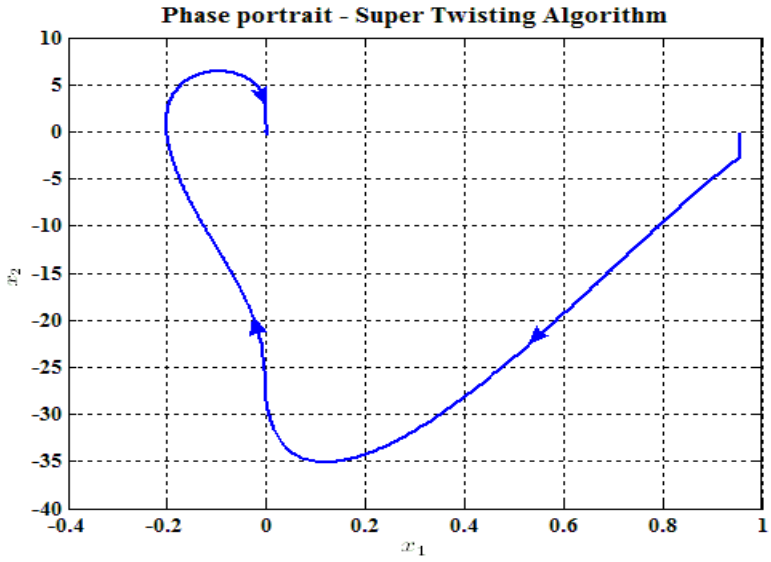

(b)

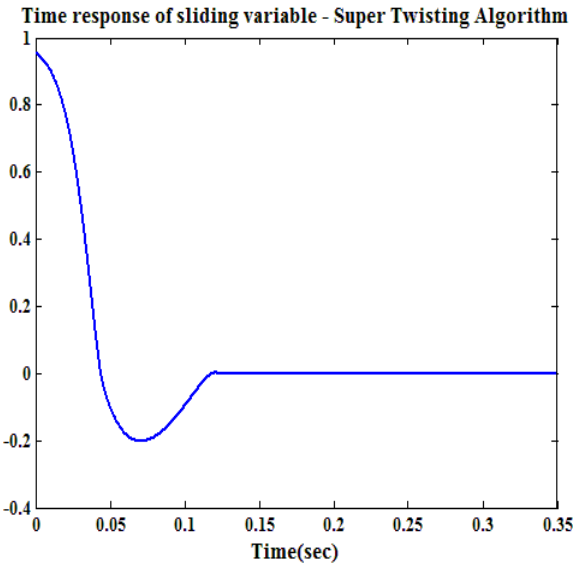

(c)

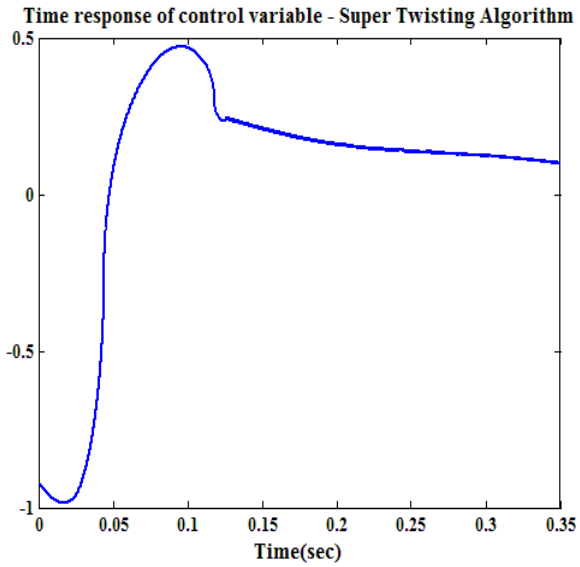

Figure 7.2: Application of Super Twisting Algorithm to illustrate HOSM. Fig. 7.2 (a) gives the phase portrait. Fig. 7.2(b) provides the variation of the sliding variable. Fig. 7.2(c) gives the applied control signal to achieve finite time convergence.

7.3 Super Twisting Observer

A first order sliding mode observer estimates all the immeasurable states with finite reaching time. An application of first order sliding mode observer to nuclear reactor system is discussed with relevant examples in Chapter 6. From the earlier discussion of this chapter, we can remove the chattering behavior by employing a second order sliding mode observer instead of boundary layered approach for reasons mentioned earlier. In comparison to twisting algorithm, super twisting algorithm is more robust and requires less information on the derivatives of sliding variable [25, 26]. Due to these merits, we formulate a super twisting observer.

7.3.1 Design of Super Twisting Observer (STO)

Let us consider a general second order system

$$\begin{aligned} \dot{x}_1 &= x_2 \\ \dot{x}_2 &= f\left(x_1, x_2, t, u\right) + \xi\left(x_1, x_2, t, u\right) \end{aligned} \tag{7.7}$$

where

$x_1, x_2 \rightarrow$ States of the system

$\left| f\left(x_1, x_2, t\right)\right| \le L \; ; L > 0$ with $L \rightarrow$ Lipschitz constant

$f\left(x_1, x_2, t\right) \rightarrow$ Known part

$\xi\left(x_1, x_2, t\right) \rightarrow$ Uncertain part

Now super twisting observer is designed as [19, 23]

$$\begin{aligned} \dot{\hat{x}}_1 &= \hat{x}_2 + \alpha_1 \left(e_1\right)^{1/2} sign\left(e_1\right) \\ \dot{\hat{x}}_2 &= f\left(x_1, \hat{x}_2, t, u\right) + \alpha_2 sign\left(e_1\right) \end{aligned} \tag{7.8}$$

where

$e_1 = x_1 - \hat{x}_1 \; ; e_2 = x_2 - \hat{x}_2$

$F\left(x_1, x_2, t, u\right) = f\left(x_1, x_2, t, u\right) - f\left(x_1, \hat{x}_2, t, u\right) + \xi sign\left(x_1, x_2, t, u\right)$

$\left|F\left(x_1, x_2, t, u\right)\right| < w > \alpha_1$

$$\alpha_2 > \sqrt{\frac{2}{\alpha_1 - w}} \cdot \frac{\left(\alpha_1 + w\right)\left(1 + p\right)}{\left(1 - p\right)} \; ; p > 0$$

This super twisting observer was first proposed by Davilla et al [19] for mechanical systems. On application the point kinetic reactor model defined in (3.4),

$$\dot{\hat{P}} = \left(\frac{\rho_r - \beta}{\Lambda}\right)\hat{P} + \lambda\hat{C} + \alpha_1(s)^{1/2}\, sign(s) \qquad 7.9$$

$$\dot{\hat{C}} = \left(\frac{\beta}{\Lambda}\right)\hat{P} - \lambda\hat{C} + \alpha_2 sign(s)$$

where the sliding variable is defined by $s = P - \hat{P}$.

In this case $\dot{\rho}_r = G_r z_r$ where $G_r \rightarrow$Control rod worth and $z_r \rightarrow$Control rod velocity

7.3.2 Simulation Results

The point kinetic data is taken from Table 5.1.

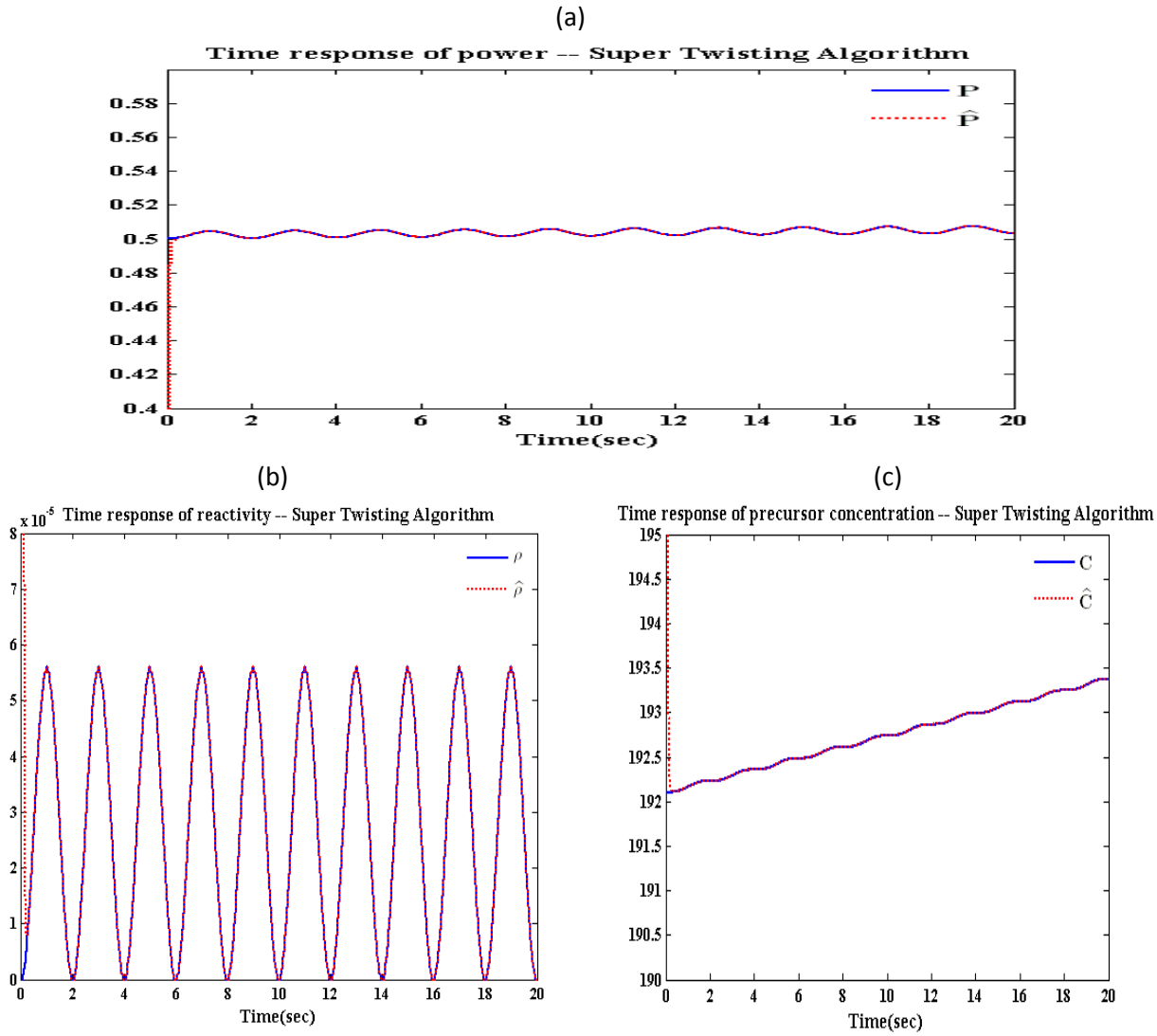

Figure 7.3: Application of Super Twisting Observer in Nuclear Reactor System. Fig. 7.3 (a) gives the reactor power. Fig. 7.3(b) and (c) provides the estimation of reactivity and delayed neutron precursor concentration using STO.

7.4 Uniform Second Order Sliding Mode (USOSM) Observer

The drawback of Super Twisting Algorithm based observer is the dependence of convergence time on the initial condition. Therefore we need to formulate an algorithm such that there is a faster convergence time irrespective of initial conditions. The observer design is a slight modification of the defined super twisting observer in section 7.3. Let us consider a general system as defined earlier in (7.7)

The USOSM observer is formulated as [30]

$$\dot{\hat{x}}_1 = \hat{x}_2 + \alpha_1\left(\mu_1|e_1|^{1/2}\,sign(e_1) + \mu_2|e_1|^{3/2}\,sign(e_1)\right)$$
$$\dot{\hat{x}}_2 = f(x_1,\hat{x}_2,t,u) + \alpha_2\left(\frac{\mu_1^2}{2}sign(e_1) + 2\mu_1\mu_2 e_1 + \frac{3}{2}\mu_2^2|e_1|^2\,sign(e_1)\right) \quad 7.10$$

where

Error terms are given by $e_1 = x_1 - \hat{x}_1$; $e_2 = x_2 - \hat{x}_2$

$\mu_1, \mu_2 \geq 0$ with gain terms represented by α_1, α_2.

The gain values are selected from the following inequality [30]

If $|F(x_1,x_2,t,u)| < \phi/2$ with a known value of ϕ, then α_1 and α_2 are selected such that (7.11) is satisfied.

$$\alpha_1^2\left(\alpha_2 - \frac{\alpha_1^2}{4}\right) > w^2;\ 2\alpha_2^2 > \alpha_1^2 \quad 7.11$$

The convergence time is independent of the initial condition of the system [30].

On comparison of (7.8) with (7.10), we note that some extra nonlinear terms are added. These terms are responsible for faster convergence time than Super Twisting Algorithm. When $\mu_1 = 1$; $\mu_2 = 0$ Uniform Sliding Mode Observer reduces to a Super Twisting observer

7.4.1 Simulation Results

Before delving into the nuclear reactor system, we illustrate the merits of this method by illustrating a mechanical system.

(a) Let us consider an example of a pendulum

$$\dot{x}_1 = x_2$$
$$\dot{x}_2 = \frac{u}{J} - \frac{g}{L}\sin(x_1) - \frac{V_s}{J}x_2 + \rho$$
$$y = x_1$$

where

x_1 is the angular position ; x_2 is the angular velocity ; ρ is the bounded disturbance

y is the output of the system

We observe that angular position is the only measured quantity and angular velocity needs to be estimated.

In this simulation, we use

$g = 9.815\,\text{m/s}^2$; $J = 0.891\,\text{kgm}^2$; $V_s = 0.18\,\text{kg.m/s}^2$

$\rho = 0.5\cos(2t) + 0.5\sin(2t)$

The Uniform Sliding Mode observer is formulated as

$$\dot{\hat{x}}_1 = \hat{x}_2 + \alpha_1\left(\mu_1 |e_1|^{1/2} sign(e_1) + \mu_2 |e_1|^{3/2} sign(e_1)\right)$$

$$\dot{\hat{x}}_2 = \frac{u}{J} - \frac{g}{L}\sin(\hat{x}_1) - \frac{V_s}{J}\hat{x}_2 + \alpha_2\left(\frac{\mu_1^2}{2} sign(e_1) + 2\mu_1\mu_2 e_1 + \frac{3}{2}\mu_2^2 |e_1|^2 sign(e_1)\right)$$

where

Error terms are given by $e_1 = x_1 - \hat{x}_1$; $e_2 = x_2 - \hat{x}_2$

The error vectors are plotted. From Fig.7.4, we can clearly observe that Super Twisting has a significantly large convergence time in comparison with Uniform Sliding Mode observer. The higher order nonlinear terms in (7.10) are responsible for better convergence of angular position and angular velocity even in the presence of bounded disturbance. The gain values represented by α_1, α_2 are selected according to the relation given by (7.11).

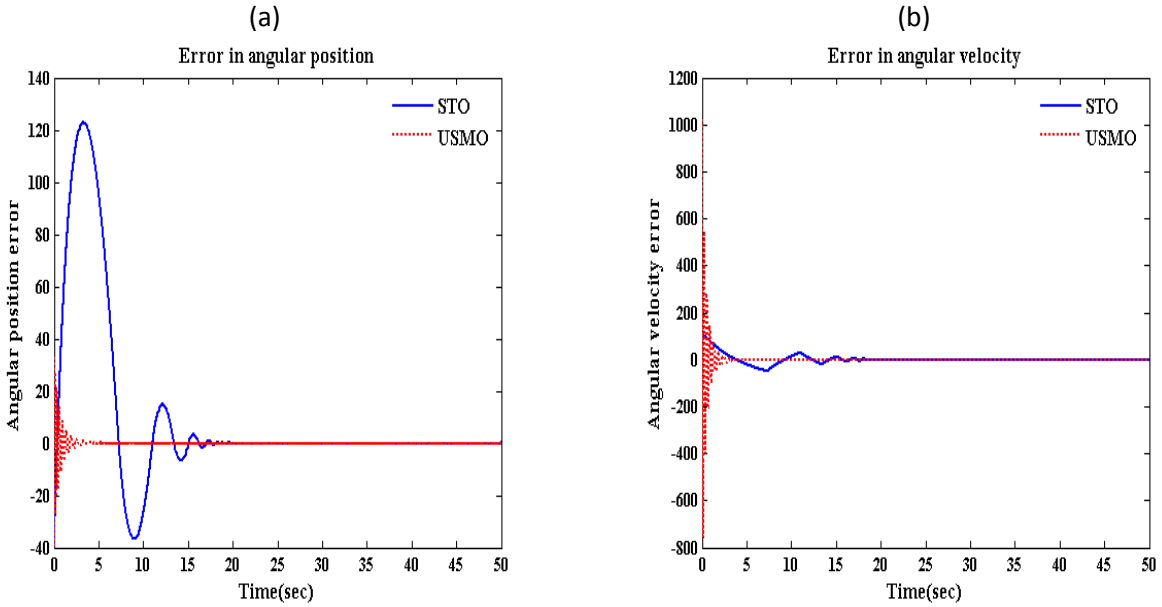

Figure 7.4: Application of USOSM for a pendulum system Fig. 7.4(a) gives the comparison of the error in estimating the angular position. Fig. 7.4(b) gives the comparison of the error in estimating the angular velocity.

Now we apply the Uniform Sliding Mode observer for analyzing nuclear reactor system dynamics. By following the general model explained in (7.10), the observer can be designed based on the point kinetic model as

$$\dot{\hat{P}} = \left(\frac{\rho_r - \beta}{\Lambda}\right)\hat{P} + \lambda\hat{C} + \alpha_1\left(\mu_1 |e_1|^{1/2} sign(e_1) + \mu_2 |e_1|^{3/2} sign(e_1)\right)$$
$$\dot{\hat{C}} = \left(\frac{\beta}{\Lambda}\right)\hat{P} - \lambda\hat{C} + \alpha_2\left(\frac{\mu_1^2}{2} sign(e_1) + 2\mu_1\mu_2 e_1 + \frac{3}{2}\mu_2^2 |e_1|^2 sign(e_1)\right) \quad 7.12$$

The output will be in terms of power. The corresponding error term is given by $e_1 = P - \hat{P}$. The gain terms are selected from the procedure illustrated above. The value of μ_1 and μ_2 is selected as 1.5.

The time response of power and precursor concentration is shown in Fig. 7.5. We note that in Fig. 7.5 (b) the value of precursor concentration is estimated in a designed manner. In addition, we note that the convergence time of the estimated precursor concentration is significantly lower than the corresponding estimation shown in Fig. 7.3(c). Therefore we can conclude that uniform second order sliding mode observer estimates the results with faster convergence time than super twisting observer.

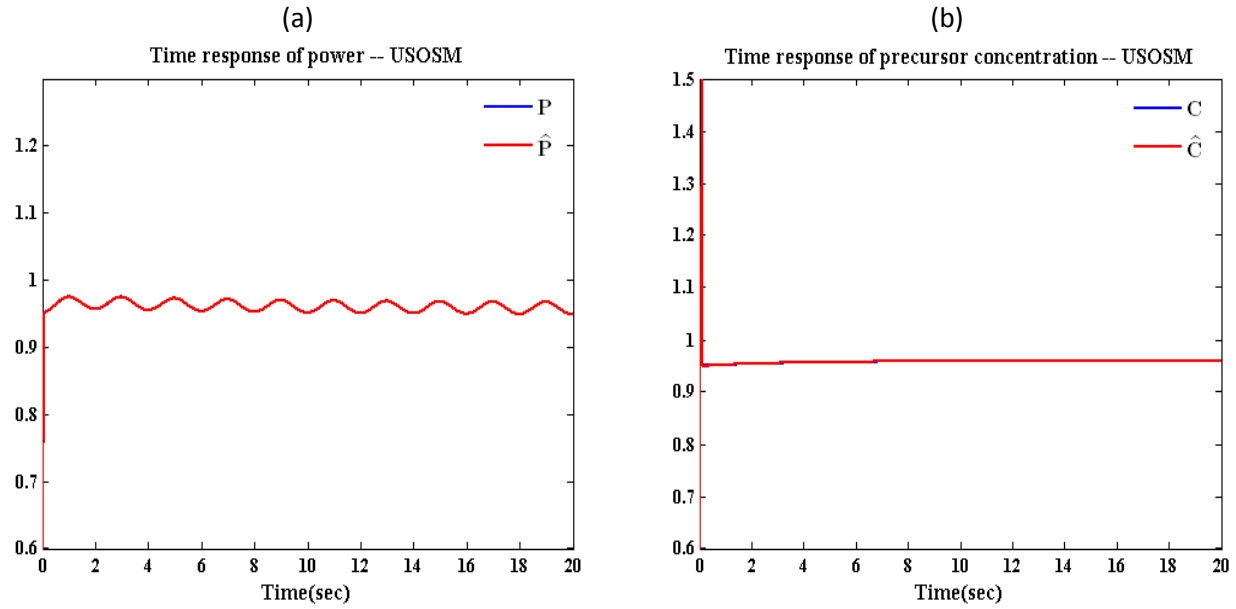

Figure 7.5: Application of USOSM for nuclear reactor system. Fig 7.5(a) provides the variation of reactor power. Fig. 7.5(b) gives the estimation of delayed neutron concentration.

Chapter 8

Conclusion and Future Scope

In this thesis, a novel attempt has been made to solve the control problem of estimating the non-measurable parameters using sliding mode observer. A first order sliding mode observer has been designed to estimate the critical parameters of a nuclear reactor system. The critical parameters considered are delayed neutron concentration, neutron source, reactivity, iodine and xenon concentration. The designed sliding mode observer is validated under input and parameter uncertainty. The disastrous effect of chattering is minimized by the effect of smooth functions at with a subsequent loss of robustness.

To preserve robustness with minimization in chattering, a second order sliding mode observer is designed. Due to a significant importance with respect to necessity of information, super twisting algorithm is used for the design. Though the focus of application is to a nuclear reactor system, simple illustrative problems are solved. An estimation of reactivity and delayed neutron precursor concentration is carried out.

To remove the dependence of super twisting algorithm on the initial condition and to obtain the estimation at a faster convergence rate, we design a uniform second order sliding mode observer.

An application of sliding mode observer is carried out in fault detection of nuclear and non-nuclear components in a nuclear power plant. The presence of an actuator or a sensor fault in power and coolant temperature is detected even in presence of measurement noise and parametric uncertainty. In addition, detection of an actuator or sensor fault influencing the measurement of water level in a steam generator is carried out. Irvin's model for a steam generator is considered with validation of the designed fault detection method during low power and high power of operation is performed.

In future, a design of sliding mode observer for nuclear reactor application can be carried out by considering a complete reactor model comprising of reactor power, delayed neutron concentration, fuel temperature, coolant temperature, iodine and xenon concentration as a single state vector.

A higher order sliding mode observer can be designed to estimate more number of parameters related to nuclear reactor. As higher order derivatives are difficult to calculate in a robust manner, a design of robust exact differentiator based on second order sliding mode observer can be carried out.

An application of higher order sliding mode in fault detection can be implemented for all the important nuclear and non-nuclear components of a nuclear power plant.

References

[1] Vadim, I. Utkin. "Survey paper variable structure systems with sliding modes." *IEEE Transactions on Automatic control* 22, no. 2 (1977).

[2] Slotine, J-JE, J. K. Hedrick, and E. A. Misawa. "Nonlinear state estimation using sliding observers." In *Decision and Control, 1986 25th IEEE Conference on*, pp. 332-339. IEEE, 1986.

[3] Chernick, J. "The dynamics of a xenon-controlled reactor." *Nuclear Science and engineering* 8, no. 3 (1960): 233-243.

[4] Wang, Peng, Tunc Aldemir, and V. I. Utkin. "Estimation of xenon concentration and reactivity in nuclear reactors using sliding mode observers." In *Decision and Control, 2001. Proceedings of the 40th IEEE Conference on*, vol. 2, pp. 1801-1806. IEEE, 2001.

[5] David, G. Luenberger "An introduction to observers." *IEEE Transactions on automatic control* 16, no. 6 (1971): 596-602.

[6] Vadim, I. Utkin. *Sliding modes in control and optimization*. Vol. 116. Berlin: Springer-Verlag, 1992.

[7] Hung, John Y., Weibing Gao, and James C. Hung. "Variable structure control: a survey." *Industrial Electronics, IEEE Transactions on* 40, no. 1 (1993): 2-22.

[8] DeCarlo, Raymond A., Stanislaw H. Zak, and Gregory P. Matthews. "Variable structure control of nonlinear multivariable systems: a tutorial." *Proceedings of the IEEE* 76, no. 3 (1988): 212-232.

[9] Drakunov, Sergey, and Vadim Utkin. "Sliding mode observers: tutorial." In *Decision and Control, 1995., Proceedings of the 34th IEEE Conference on*, vol. 4, pp. 3376-3378. IEEE, 1995.

[10] Edwards, Christopher, Sarah K. Spurgeon, and Ron J. Patton. "Sliding mode observers for fault detection and isolation." *Automatica* 36, no. 4 (2000): 541-553.

[11] Spurgeon, Sarah K. "Sliding mode observers: a survey." *International Journal of Systems Science* 39, no. 8 (2008): 751-764.

[12] Young, K. David, Vadim I. Utkin, and Umit Ozguner. "A control engineer's guide to sliding mode control." *IEEE transactions on control systems technology* 7, no. 3 (1999): 328-342.

[13] Luenberger, David G. "Observers for multivariable systems." *Automatic Control, IEEE Transactions on* 11, no. 2 (1966): 190-197.

[14] Luenberger, David G. "Observing the state of a linear system." *Military Electronics, IEEE Transactions on* 8, no. 2 (1964): 74-80.

[15] Edwards, Christopher, Leonid Fridman, and Arie Levant. *Sliding mode control and observation*. Birkhäuser, 2014.

[16] Utkin, Vadim, Jürgen Guldner, and Jingxin Shi. *Sliding mode control in electro-mechanical systems*. Vol. 34. CRC press, 2009.

[17] Levant, Arie. "Robust exact differentiation via sliding mode technique."*Automatica* 34, no. 3 (1998): 379-384.

[18] Levant, Arie. "Sliding order and sliding accuracy in sliding mode control." *International journal of control* 58, no. 6 (1993): 1247-1263.

[19] Davila, Jorge, Leonid Fridman, and Arie Levant. "Second-order sliding-mode observer for mechanical systems." *IEEE transactions on automatic control* 50, no. 11 (2005): 1785-1789.

[20] Emel'yanov, S. V., S. K. Korovin, and A. Levant. "High-order sliding modes in control systems." *Computational mathematics and modeling* 7, no. 3 (1996): 294-318.

[21] Tan, Wen. "Water level control for a nuclear steam generator." *Nuclear Engineering and Design* 241, no. 5 (2011): 1873-1880.

[22] Na, Man Gyun, and Hee Cheon No. "Quantitative evaluation of swelling or shrinking level contributions in steam generators using spectrum analysis." *Annals of Nuclear Energy* 20, no. 10 (1993): 659-666.

[23] Davila, Jorge, Leonid Fridman, and Alexander Poznyak. "Observation and identification of mechanical systems via second order sliding modes." *International Journal of Control* 79, no. 10 (2006): 1251-1262.

[24] Chen, F., and M. W. Dunnigan. "Comparative study of a sliding-mode observer and Kalman filters for full state estimation in an induction machine." *IEE Proceedings-Electric Power Applications* 149, no. 1 (2002): 53-64.

[25] Moreno, Jaime A., and Marisol Osorio. "A Lyapunov approach to second-order sliding mode controllers and observers." In *Decision and Control, 2008. CDC 2008. 47th IEEE Conference on*, pp. 2856-2861. IEEE, 2008.

[26] Fridman, Leonid, and Arie Levant. "Higher order sliding modes." *Sliding mode control in engineering* 11 (2002): 53-102.

[27] Sira-Ramirez, H. "Variable structure control of non-linear systems." *International journal of systems science* 18, no. 9 (1987): 1673-1689.

[28] Barbot, J., M. Djemai, and T. Boukhobza. "Sliding mode observers." *Sliding Mode Control in Engineering* 11 (2002).

[29] Slotine, J. J, and Shankar S. Sastry. "Tracking control of non-linear systems using sliding surfaces, with application to robot manipulators." *International journal of control* 38, no. 2 (1983): 465-492.

[30] Cruz-Zavala, Emmanuel, Jaime A. Moreno, and Leonid Fridman. "Uniform second-order sliding mode observer for mechanical systems." In *Variable Structure Systems (VSS), 2010 11th International Workshop on*, pp. 14-19. IEEE, 2010.

[31] Cruz-Zavala, Emmanuel, Jaime A. Moreno, and Leonid M. Fridman. "Uniform robust exact differentiator." *Automatic Control, IEEE Transactions on* 56, no. 11 (2011): 2727-2733.

[32] Ablay, Günyaz, and Tunc Aldemir. "Observation of the dynamics of nuclear systems using sliding mode observers." *Nuclear Technology* 174, no. 1 (2011): 64-76.

[33] Na, Man Gyun, and Hee Cheon No. "Quantitative evaluation of swelling or shrinking level contributions in steam generators using spectrum analysis." *Annals of Nuclear Energy* 20, no. 10 (1993): 659-666.

[34] Edwards, Robert M., Kwang Y. Lee, and Asok Ray. "Robust optimal control of nuclear reactors and power plants." *Nuclear Technology* 98, no. 2 (1992): 137-148.

[35] Hwang, Inseok, Sungwan Kim, Youdan Kim, and Chze Eng Seah. "A survey of fault detection, isolation, and reconfiguration methods." *Control Systems Technology, IEEE Transactions on* 18, no. 3 (2010): 636-653.

[36] Glasstone, Samuel, and Alexander Sesonske. "Nuclear reactor engineering.", *CBS Publishers*

[37] Burton, J. A., and Alan SI Zinober. "Continuous approximation of variable structure control." *International journal of systems science* 17, no. 6 (1986): 875-885.

[38] Spurgeon, S. K., and R. Davies. "A nonlinear control strategy for robust sliding mode performance in the presence of unmatched uncertainty." *International Journal of Control* 57, no. 5 (1993): 1107-1123.

Appendix

Relative Degree

Considering the importance of relative degree in application of sliding mode, a brief discussion is provided. Let us divide the discussion into two as

Linear Systems

The equation for a general system in state space representation is given by

$$\dot{x} = Ax + Bu$$

$$y = Cx$$

where the terms are already described in Chapter 4.

The transfer function of a general system can be defined as $\frac{y(s)}{x(s)} = C(sI - A)^{-1} B$.

In simple words, relative degree is defined as the difference in the order of the denominator polynomial and numerator polynomial.

Definition: *Relative degree of a system* r *is the smallest integer for which* $CA^{r-1}B \neq 0$.

By taking successive derivatives of the output, we get

$$\dot{y} = CAx \ ;$$

$$\ddot{y} = CA^2 x \ .....$$

$$\frac{d^{r-1}y}{dt^{r-1}} = CA^{r-1}x;$$

$$\frac{d^{r}y}{dt^{r}} = CA^{r}x + CA^{r-1}Bu$$

From the above set of equations, we can easily infer that relative degree corresponds to the lowest order derivative which explicitly depends on the control input.

Nonlinear Systems

The general equation representing a nonlinear system is given by

$$\dot{x} = f(x) + g(x)u$$

$$y = h(x)$$

Definition*: Relative degree* r *is the smallest integer for which* $L_g L_f^{r-1} h(x) \neq 0$ *and* $L_g L_f^{r-2} h(x) = 0 \ \ \forall x$ *in some neighborhood of the operating point.*

Similar to the earlier case of taking successive derivatives of output, we get

$$\dot{y} = \frac{dh}{dt} = \frac{\partial h}{\partial x} \cdot \frac{dx}{dt} = L_f h(x)$$

$$\ddot{y} = L_f^2 h(x)$$

$$\vdots$$

$$\frac{d^{r-1} y}{dt^{r-1}} = L_f^{r-1} h(x)$$

$$\frac{d^{r} y}{dt^{r}} = L_f^{r} h(x) + L_g L_f^{r-1} h(x) u$$

where

$L_f \rightarrow$ Lie derivative of $f(x)$

$L_g \rightarrow$ Lie derivative of $g(x)$

For nonlinear systems also, relative degree corresponds to the lowest order derivative which explicitly depends on the control input.